Development and Application of Modern Optimal Controllers for a Membrane Structure Using Vector Second Order Form

Ipar Ferhat

Dissertation submitted to the faculty of the Virginia Polytechnic Institute and State University in partial fulfillment of the requirements for the degree of

Doctor of Philosophy
In
Aerospace and Ocean Engineering

Cornel Sultan, Chair
Rakesh K. Kapania
Craig Woolsey
Michael Philen

May 1st 2015
Blacksburg, Virginia

Keywords: Thin / membrane structures, piezoelectric actuators, smart materials, control of structures, distributed control, vector second order form.

Development and Application of Modern Optimal Controllers for a Membrane Structure Using Vector Second Order Form

Ipar Ferhat

ABSTRACT

With increasing advancement in material science and computational power of current computers that allows us to analyze high dimensional systems, very light and large structures are being designed and built for aerospace applications. One example is a reflector of a space telescope that is made of membrane structures. These reflectors are light and foldable which makes the shipment easy and cheaper unlike traditional reflectors made of glass or other heavy materials. However, one of the disadvantages of membranes is that they are very sensitive to external changes, such as thermal load or maneuvering of the space telescope. These effects create vibrations that dramatically affect the performance of the reflector.

To overcome vibrations in membranes, in this work, piezoelectric actuators are used to develop distributed controllers for membranes. These actuators generate bending effects to suppress the vibration. The actuators attached to a membrane are relatively thick which makes the system heterogeneous; thus, an analytical solution cannot be obtained to solve the partial differential equation of the system. Therefore, the Finite Element Model is applied to obtain an approximate solution for the membrane actuator system.

Another difficulty that arises with very flexible large structures is the dimension of the discretized system. To obtain an accurate result, the system needs to be discretized using smaller segments which makes the dimension of the system very high. This issue will persist as long as the improving technology will allow increasingly complex and large systems to be designed and built. To deal with this difficulty, the analysis of the system and controller development to suppress the vibration are carried out using vector second order form as an alternative to vector first order form. In vector second order

form, the number of equations that need to be solved are half of the number equations in vector first order form.

Analyzing the system for control characteristics such as stability, controllability and observability is a key step that needs to be carried out before developing a controller. This analysis determines what kind of system is being modeled and the appropriate approach for controller development. Therefore, accuracy of the system analysis is very crucial. The results of the system analysis using vector second order form and vector first order form show the computational advantages of using vector second order form.

Using similar concepts, LQR and LQG controllers, that are developed to suppress the vibration, are derived using vector second order form. To develop a controller using vector second order form, two different approaches are used. One is reducing the size of the Algebraic Riccati Equation to half by partitioning the solution matrix. The other approach is using the Hamiltonian method directly in vector second order form. Controllers are developed using both approaches and compared to each other. Some simple solutions for special cases are derived for vector second order form using the reduced Algebraic Riccati Equation. The advantages and drawbacks of both approaches are explained through examples.

System analysis and controller applications are carried out for a square membrane system with four actuators. Two different systems with different actuator locations are analyzed. One system has the actuators at the corners of the membrane, the other has the actuators away from the corners. The structural and control effect of actuator locations are demonstrated with mode shapes and simulations. The results of the controller applications and the comparison of the vector first order form with the vector second order form demonstrate the efficacy of the controllers.

مەن بۇ ئىلمىي ماقالەمنى ئائىلەمگە ۋە ئۇيغۇر خەلقىگە بېغىشلايمەن.

I would like to dedicate this dissertation to my family and Uyghur people.

ACKNOWLEDGEMENT

I would like to thank my advisor Dr. Cornel Sultan for his guidance and support during my research, and the National Science Foundation for their support via the NSF CMMI-0952558 and NSF IIP-1307827 grants.

I would also like to thank Dr. Rakesh K. Kapania, Dr. Craig Woolsey and Dr. Michael Philen serving on my Ph.D. committee and for their valuable advice.

I am very grateful to my family and my friends for their support, patience and understanding during my Ph.D.

Lastly, I would like to thank my lab mates Tri Ngo, Shu Yang, Maria Rye, Praneeth Reddy Sudalagunta and Javier Gonzalez Rocha for their support and friendship.

TABLE OF CONTENTS

LIST OF FIGURES

LIST OF TABLES

NOMENCLATURE

ρ	material density
t	time
N	prestress
w	transverse displacement
f	external force
h	thickness
ε	direct strain
γ	shear strain
E	elasticity modulus
υ	Poisson's ratio
σ	direct stress
τ	shear stress
M	moment
D	flexural stiffness
G	shear stiffness
Ω	domain
δ	Kelvin-Voigt damping coefficient
S_{ij}	mechanical strain tensor
T_{ij}	mechanical stress tensor
s_{ijkl}	compliance tensor
d_{kij}	piezoelectric coefficient tensor
$\mathbf{E}$	electric field vector
V_i	voltage applied to actuator i
M	mass matrix

C	damping matrix
K	stiffness matrix
$\bar{F}$	contral matrix
ψ_i	basis function
q	generalized coordinates
ω	natural frequency
A	state matrix
B	input matrix
u	control input
λ	eigenvalues of the state matrix
$\mathbb{C}$	controllability matrix
O	observability matrix
V	cost function
Q	state penalty matrix
R	control penalty matrix
x	state vector
y	output vector
H	output matrix
w_p, v_p	Gaussian white noise
L	disturbance input matrix
T	observer gain
ζ	Kalman gain

Subscripts

a	actuator properties
m	membrane properties
x	values in the x direction
y	values in the y direction
i, j	index of variable or property

ACRONYMS

NASA	National Aeronautic and Space Administration
PZT	Lead Zirconate Titanate
PVDF	Polyvinplidene Fluoride
MFC	Micro Fiber Composite
SMA	Shape Memory Alloy
FEM	Finite Element Method
LQR	Linear Quadratic Regulator
LQG	Linear Quadratic Gaussian

Chapter 1

INTRODUCTION

The most basic and simple definition of membranes is: membranes are two dimensional structures with very low thickness to length ratio. They do not carry compression loads but are used in many areas when they are under tensile loads. Throughout the history, membranes have been used in many areas due to their flexible, light-weight, and compliance features. One example is their common usage as tents since ancient times. With developing technology, usage of membranes has increased throughout the history. This vast application of very thin plates and membrane structures has aroused the necessity for classification of membrane structures. Basically, for practical applications there are three different types of membrane structures: air supported structures, air inflated structures and suspended membrane structures [1]. Air supported structures have been used throughout the last century in many areas such as roofing over sport halls, swimming pools, or some temporary shelters [1]. Fig. 1.1 shows an air supported membrane structure [2].

Figure 1.1: Gotham Stadium at Mill Pond Park - New York, NY,
(Used under fair use, Ref. [2], 2014)

Air inflated structures, such as Gossamer structures, have become popular during the last few decades, especially in space applications due to their flexibility, low packaging volume, and cheaper launching/shipment cost. Gossamer structure is a general name for the category of ultra low mass structures [3]. These structures are mostly air inflated membrane structures. Application areas for Gossamer structures have a very wide range such as solar arrays, satellite communication systems, human habitats, planetary surface explorations, radars and reflectors, solar concentrators, and solar shades. The usage of Gossamer structures have been an ideal concept for very long time, even though there were few applications due technological constraints. One of the first application of Gossamer structure was carried out by Goodyear Corporation. They developed a search radar antenna, radar calibration sphere and lenticular inflatable parabolic reflector in the 1950s and 1960s as seen in Figs. 1.2-1.4 [3].

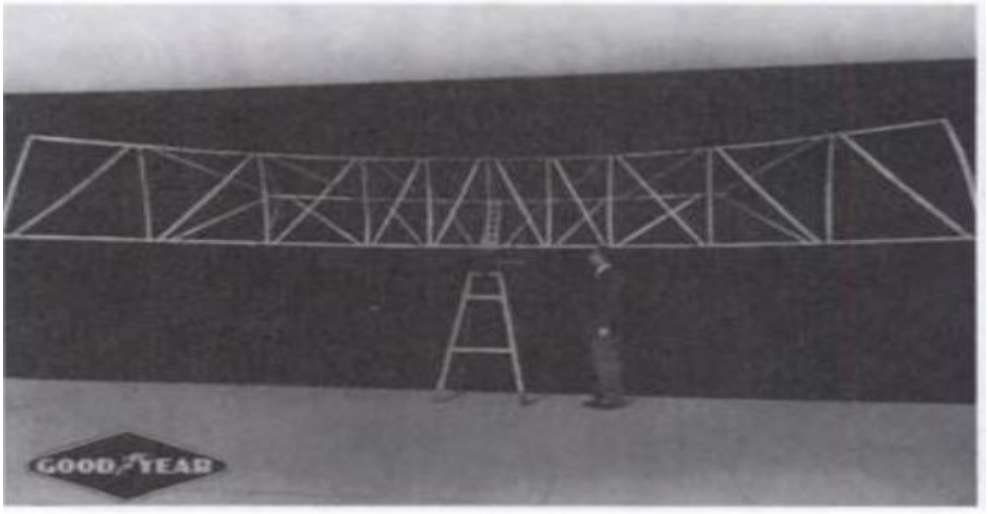

Figure 1.2: Inflatable search radar antenna, the 1950s.
(Used under fair use, Ref. [3])

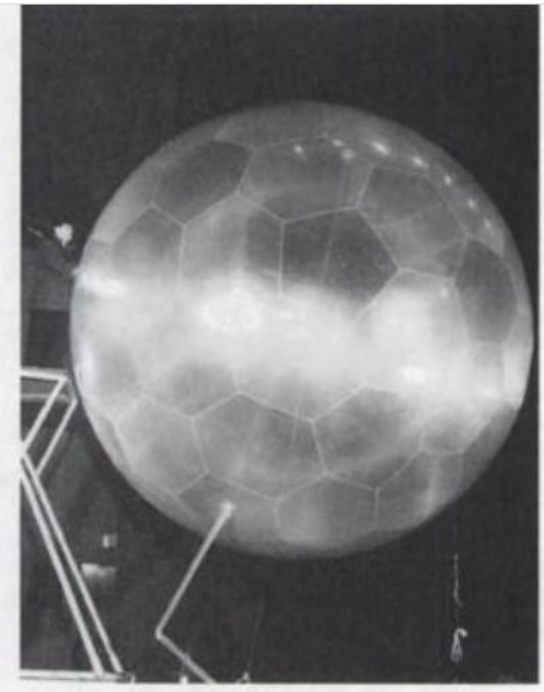

Figure 1.3: Radar calibration sphere, the 1950s.
(Used under fair use, Ref. [3])

Figure 1.4: Lenticular inflatable paragoric reflector, the 1950s.
(Used under fair use, Ref. [3])

The other early application of Gossamer structure was implemented by NASA with Echo balloons that were used to provide a passive space based communication reflector. Echo I (Fig. 1.5) was successfully launched on August 12, 1960 [4]. Echo I operated as a low earth orbit receiving a signal and reflecting it back.

Figure 1.5: ECHO satellite, the 1960s.
(Used under fair use, Ref. [4], 2014)

One of the later examples of Gossamer structures is a reflector antenna for a very large baseline interferometry and land mobile communications. ESA-ESTAC developed a 6m inflatable reflector antenna in the 1980s seen in Fig. 1.6 [3].

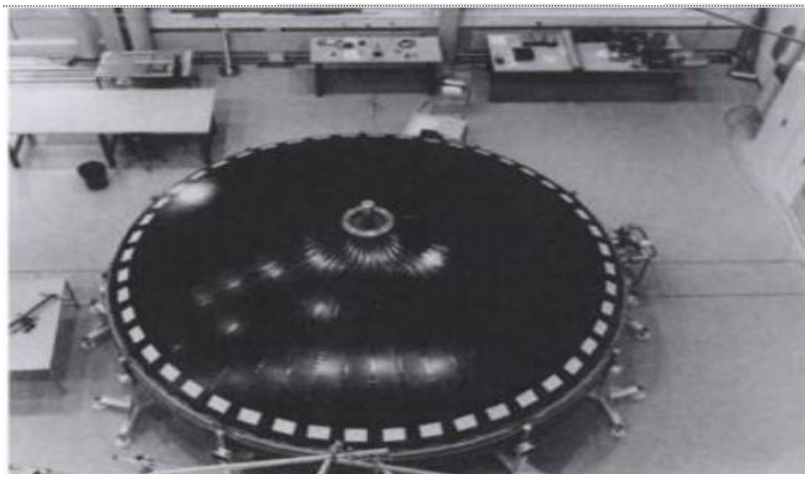

Figure 1.6: Inflatable very long baseline interferometry antenna, the 1980s.
(Used under fair use, Ref. [3])

Just before the 21st century, NASA developed an inflatable antenna. They launched the NASA's Inflatable Antenna Experiment (IAE) on May 19, 1996 [3]. The photograph of IAE is seen in Fig. 1.7.

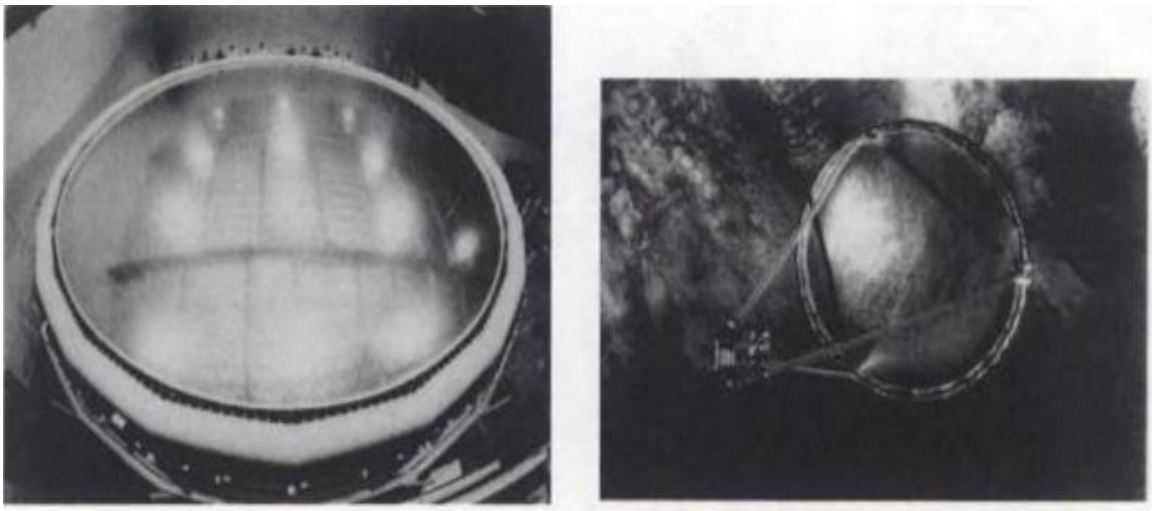

Figure 1.7: Inflatable Antenna Experiment by NASA, the 1990s.
(Used under fair use, Ref. [3])

For suspended membrane structures, a very recent example is a tensegrity structure with an attached membrane (Fig. 1.8) whose feasibility as a passive device in energy harvesting using smart materials is illustrated in reference [5].

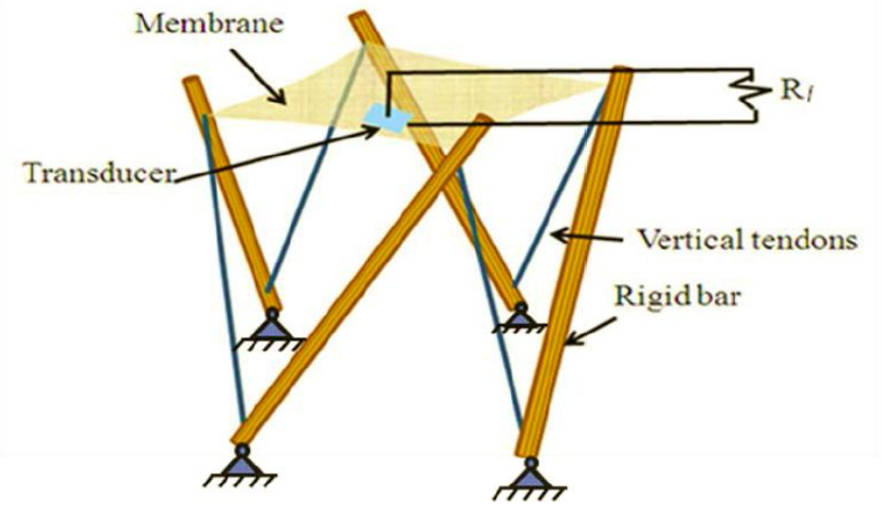

Figure 1.8: Tensegrity structure with a membrane.
(Used under fair use, Ref. [5])

Even though the usage of membranes in our daily lives is very extensive, aerospace applications of the membranes have increased dramatically only during the last decades. Because they are very thin structures sensitive to external disturbances that cause vibration and the control implementation can be very difficult. Another difficulty is dealing with distributed systems with very high dimensions. However, the significance of the advantages of using membrane structures in aerospace applications has led many researchers to focus on this area.

1.1 Control of Thin Structures

One of the key advancements in technology that allowed the control of thin structures is the discovery of smart materials. Piezoelectric materials enable us to control large plate-like structures using distributed actuators. This system is based on the shape changing characteristics of the piezoelectric material under an electric voltage. Nowadays, smart materials are used in many areas from underwater vehicles to aerospace applications [93]. One futuristic example to aerospace application is morphing wing airplanes. With this kind of control, the airplane wings can mimic a bird's wing movement very closely leading to a safe and efficient flight. Fig. 1.9 shows a concept of a morphing wing airplane mimicking a bird [6].

Figure 1.9: Morphing wing airplane mimicking an eagle.
(Used under fair use, Ref. [6], 2014)

An example of a thin structure used as a mirror in space applications shows how important it is to be able to control thin structures used as reflectors. In Fig. 1.10 the image of a reflector is shown for various control conditions [7]. It is clear that an image changes substantially even with a small aberration in the mirror.

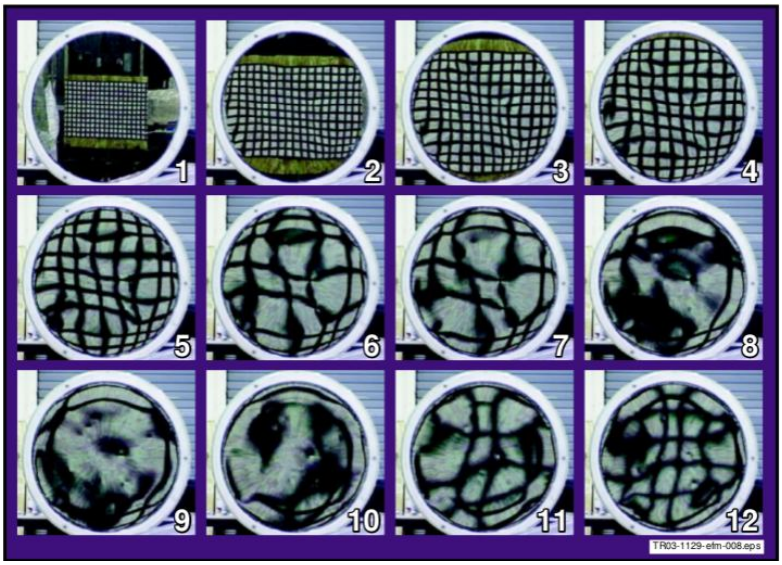

Figure 1.10: The effect of decreasing the radius of curvature on a membrane mirror. (Used under fair use, Ref. [7])

One of the difficulties of controlling thin structures is that most control applications are empirical and many experiments are necessary due to the difficulties of the precise modeling of the distributed system. Furthermore, the equations of motion are derived as partial differential equations; and to have the exact model of a distributed system, we need to have infinite number of coordinates, which is impossible in real applications. For control design, we need ordinary differential equations and finite number of coordinates. Even though we obtain a finite number of coordinates and ordinary differential equations by discretizing the system, this is a qualitative approximation of the original model based on partial differential equations. A common tendency to improve the accuracy of the approximate model is to increase the number of coordinates used in the ordinary differential equations. However this creates other problems because reliable computations are very difficult for very high dimensional systems.

1.2 Control Using Vector Second Order Form

Developments in space technology have always been parallel to developments in computing power and control of space structures. Nowadays, computers are capable of computing online solutions for high dimensional systems, which also enables the control of flexible distributed systems. However, being able to describe a system with fewer number of dimensions is still crucial in order to have more advanced design capability or to be able to design even larger systems. This demand will never diminish since humankind will always be exploring more and inventing more to achieve further advancements.

First order ordinary differential equations are the most common and general type of equations that are used to describe the system dynamics when we want to apply control. When the control theory was developed, it was developed by control engineers mostly for electrical systems that are in first order form [8]. As a result, conventional control theory has been developed based on first order differential equations. However most mechanical systems are described by second order differential equations. To apply classical control we have to convert the system's dynamic equations into first order form by redefining the state vector. This is an extra step in computation and it doubles the number of equations that need to be solved. Another advantage of using vector second order form is having a more familiar mathematical expression for scientists with expertise in mechanics. Furthermore, when LQR developed for vector second order form using the Hamiltonian method we do not need to solve the nonlinear Algebraic Riccati Equation. Therefore, developing control theory using vector second order form can be very beneficial in controlling high dimensional structures, such as membrane structures.

1.3 Research Objectives

The main goal of this work is to accurately model and control a membrane structure with bimorph actuators. As a result, we can have a more reliable model and control design that will decrease the effort and cost related to experiments. The interdisciplinary approach for structural modeling and controller design will be a crucial part of the modeling process. The control aim is suppressing the vibration of the membrane. For the system analysis and control application, the linear vector second order form will be used as an effective approach to deal with high dimensional systems.

Most of the time, structural modeling is solely based on static parameters such as displacements and stresses. However, when active control needs to be applied, it is important to consider the dynamic parameters such as natural frequencies and mode shapes too. This helps to have structural and control design process in a harmonious way. From this point of view, two different systems depending on actuator placements (Figs. 1.11-1.12) will be analyzed. One system has the actuators away from the corners to have a better control capability at every point of the membrane. The other system has the actuators at the corners to have a larger homogenous central area for improved mission performance. For example, the mission can require to have a large area to be used as a reflector on a space antenna or a smooth surface on an airplane wing for aerodynamic efficiency. Both systems will be analyzed from the structural and control perspective.

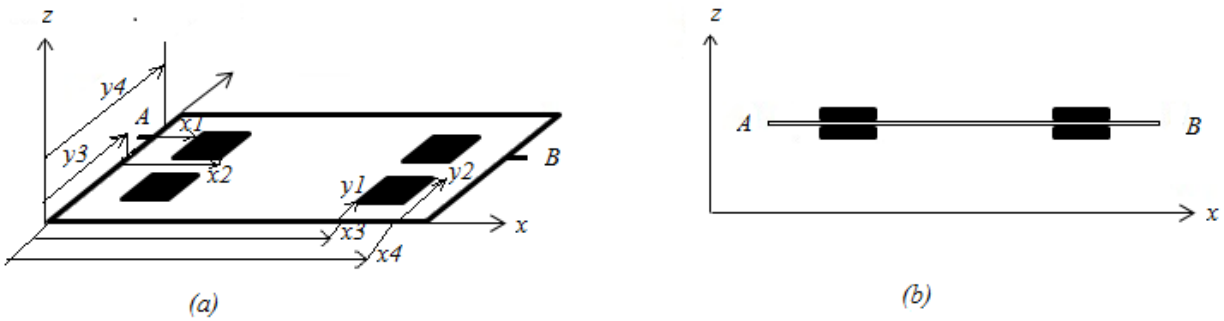

Figure 1.11: (a) System I. The membrane with four bimorph actuators away from the corners, (b) A-B intersection of System I

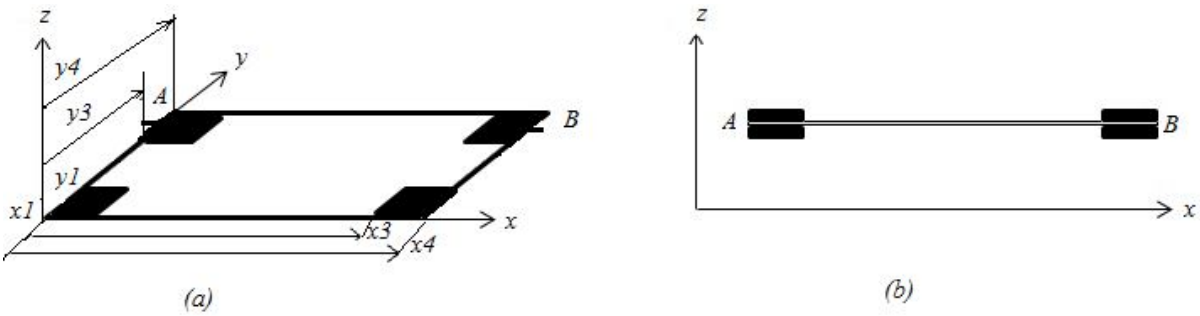

Figure 1.12: (a) System II. The membrane with four bimorph actuators at the corners, (b) A-B intersection of System II

The bimorph actuators are made of piezoelectric materials. The bimorph layers are used to create a bending moment by contracting one layer and expanding the other layer. This kind of

control can only be applied if the material has bending resistance. Therefore, the membrane that is used is actually a leaf-like material that has considerable bending resistance under inplane load. Even though it is classified as membrane due to it is thickness, it is actually a very thin plate with bending resistance that is created by the material's strength and the inplane load.

To have a reliable control application, the systems will be analyzed using linear vector second order form as well as linear vector first order form. The main objective is to show the capabilities and the advantages of the vector second order form. Since we are trying to suppress the vibration of the membrane with piezoelectric actuators, LQR and LQG controllers, that optimize the displacement and electric usage, will be developed using both vector first order and vector second order form. The key novelties are rigorous system analysis using vector second order form, development of control theories using vector second order form, and their application to practical systems.

1.4 Outline of Dissertation

The layout of this dissertation is as follows: the works that have been done in related areas are summarized in Chapter 2. Chapter 3 is devoted to mathematical modeling and the Finite Element Modeling of the system. The rigorous system analysis is carried out in Chapter 4 as a prerequisite work for the controller development and applications. In Chapter 5, LQR and LQG controller are developed for vector first order form and vector second order form. The control applications and results are demonstrated in Chapter 6. The conclusion, discussion and contributions is summarized in Chapter 7.

Chapter 2

LITERATURE REVIEW

2.1 Introduction

Knowledge and understanding of previous works are one of the crucial beginning steps in improvement of research and technology since it allows us to gain more insight into the physical phenomena analyzed and improve the engineering design process of any project. Furthermore, it prevents repetition of past mistakes. This chapter is a review of previous works that were published in the areas related to this dissertation. Section 2.2 summarizes some works that are relevant to the modeling of membrane and flexible structures as well as control of membrane and large structure. Finally, as a new approach to control theory and its applications, results that address the vector second order form of linearized equations of motion are summarized in Section 2.3. The concluding remarks of the literature review is discussed in Section 2.4.

2.2 Modeling and Control of Membrane Structures

One of the earliest rigorous published works on control of membrane structures was carried out by Balas [9]. His approach is more general considering that he studied general flexible structures. He discretizes the system as lumped masses and applies modal control converting the system to vector first order form. He also considers the spillover effects. Another work that focuses more on the control characteristics of flexible structures was done by Hughes and Skelton [10]. They analyze the controllability and observability conditions of a flexible system, and investigate the most feasible placement of the sensors. Gibson and Adamian applied an LQG control to a flexible structures by discretizing the systems to obtain mathematical models of a finite dimension [11]. They solve two Riccati equations in finite dimension, one for optimal control and the other for optimal state estimation. The importance of the interaction

between the modeling and control development process was emphasized by Liu and Skelton [12]. They try to reduce the iteration number in the control design process by applying Q-Markov covariance equivalent realization, Modal Cost Analysis, model reduction algorithm, and an Output Variance Constraint controller design algorithm to a flexible system.

With the invention of piezoelectric materials, the distributed piezoelectric actuators and sensors have become an important tool for structural control. The early works on control of structures with piezoelectric actuators were done by Forward [13]. Forward uses two piezoelectric ceramic actuators to dampen a cylindrical mass. Even though the mode frequencies are close, he is able to obtain substantial damping. He also demonstrates the effects of using only one actuator. He validates his results with experiments. In another study, the design and control of a deformable two dimensional glass mirror was carried out by Sato et al. [14]. They bound multiple layer electrostrictive laminar sheets to the backside of the mirror. Each layer generates a different wave front, and the displacement is the sum of the weighted values of these wave fronts. They show that this provides desired damping. Similarly, Sato, Ishikawa and Ikeda designed a one dimensional mirror controlled with multi layer PVDF actuators [15]. Similar to reference [14], each layer generates a different wave front and the desired profile is achieved as the weighted sum of these wave fronts. In another work, Bailey and Ubbard use a distributed piezoelectric (PVDF) actuator to control a beam with the purpose of avoiding the disadvantages of using lumped actuators, such as the necessity to truncate the model [16]. They also propose a control law based on Lyapunov's second law to be able to control all modes. Crawley and Luis carried out an extensive work on piezoelectric actuators [17]. They develop analytical models for distributed actuators and simulate a beam structure with piezoelectric actuators attached. They compare the various types of PZT and PVDF actuators to show the effectiveness of material choices on the performance of the structure.

To design an efficient system that is light and has a high control capacity, we need to consider the trade-off between the number of actuators and sensors for the control ability and measuring, and the weight of the system. For this purpose there have been a large amount of work on the optimization of the number and the placement of actuators and sensors. Some of the works in this area were done by Gawronski and Lim. They studied the efficient actuator and sensor placement on flexible structures using Henkel singular values [18]. By this approach they try to develop a methodology to optimize the controllability and observability of the system with

the most efficient number of actuators and sensors. Another optimal actuator placement study was carried out by Mirza and Van Niekerk [19]. They use the cost function based on the disturbance sensitivity grammian. They show that by minimizing the size of the grammian matrix, the control effectiveness of the actuator can be maximized. They use an L shaped membrane for the application of their approach.

Baven studied the optimal placement of a piezoceramic actuator on a rectangular panel to suppress the noise actively in his Ph.D. dissertation [20]. He adds a curved panel structure to reduce the noise of a subsonic aircraft with an active control. He uses genetic algorithms to determine the optimal placement of the piezoceramic actuators. Quek, Wang and Ang developed a simple method to determine the optimal placement of collocated piezoelectric actuators attached to a composite plate [21]. They apply a direct pattern search method to optimize a cost performance based on normal strains and controllability of the system. They demonstrate with examples that the number of iterations is fewer than the initial blind discrete pattern search approach. Halim and Moheimani developed an optimization approach based on modal and spatial controllability measures for collocated piezoelectric actuators and sensors on a very thin plate [22]. They show that this approach can be used on collocated actuator-sensor pairs without damaging the observability performance. They demonstrate their results using a simple supported thin plate. The precise shape and vibration control of a paraboloidal membrane shell was investigated by Yue, Deng and Tzou by analyzing the microscopic control actions of segmented actuator patches laminated on a membrane shell while optimizing the actuator locations [23]. Development and analysis of a distributed actuator attached to a hemispherical shell was carried out by Smithmaitrie and Tzou [24]. They investigate certain parameters such as actuator placements and sizes, shell thickness, distributed control forces etc., to see the effect on different situations.

Philen studied active shape control and vibration suppression of plate structures in his Ph.D. dissertation [25]. He uses directionally decoupled piezoelectric actuators as an ideal actuator for two dimensional structures. He proposes two directional decoupling methods for high-precision shape and vibrational control as Active Stiffener and Micro Fiber Composites. A doubly curved membrane shell with multiple layers of active materials was studied by Bastaits et al. [26]. They show that four layers of active material provide independent control of in-plane forces and bending moments by guaranteeing optimal morphing with an arbitrary profile.

Feedback control of a beam with piezoelectric actuators and sensors was investigated by Hanagud, Obal and Calise [27]. They apply optimal control with quadratic cost index of the state and control input. They carry simulations with different cost penalties to show the effect of penalty weightings of the cost. Scott and Weisshaar used piezoelectric actuators (PZT and PVDF) and shape memory alloys to control the flutter of a panel [28]. They apply both transverse and inplene controls for flutter suppression and show that inplane control is more effective. They compare the SMAs and piezoelectric actuators in terms of effectiveness and suppression time. They also derive an analytical formula to compare the effectiveness of piezoelectric actuators. The effectiveness consists of material terms, such as elasticity modulus, and geometrical features, such as the thickness ratio of the actuator to the plate. Renno and Inman [29] modeled a 1-D membrane strip with multiple actuators that actuate the system producing bending and tension effects. Control of flexural vibrations of a circular plate was carried out by Nader et al. [30]. They use multi layer piezoelectric actuators to suppress the vibration. They develop an analytical solution to their problem and verify their results using 3-D Finite Element Method. Sun and Tong developed an optimal control for the shape of piezoelectric structures [31]. They consider two constraints, control energy and control voltage. They emphasize the importance of the control voltage constraints for piezoelectric materials since the voltages higher than the critical value can depolarize the material.

Williams studied the piezoelectric actuators attached on membrane structures in his master's thesis [32]. His motivation is modeling an inflated torus space structure. He emphasizes the shortages of the conventional membrane theory when applied to very thin membranes with relatively thick actuators, and he uses thin plate theory to model the system. To discretize and solve the system numerically, he uses the Finite Element Method. A very extensive work on gossamer structures was carried out by Jenkins [3, 33]. He summarizes the history, design, manufacturing, and control developments of gossamer structures comprehensively in his books. Park, Kim and Inman used piezoelectric sensor and actuators to apply feedback control to an inflated torus structure made of membrane materials [34]. They use PVDF for sensors and actuators and MFC for actuators. They carry out experiments to demonstrate the effectiveness of using piezoelectric actuators to suppress the vibration of the torus. In another work, Park, Ruggiero and Inman carried out similar work to reference [34]. They use PVDF sensors and MFC actuators to suppress the vibration of an inflated membrane torus. They demonstrate

experimental results as well as theoretical [35]. A review of Shape Memory Alloys and their aerospace applications was carried out by Hartl and Lagoudas [36]. They provide a general overview of SMAs to discuss their advantages and difficulties in engineering applications. They review the usage of SMAs on structures for atmospheric earth flights as well as space flights.

Rogers and Agnes modeled an active optical membrane using the Method of Integral Multiple Scales (MIMS) [37]. The system consists of laminated inflatable structures and piezo-polymer sheets. Their analysis show that the piezoelectric polymer layer has a significant effect on the deflection of the reflectors when actuated. Ruggiero and Inman extended the 1-D work to a 2-D membrane mirror with one bimorph actuator [38]. They develop a 2-D LQR for vibration control of the membrane mirror. Ruggiero modeled a 1-D strip of a membrane satellite mirror with a lead zicronate titanate (PZT) bimorph actuator using the finite element method and applied a Linear Quadratic Regulator (LQR) to eliminate vibrations [39]. He also applies the same work to a two dimensional mirror. He models the membrane strip as an Euler-Bernoulli beam and membrane plate as a Kirchoff plate to capture the bending characteristics of the system. Renno and Inman analyzed a 1-D membrane strip with a single piezoelectric bimorph actuator attached to it [40]. They model the membrane strip as an Euler-Bernoulli beam using the finite element method and apply Proportional-Integral (PI) control. Renno modeled a 2-D circular membrane with smart actuators for adaptive optics applications in his Ph.D. dissertation [41]. Tarazaga worked on improving the performance of an optical membrane to suppress the vibration of a membrane, backed with air cavity, with a new control approach that uses a centralized acoustic source in the cavity to actuate the system [42]. The key advantage of this approach is not adding a mass load to the membrane.

Kiely, Washington, and Bernhard increased the bandwidth of a micro strip patch antenna with a parasitic element using piezoelectric actuators attached to a micro strip patch antenna and a parasitic element [43]. To obtain relatively large displacements, they use RAINBOW piezoelectric stack actuators. They are able to increase the bandwidth of the antenna with small displacement changes, since antennas operating in high frequencies are very sensitive to small displacement changes. Varadarajan, Chandrashekhara and Agarwal carried out a shape control problem of a laminated composite plate with piezoelectric actuators [44]. They use various kinds of locations to attach the piezoelectric patches. They use the Finite Element Model to solve their system. They minimize the error between the desired shape and the obtained shape by applying

an optimal voltage. They carry out their work for cases of quisistatically varying loads. Ferhat and Sultan applied LQG controller to a membrane with bimorph PZT actuators [45]. They carry a robustness study to determine the sensitivity of certain material properties and the tension being applied. Hon, Dean and Winzer developed a static nonlinear model of a mirror with multiple piezoelectric actuators [46]. They construct an array of actuators using multi layer actuators. Using a feedback control, they show that the mirror can correct the distortion of the wave front effectively. They compare their Finite Element result with their experiments. Jekins et al. developed a nonlinear model of membrane antennas and reflectors, and apply nonlinear control to obtain a high performance [47]. They emphasize that the performance of reflectors and antennas is strictly related to surface precision. Their approach to having an adaptive mirror includes a state estimation, parameter identification and feedback control.

Maji and Starnes used piezoelectric actuators to control the shape of a deployable membrane [48]. Their goal is to correct the surface shape inaccuracies due to geometric nonlinear deformations of an inflated membrane. They use piezoplymer (PVDF) actuators for active control of transverse displacement of the membrane in micron levels. Paterson, Munro and Dainty constructed a low cost adaptive optics system using a membrane mirror. They carry out the numerical modeling to determine the optimum number of actuators, modes and the diameter of the membrane [49]. Their system consists of almost entirely commercially available components which makes it low cost. Martin and Main used noncontact electron gun actuator to control a thin film bimorph mirror laminated with piezopolymers (PVDF). They show the control effect of the system theoretically and experimentally. They note that even though PVDF is chosen for the system, a piezoceramic layer would be more efficient in space environments [50]. Durr et al. carried out an extensive work on design, development and manufacturing of an adaptive lightweight mirror for space applications [51]. They use piezoelectric actuators to control the surface of the mirror. They investigate several cases using the Finite Element Model. Design, development and control of a modular adaptive mirror for large degree of freedom was carried out by Rodrigues et al. [52]. The mirror is made of silicon wafer and PZT attached to the structure. They use Finite Element Model for numerical simulations.

Another approach to suppress the vibration in membrane structure can be achieved by creating more damping. Membranes are inherently very flexible and usually have very little material damping; therefore, to create more damping in the system, one idea is to generate

external damping. One method to achieve this is via magnetic damping and it was studied by Sodano in his Ph.D. dissertation [53]. He creates magnetic damping using eddy currents. Eddy currents are generated in a conductive material that experiences a time varying magnetic field. Zhao studied the stability of flexible distributed parameter structures in his Ph.D. dissertation [54]. He applies passive control, Iterative Learning Control, and Repetitive Learning control to reduce tracking or regulation errors in response to bounded periodic inputs. He applies the developed controller to membranes structures too. Another passive control design of membrane structures was carried out by Horn and Sokolowski [55]. They use a shape memory alloy made as a wire and attached to a membrane structure to create damping by heat dissipation. They prove that with correct initial and boundary conditions, the energy of the entire system is a decreasing function. The suppression of the transverse vibration of an axially moving membrane system was carried out by Nguyen and Hong [56]. They develop a control algorithm that optimally minimizes the vibration energy of the membrane by regulating the axial transport velocity.

Renno, Kurdila and Inman developed a switching sliding mode controller for a 1-D membrane strip with two Micro Fiber Composite (MFC) bimorph actuators attached to it [57]. The sliding mode controller guarantees the system's stability robustness in the presence of uncertainties. Renno and Inman [58] applied a nonlinear controller to a membrane strip with two bimorph actuators that are effective axially and in bending to achieve shape control. Ruppel, Dong, Rooms, Osten and Sawodny developed feedforward control for a deformable membrane mirror using voice coil actuators [59]. Jha and Inman developed a sliding mode control to suppress the vibration of a gossamer structure with piezoelectric actuators and sensors [60]. They use PVDF as sensors and MFC as actuators that are both attached to an inflated membrane torus. A rigorous work of a structural design, manufacturing and analysis of mechanical properties of an inflatable antenna reflector was done by Xu and Guan [61]. They show that the accuracy of an inflatable membrane antenna reflector can be significantly improved by optimizing the design and manufacturing process that takes into account material and mechanical conditions as well as the environmental factors.

2.3 Vector Second Order Form in Control Theory and Applications

Despite the fact that many physical systems can be modeled using mathematical systems of the second order ordinary differential equations (i.e. vector second order from systems), few researchers advocated the usage of the vector second order form to develop control theories. The conventional linear, as well as nonlinear control theories were developed based on first order forms of ordinary differential equations (linear or nonlinear). In theory, systems expressed in the vector second order form can be easily converted to vector first order forms and control tools that already exist for these forms can be applied. In practice however, when the dimension of the system (e.g., the number of equations) grows, one would like to apply control design tools directly to the second order form. There are many advantages associated with the vector second order from that are mentioned in Section 1.2.

One of the earliest contributions to the area of control for linear vector second order systems was made by Hughes and Skelton [62]. They develop theories to check the controllability and observability of a vector second order system without converting the system to a vector first order form. They demonstrate that these theories are efficient and reliable. Another work on controllability and observability was carried out by Laub and Arnold. They develop methods to check stabilizability, controllability, observability and detectability using vector second order systems [63]. Their methods can be applied to damped and undamped systems. Wu and Duan developed an observer for vector second order form using the generalized eigenstructure assignment method [64].

A work on checking the stability of a system using vector second order form was carried out by Shieh, Mehio and Dib. They derive the sufficient conditions for the stability and instability for second order polynomials using the Lyapunov theory [65]. Bernstein and Bhat investigated the Lyapunov stability, semistability and asymptotic stability of second order systems [66]. Another work on the stability criteria of vector second order forms was carried out by Diwekar and Yadavalli [67]. They derive both sufficient and necessary conditions for the system under different types of loading.

Skelton and Hughes developed Modal Cost Analysis for vector second order systems in another work [68]. Skelton continued his work on vector second order systems and developed an

adaptive orthogonal filter to estimate the compensation error [69]. Sharma and George derived another necessary and sufficient condition for the controllability of the linear vector second order systems [70]. In addition, they also derive a sufficient condition for controllability of nonlinear vector second order systems.

Skelton developed a Linear Quadratic Regulator based on vector second order form [71]. He obtains a sequence of 3 independent equations by partitioning the Algebraic Riccati Equation that is typical in LQR design for the vector first order form. These equations are reduced to the Algebraic Riccati Equations under certain conditions for damped systems. He also obtains an analytical LQR controller for undamped systems with collocated actuators. Yipaer and Sultan applied vector second order form to analyze a membrane structure with piezoelectric actuators [72]. They apply the reduced Algebraic Riccati Equation to develop LQR. Ferhat and Sultan carried out the work on a membrane with bimorph PZT actuators using vector second order form and developed an LQR for undamped collocated actuator sensor case [73].

Another approach to develop an LQR using vector second order form is deriving the controller using the Hamiltonian method. Ram and Inman developed an LQR based on vector second order form using variational calculus for square input matrix [74]. This method allows them to avoid the nonlinear Algebraic Riccati Equations. Zhang extended this work for a non-square input matrix case in his work [75]. Ferhat and Sultan applied an LQR for vector second order form using the Hamiltonian method to a membrane structure with bimorph actuators [76]. They compare their results with the vector first order form LQR.

With a similar approach to LQR development partitioning the Algebraic Riccati Equation, Hashemipour and Laub developed a Kalman filter for vector second order systems [77]. They obtain the Algebraic Riccati equations for discrete and continuous systems. The solutions for these equations that were obtained using square root estimation algorithm can be found in a work done by Oshman, Inman and Laub [78]. Juang and Maghami used the vector second order form to develop a robust state estimator by eigensystem assignment [79]. They develop three design methods for state estimation and also compare them to the vector first order form results.

A stabilizing passive controller was developed by Juang and Phan using vector second order form [80]. This robust controller can also be applied as an active controller. Another active

control method to stabilize mechanical systems using vector second order form was developed by Datta and Rincon [81]. They propose two feedback control algorithms. One of them does not require the knowledge of the stiffness or damping which makes it very easy to apply. One of the most used control methodology in vector first order form is pole assignment. Chu and Datta derived this approach based on vector second order form [82]. They demonstrate the robustness of their method by examples. Chu generalized this work to a multi-input and non-symmetric case in another work [83]. Diwekar and Yadavalli applied an active control, which is developed using vector second order form, to a beam with piezoelectric actuator [84]. They emphasize the advantages of vector second order forms over vector first order forms. Duan and Liu worked on eigenstructure assignment for linear vector second order form systems [85]. Duan extended the eigenstructure assignment work in another work [86]. Whang and Duan developed a robust algorithm for pole assignment using vector second order form [87]. They use the derivation of Duan`s previous works [85, 86] as the basis for the pole assignment and develop a robust algorithm.

2.4 Chapter Summary

It is quite clear that there have been a dramatic increase in application of membrane structures in aerospace technology. Invention of smart materials contributed tremendously to this advent as well as the increasing computational capacity as seen in Section 2.2. This advancement comes with an issue of high dimensional systems that has been remedied mostly with modal order reduction techniques. However, this requires us to compromise on accuracy.

In Section 2.3 the works on control development using vector second order form are summarized. This is an alternative and complementary approach to the vector first order form. However, the works in this area are very few and need to be improved to become a more common control method.

Chapter 3

MODELING OF A MEMBRANE-ACTUATOR SYSTEM

3.1 Introduction

Modeling of physical systems is always an approximation of the real systems. Even though we tend to think the closest model to the real physical system is the best model, modeling is actually an optimization process that depends on what we would like to obtain from a model. Therefore, modeling needs to be approached as an objective oriented and iterative process. For example, when we examine the motions of an airplane between two points, the optimal approach would be assuming the plane as a point mass with 3 degree of freedom. However, when we are trying to measure the performance of the airplane, we need to consider the geometric characteristics and take into account the 6 degree of freedom as the system is a rigid body. Also, when we are studying the aeroelastic characteristics of a wing, the rigid body assumption is no longer valid. We must model the wing of the plane as flexible distributed structures. Therefore, we can summarize the modeling process as follows: when we model a physical system, first we define the parameters that we would like to obtain from a model, and then we decide on what kind of model would be suitable for us to obtain the parameters that we are analyzing. Lastly, we have to decide on the convergence of the numerical results that needs to be achieved for our purpose.

The logical flow of the modeling process is exemplified in relation to the work presented herein. In this dissertation, the goal is to control the vibration of membrane structures used in aerospace applications. The vibration phenomena is observed as the displacement of the membrane. Therefore, the parameters that need to be obtained from the model are amplitude and frequency of the vibration. To obtain these characteristics, the system is modeled as a distributed parameter system. The next step is to determine the sensitivity, that is desired to be obtained

from the numerical calculation, to obtain optimal convergence of desired parameters. Since the system is a dynamic system, it is more suitable to use dynamic parameters as well as static parameters to determine the optimal convergence rate. The optimal convergence rate will be determined according to the structural accuracy and the control feasibility. This step needs to be iterative considering the interaction between structural analysis and control design/application.

The fundamental theories that are used to model two dimensional distributed parameter systems and the mathematical modeling process for a membrane structure with piezoelectric bimorph actuators are described and studied in Section 3.2. In Subsections 3.2.1 and 3.2.2, the membrane and plate theories are explained in detail with advantages and shortcomings for this system, emphasizing why a leaf-like structure needs to be modeled as a plate even though it is perceived and referred to as a "membrane". This need is further demonstrated with the addition of piezoelectric actuators to the system in Subsection 3.2.3. The next step in modeling is computational modeling which is derived in Section 3.3. Subsection 3.3.1 derives the weak form Finite Element Modeling of the membrane system. The determination of the convergence rate for the static and dynamic parameters is carried out in Subsection 3.3.2. The chapter is summarized in Section 3.4.

3.2 Mathematical Modeling

Since the accuracy of a mathematical model strongly depends on the modeling assumptions, it is very important to make correct assumptions when we start modeling a physical system. When a structure has its two dimensions relatively larger than its third dimension, it is considered a two dimensional structure. Most common two dimensional structures used in aerospace applications are plates, shells and membranes. Two dimensional structures that are flat when there is no load applied are called plates; if the structures are curved under no load, they are called shells. Plates are identified as membranes when the thickness is very small. In this case, the bending resistance is assumed to be negligible. More refined classifications of plates and membranes are defined based on the ratio between the thickness and the length. According to this definition, for a plate seen in Fig 3.1, where h represent thickness, and l represents length, when $l/h \le 8$, the plate is identified as thick plate. Thin plates have the length to thickness ratio as $8 \le l/h \le 80$. If the two dimensional structure has ratio of $l/h \ge 80$, it is

classified as a membrane [88]. It should be noted that this is not a discrete classification. There is a gray area around the limits of the ratios. Same structure can be approached with two different identifications if the length to thickness ratio is closer to its limits. The decision can be made based on the design objective or convergence criteria.

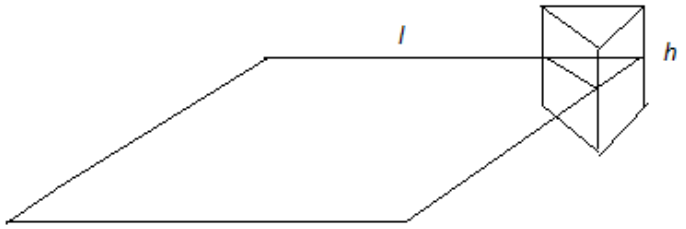

Figure 3.1: Plate classification according to length to thickness ratio.

The membrane structure that is being modeled in this work is a square membrane with bimorph actuators attached to it. Since the thickness is very small in the membrane material, it is inherently considered a two dimensional distributed system. Conventionally, the ratio of the thickness to the length classifies the system as membranes and neglects the bending properties. However, it is observed that certain materials still have non-negligible bending characteristics even when they are very thin. Also having a tension load makes membranes behave like thin plates for certain materials. In this case, this property actually allows us the use of bending characteristics of the piezoelectric actuators to control the membrane-bimorph actuator system. The two theories that are used for modeling a two dimensional thin structure are the membrane and thin plate theories. The fundamentals basics, advantages and shortcomings of these theories, and the effect of the bimorph actuators in modeling are further studied in the following subsections.

3.2.1 Membrane Theory

The first mathematical membrane theory was developed by L. Euler (1707-1783) in 1766 [89]. He assumed that membranes are systems of stretched strings perpendicular to each other. He studied the vibration of various shapes of membranes and derived some analytical results. Neither strings nor membranes carry bending loads and their mechanical behavior is to some extent similar. For example we can assume that membranes are 2-dimensional form of strings.

The basic assumptions for the linear isotropic membrane structures can be summarized as follows:

- The material is homogenous, isotropic and elastic, obeying Hooke's law.
- The membrane is flat initially.
- The mid surface of the membrane remains unstrained during deformation.
- Displacements are very small compared to the thickness of the membrane which also allows us to ignore wrinkling.
- There is no flexural rigidity (no resistance to bending).
- Normal strains and stresses are negligible.

Under these assumptions, the equation of motion for a membrane under uniform tension is derived in Cartesian coordinates using the geometrical characteristics of the membrane seen in Figs. 3.2-3.4:

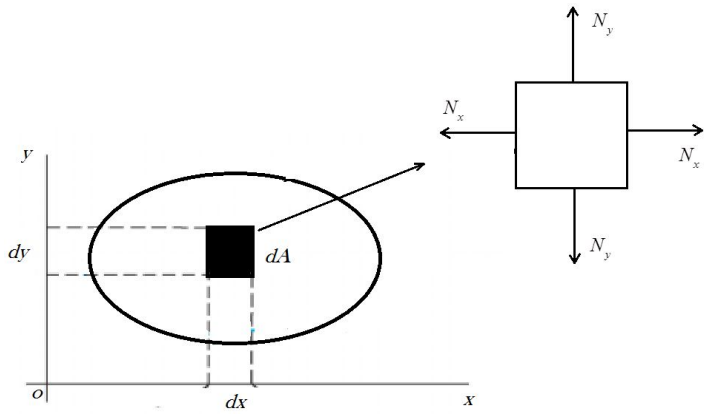

Figure 3.2: Membrane structure under tension in Cartesian coordinates

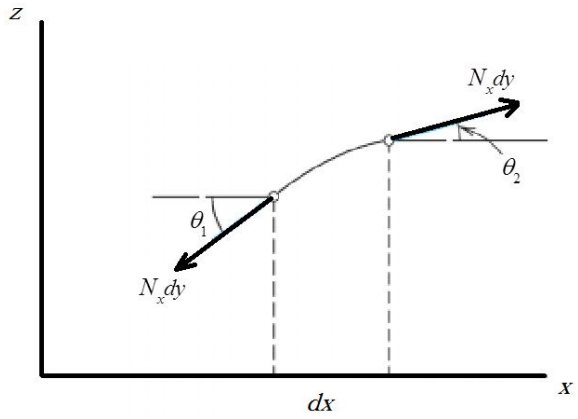

Figure 3.3: *x-z* profile of the membrane structure

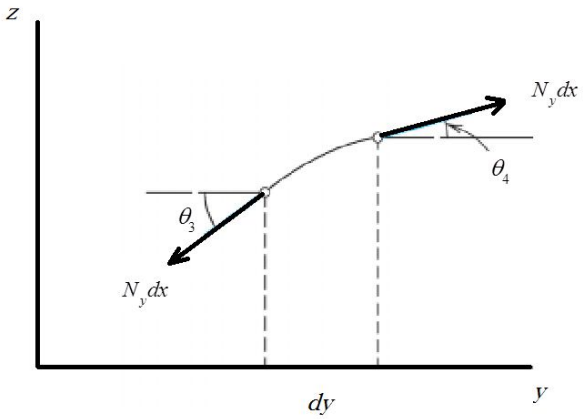

Figure 3.4: *y-z* profile of the membrane structure

As it has been demonstrated in Figs. 3.2-3.4, N_x and N_y are the prestesses in terms of force per meter in the *x* and *y* directions, respectively, *dx* and *dy* are the infinitely small lengths of the membrane piece. θ_1, θ_2, θ_3 and θ_4 are the angles of the curvature. The total force in the *z* direction created by $N_x dy$ is:

$$N_x dy \sin\theta_2 - N_x dy \sin\theta_1 \tag{3.2.1}$$

The total force in the z direction created by $N_y dx$ is:

$$N_y dx \sin\theta_4 - N_y dx \sin\theta_3 \tag{3.2.2}$$

By Newton's second law the sum of the forces in the *z* direction is equal to acceleration of the mass in the *z* direction, and mathematically expressed such that:

$$\rho dxdy\frac{\partial^2 w}{\partial t^2} = N_x dy\sin\theta_2 - N_x dy\sin\theta_1 + N_y dx\sin\theta_4 - N_y dx\sin\theta_3 \tag{3.2.3}$$

Since the curvature angles are assumed to be very small, the following assumptions can be made:

$$\sin\theta_1 \cong \theta_1 = \frac{\partial w}{\partial x} \tag{3.2.4}$$

$$\sin\theta_2 \cong \theta_2 = \frac{\partial w}{\partial x} + \frac{\partial}{\partial x}\left(\frac{\partial w}{\partial x}\right)dx \tag{3.2.5}$$

$$\sin\theta_3 \cong \theta_3 = \frac{\partial w}{\partial y} \tag{3.2.6}$$

$$\sin\theta_4 \cong \theta_4 = \frac{\partial w}{\partial y} + \frac{\partial}{\partial y}\left(\frac{\partial w}{\partial y}\right)dy \tag{3.2.7}$$

Rewriting Equ. (3.2.3), the equation of motion for a tensioned membrane under free vibration is obtained as follows:

$$\rho\frac{\partial^2 w}{\partial t^2} = N_x\frac{\partial^2 w}{\partial x^2} + N_y\frac{\partial^2 w}{\partial y^2} \tag{3.2.8}$$

For $N_x = N_y$, the two dimensional wave equation that shows the wave speed of the membrane as a parameter *c* can be obtained as:

$$\frac{1}{c^2}\frac{\partial^2 w}{\partial t^2} = \nabla^2 w \tag{3.2.9}$$

$$c = \sqrt{\frac{N}{\rho}} \tag{3.2.10}$$

Here, ∇ is the Laplace operator. Analyzing the term for wave speed, it can be concluded that if a membrane is under high stress, it vibrates with higher frequency. Same way, lighter materials will vibrate faster as it is expected physically.

3.2.2 Thin Plate Theory

Mathematical development of the plate theory comes just after the development of the membrane theory by Euler. Jacques Bernoulli (1759-1789), student of Euler, extended his membrane theory to a plate theory replacing the strings with beams [89]. Based on this derivation, plates can be considered as 2-dimensional beams. This approach allows the 2-dimensional structure to have bending stiffness. In addition to the contributions to the general plate theory by other scientists, Gustav R. Kirchhoff (1824-1887) fully developed the thin plate theory. The thin plate theory is also named Bernoulli Kirchhoff Plate Theory or just Kirchhoff plate theory [90]. The general assumptions of the Kirchhoff plate theory are [91]:

- The material is homogenous, isotropic and elastic, obeying Hooke's law.
- The plate is flat initially.
- The mid surface of the plate remains unstrained during deformation.
- Displacements are very small compared to the thickness of the plate.
- Normal stresses in the transverse direction are negligible.

The general approach in deriving the equation of motion for thin plates is assuming that the inplane loads have no effect on the vibration of the plates. However, in this case it is strictly required to take into account the inplane loads while deriving the equation of motion for the plate. For very thin plates, the tension creates transverse vibration just like in the membranes. The Figs. 3.5-3.7 show the loads that a plate element carries and the deformation of a plate under these loads [92].

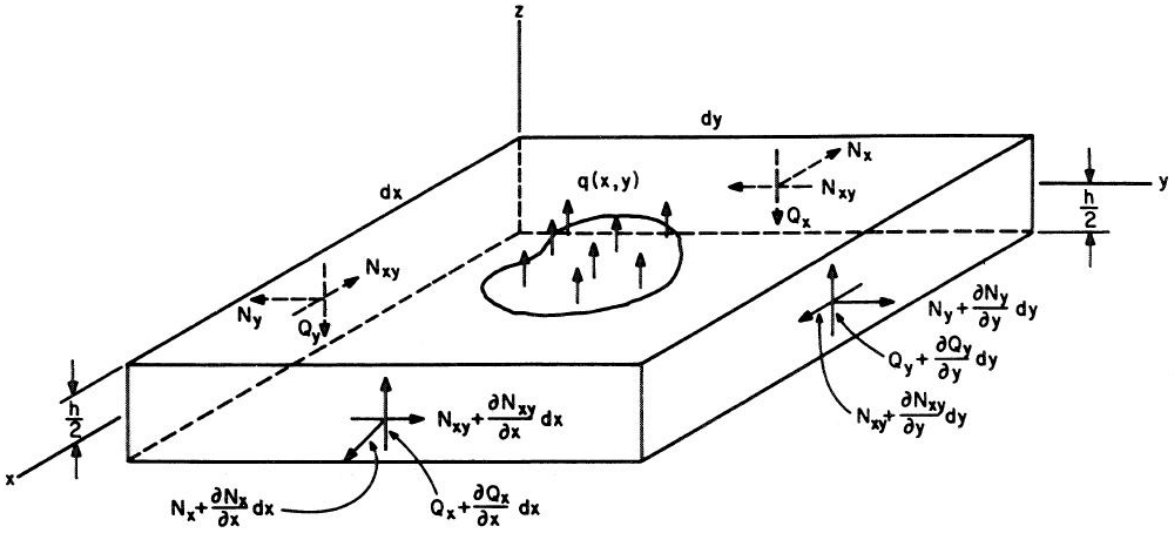

Figure 3.5: Forces acting on a plate element. (Used under fair use, Ref. [92])

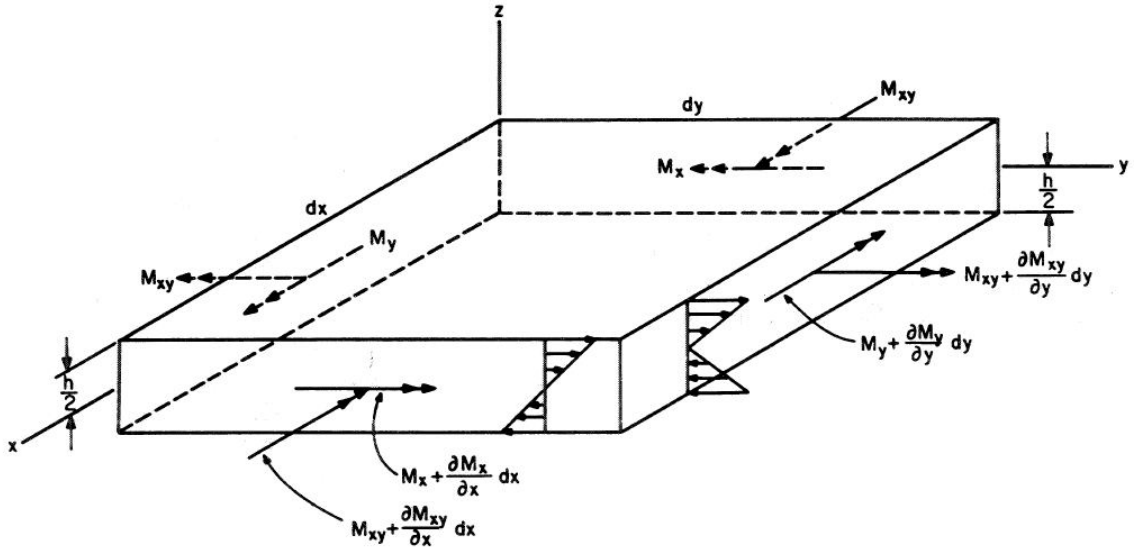

Figure 3.6: Moments acting on a plate element. (Used under fair use, Ref. [92])

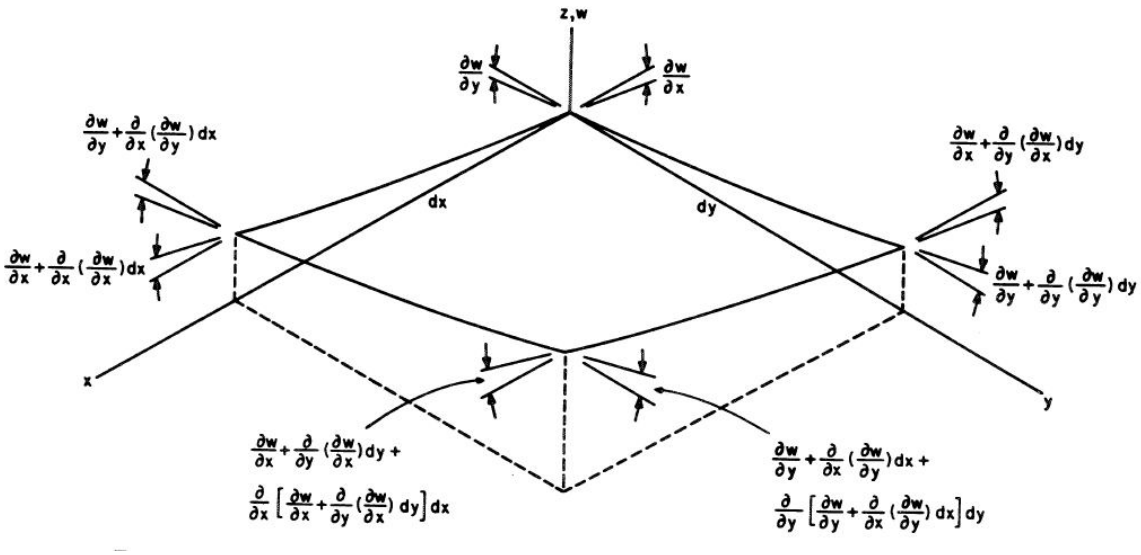

Figure 3.7: Deformed plate element. (Used under fair use, Ref. [92])

The equation of motion for a plate element based on Figs. 3.5-3.7 is derived in reference [92]. The plate is parallel to the $x-y$ plane and all its edges are clamped. Here *x* and *y* denote two orthogonal directions in the plane of the plate, ρ is material's density, *w* is the transverse displacement and *h* is the thickness of the plate. *E* is Young's Modulus, υ is Poisson's ratio of the membrane, and *f* is the externally applied force. The total force in the *z* direction created by transverse shearing forces Q_x and Q_y are:

$$Q_x + \frac{\partial Q_X}{\partial x} dx - Q_x + Q_y + \frac{\partial Q_y}{\partial y} dy - Q_y \tag{3.2.11}$$

The total force in the *z* direction created by inplane shearing forces N_x, N_y, and N_{xy} are:

$$
\begin{aligned}
&\left(N_x+\frac{\partial N_x}{\partial x}dx\right)\left(\frac{\partial w}{\partial x}+\frac{\partial^2 w}{\partial x^2}dx\right)dy-N_x\frac{\partial w}{\partial x}dy\\
&+\left(N_y+\frac{\partial N_y}{\partial y}dy\right)\left(\frac{\partial w}{\partial y}+\frac{\partial^2 w}{\partial y^2}dy\right)dx-N_y\frac{\partial w}{\partial y}dx\\
&+\left(N_{xy}+\frac{\partial N_{xy}}{\partial y}dy\right)\left(\frac{\partial w}{\partial x}+\frac{\partial^2 w}{\partial x\partial y}dy\right)dx-N_{xy}\frac{\partial w}{\partial x}dx\\
&+\left(N_{xy}+\frac{\partial N_{xy}}{\partial x}dx\right)\left(\frac{\partial w}{\partial y}+\frac{\partial^2 w}{\partial x\partial y}dx\right)dy-N_{xy}\frac{\partial w}{\partial y}dy
\end{aligned}
\tag{3.2.12}
$$

Using Newton's second law, the total force in the *z* direction can be equated to acceleration of the mass in the *z* direction as:

$$
\begin{aligned}
&Q_x+\frac{\partial Q_x}{\partial x}dx-Q_x+Q_y+\frac{\partial Q_y}{\partial y}dy-Q_y\\
&+\left(N_x+\frac{\partial N_x}{\partial x}dx\right)\left(\frac{\partial w}{\partial x}+\frac{\partial^2 w}{\partial x^2}dx\right)dy-N_x\frac{\partial w}{\partial x}dy\\
&+\left(N_y+\frac{\partial N_y}{\partial y}dy\right)\left(\frac{\partial w}{\partial y}+\frac{\partial^2 w}{\partial y^2}dy\right)dx-N_y\frac{\partial w}{\partial y}dx\\
&+\left(N_{xy}+\frac{\partial N_{xy}}{\partial y}dy\right)\left(\frac{\partial w}{\partial x}+\frac{\partial^2 w}{\partial x\partial y}dy\right)dx-N_{xy}\frac{\partial w}{\partial x}dx\\
&+\left(N_{xy}+\frac{\partial N_{xy}}{\partial x}dx\right)\left(\frac{\partial w}{\partial y}+\frac{\partial^2 w}{\partial x\partial y}dx\right)dy-N_{xy}\frac{\partial w}{\partial y}dy\\
&+f=\rho h\frac{\partial^2 w}{\partial t^2}
\end{aligned}
\tag{3.2.13}
$$

Assuming small curvature, the high order derivative terms are neglected; and rewriting Equ. (3.2.13) in a more simple form, the expression is obtained such that:

$$
\frac{\partial Q_x}{\partial x}+\frac{\partial Q_y}{\partial y}+N_x\frac{\partial^2 w}{\partial x^2}+N_y\frac{\partial^2 w}{\partial y^2}+2N_{xy}\frac{\partial^2 w}{\partial x\partial y}+f=\rho h\frac{\partial^2 w}{\partial t^2}
\tag{3.2.14}
$$

To derive strain-displacement relations, the longitudinal displacements in *x* and *y* directions are defined as *u* and *v* respectively such that:

$$u = u_0 - z\frac{\partial w}{\partial x} \tag{3.2.15a}$$

$$v = v_0 - z\frac{\partial w}{\partial y} \tag{3.2.15b}$$

Here u_0 and v_0 represents the initial displacement in the *x* and *y* directions respectively. Direct and shear strains ε_x, ε_y and γ_{xy} are formulated in terms of displacements for two dimensional plate elements as:

$$\varepsilon_x = \frac{\partial u}{\partial x} \tag{3.2.16a}$$

$$\varepsilon_y = \frac{\partial v}{\partial y} \tag{3.2.16b}$$

$$\gamma_{xy} = \frac{\partial u}{\partial x} + \frac{\partial v}{\partial y} \tag{3.2.16c}$$

Substituting Equ. (3.2.15a) and Equ. (3.2.15b) into Equ. (3.2.16a–3.2.16c), the strain displacement relations in terms of displacement in the z direction is derived as:

$$\varepsilon_x = \frac{\partial u_0}{\partial x} - z\frac{\partial^2 w}{\partial x^2} \tag{3.2.17a}$$

$$\varepsilon_y = \frac{\partial u_0}{\partial y} - z\frac{\partial^2 w}{\partial y^2} \tag{3.2.17b}$$

$$\gamma_{xy} = \left(\frac{\partial u_0}{\partial x} + \frac{\partial v_0}{\partial y}\right) - 2z\frac{\partial^2 w}{\partial x \partial y} \tag{3.2.17c}$$

Strains can be defined in terms of stresses for two dimensional plate structures for orthotropic and isotropic materials as:

$$\varepsilon_x = \frac{1}{E}\left(\sigma_x - \upsilon\sigma_y\right) \tag{3.2.18a}$$

$$\varepsilon_y = \frac{1}{E}\left(\sigma_y - \upsilon\sigma_x\right) \tag{3.2.18b}$$

$$\gamma_{xy} = \frac{2(1+\upsilon)}{E}\tau_{xy} \tag{3.2.18c}$$

Here, σ_x and σ_y represents the direct stresses in the *x* and *y* direction respectively and τ_{xy} represents the shear stress. Similarly, Equ. (3.2.18a-3.2.18c) can be restructured to write the stresses in terms of strains and displacement in the z direction in the form of:

$$\sigma_x = \frac{E}{1-\nu^2}\left(\varepsilon_x + \upsilon\varepsilon_y\right) \tag{3.2.19a}$$

$$\sigma_y = \frac{E}{1-\nu^2}\left(\varepsilon_y + \upsilon\varepsilon_x\right) \tag{3.2.19b}$$

$$\tau_{xy} = \frac{E}{2(1+\upsilon)}\gamma_{xy} \tag{3.2.19c}$$

To derive the equation of motion for a plate in terms of displacement in the transverse direction, the forces and moments need to be expressed in terms of the transverse displacement. The expressions of these terms are described as:

$$N_x = \int_{-h/2}^{h/2} \sigma_x dz \tag{3.2.20a}$$

$$N_y = \int_{-h/2}^{h/2} \sigma_y dz \tag{3.2.20b}$$

$$N_{xy} = \int_{-h/2}^{h/2} \tau_{xy} dz \tag{3.2.20c}$$

$$M_x = \int_{-h/2}^{h/2} \sigma_x z dz \tag{3.2.21a}$$

$$M_y = \int_{-h/2}^{h/2} \sigma_y z dz \tag{3.2.21b}$$

$$M_{xy} = \int_{-h/2}^{h/2} \tau_{xy} z dz \tag{3.2.21c}$$

Substituting the stress terms obtained in terms of transverse displacement and carrying out the integration through the thickness, the following force expressions in terms of transverse displacement are obtained as:

$$\begin{aligned} N_x &= \int_{-h/2}^{h/2} \frac{E}{1-\upsilon^2}\left(\left(\frac{\partial u_0}{\partial x} + \upsilon\frac{\partial v_0}{\partial y}\right) - z\left(\frac{\partial^2 w}{\partial x^2} + \upsilon\frac{\partial^2 w}{\partial y^2}\right)\right) dz \\ &= \frac{E}{1-\upsilon^2}\left[\left(\frac{\partial u_0}{\partial x} + \upsilon\frac{\partial v_0}{\partial y}\right) z\Big|_{-h/2}^{hl2} - \frac{1}{2}\left(\frac{\partial^2 w}{\partial x^2} + \upsilon\frac{\partial^2 w}{\partial y^2}\right) z^2\Big|_{-h/2}^{h/2}\right] \\ &= \frac{E}{1-\upsilon^2}\left(\frac{\partial u_0}{\partial x} + \upsilon\frac{\partial v_0}{\partial y}\right) h \end{aligned} \tag{3.2.22}$$

$$\begin{aligned} N_y &= \int_{-h/2}^{h/2} \frac{E}{1-\upsilon^2}\left(\left(\frac{\partial v_0}{\partial y} + \upsilon\frac{\partial u_0}{\partial x}\right) - z\left(\frac{\partial^2 w}{\partial y^2} + \upsilon\frac{\partial^2 w}{\partial x^2}\right)\right) dz \\ &= \frac{E}{1-\upsilon^2}\left[\left(\frac{\partial v_0}{\partial y} + \upsilon\frac{\partial u_0}{\partial x}\right) z\Big|_{-h/2}^{h/2} - \frac{1}{2}\left(\frac{\partial^2 w}{\partial y^2} + \upsilon\frac{\partial^2 w}{\partial x^2}\right) z^2\Big|_{-h/2}^{h/2}\right] \\ &= \frac{E}{1-\upsilon^2}\left(\frac{\partial v_0}{\partial y} + \upsilon\frac{\partial u_0}{\partial x}\right) h \end{aligned} \tag{3.2.23}$$

$$
\begin{aligned}
N_{xy} &= \int_{-h/2}^{h/2} \frac{E}{2(1+\upsilon)}\left(\left(\frac{\partial u_0}{\partial x}+\frac{\partial v_0}{\partial y}\right)-2z\left(\frac{\partial^2 w}{\partial x \partial y}\right)\right)dz \\
&= \frac{E}{2(1+\upsilon)}\left[\left(\frac{\partial u_0}{\partial x}+\frac{\partial v_0}{\partial y}\right)z\Big|_{-h/2}^{h/2}-\left(\frac{\partial^2 w}{\partial x \partial y}\right)z^2\Big|_{-h/2}^{h/2}\right] \\
&= \frac{E}{2(1+\upsilon)}\left(\frac{\partial u_0}{\partial x}+\frac{\partial v_0}{\partial y}\right)h
\end{aligned}
\tag{3.2.24}
$$

Similar to force derivations, substituting the stress terms obtained in terms of transverse displacement and carrying out the integration through the thickness, the following moment expressions in terms of transverse displacement are obtained as:

$$
\begin{aligned}
M_x &= \int_{-h/2}^{h/2} \frac{E}{1-\upsilon^2}\left(\left(\frac{\partial u_0}{\partial x}+\upsilon\frac{\partial v_0}{\partial y}\right)-z\left(\frac{\partial^2 w}{\partial x^2}+\upsilon\frac{\partial^2 w}{\partial y^2}\right)\right)zdz \\
&= \frac{E}{1-\upsilon^2}\left[\frac{1}{2}\left(\frac{\partial u_0}{\partial x}+\upsilon\frac{\partial v_0}{\partial y}\right)z^2\Big|_{-h/2}^{h/2}-\frac{1}{3}\left(\frac{\partial^2 w}{\partial x^2}+\upsilon\frac{\partial^2 w}{\partial y^2}\right)z^3\Big|_{-h/2}^{h/2}\right] \\
&= -\frac{Eh^3}{12(1-\upsilon^2)}\left(\frac{\partial^2 w}{\partial x^2}+\upsilon\frac{\partial^2 w}{\partial y^2}\right)
\end{aligned}
\tag{3.2.25}
$$

$$
\begin{aligned}
M_y &= \int_{-h/2}^{h/2} \frac{E}{1-\upsilon^2}\left(\left(\frac{\partial v_0}{\partial y}+\upsilon\frac{\partial u_0}{\partial x}\right)-z\left(\frac{\partial^2 w}{\partial y^2}+\upsilon\frac{\partial^2 w}{\partial x^2}\right)\right)zdz \\
&= \frac{E}{1-\upsilon^2}\left[\frac{1}{2}\left(\frac{\partial v_0}{\partial y}+\upsilon\frac{\partial u_0}{\partial x}\right)z^2\Big|_{-h/2}^{h/2}-\frac{1}{3}\left(\frac{\partial^2 w}{\partial y^2}+\upsilon\frac{\partial^2 w}{\partial x^2}\right)z^3\Big|_{-h/2}^{h/2}\right] \\
&= -\frac{Eh^3}{12(1-\upsilon^2)}\left(\frac{\partial^2 w}{\partial y^2}+\upsilon\frac{\partial^2 w}{\partial x^2}\right)h
\end{aligned}
\tag{3.2.26}
$$

$$
\begin{aligned}
M_{xy} &= \int_{-h/2}^{h/2} \frac{E}{2(1+\upsilon)}\left(\left(\frac{\partial u_0}{\partial x}+\frac{\partial v_0}{\partial y}\right)-2z\left(\frac{\partial^2 w}{\partial x \partial y}\right)\right)zdz \\
&= \frac{E}{2(1+\upsilon)}\left[\frac{1}{2}\left(\frac{\partial u_0}{\partial x}+\frac{\partial v_0}{\partial y}\right)z^2\Big|_{-h/2}^{h/2}-\frac{2}{3}\left(\frac{\partial^2 w}{\partial x \partial y}\right)z^3\Big|_{-h/2}^{h/2}\right] \\
&= -\frac{Eh^3}{24(1+\upsilon)}\left(\frac{\partial^2 w}{\partial x \partial y}\right)
\end{aligned}
\tag{3.2.27}
$$

The equilibrium between moments and forces can be evaluated as below:

$$
Q_x = \frac{\partial M_x}{\partial x}+\frac{\partial M_{xy}}{\partial y} \tag{3.2.28}
$$

$$
Q_y = \frac{\partial M_y}{\partial y}+\frac{\partial M_{xy}}{\partial x} \tag{3.2.29}
$$

Substituting all terms, that are defined in terms of displacement, into the Equ. (3.2.14) and assuming that the shear forces can be neglected, the simple equation of motion for vibrating plates is derived as:

$$
\begin{aligned}
&\rho h\frac{\partial^2 w}{\partial t^2}+D\left(\frac{\partial}{\partial x^2}\left(\frac{\partial^2 w}{\partial x^2}+\upsilon\frac{\partial^2 w}{\partial y^2}\right)\right)+D\left(\frac{\partial^2}{\partial y^2}\left(\frac{\partial^2 w}{\partial y^2}+\upsilon\frac{\partial^2 w}{\partial x^2}\right)\right) \\
&+2G\frac{\partial^2}{\partial x \partial y}\left(\frac{\partial^2 w}{\partial x \partial y}\right)+2G\frac{\partial^2}{\partial y \partial x}\left(\frac{\partial^2 w}{\partial y \partial x}\right)+\left(N_x\right)\frac{\partial^2 w}{\partial x^2}+\left(N_y\right)\frac{\partial^2 w}{\partial y^2}= f
\end{aligned}
\tag{3.2.30}
$$

$$
D = \frac{Eh^3}{12\left(1-\upsilon^2\right)},\quad G = \frac{Eh^3}{24(1+\upsilon)} \tag{3.2.31}
$$

Here, *D* is the flexural stiffness of the plate, *G* is the shear stiffness of the plate. For damping, Kelvin-Voigt damping model is assumed; because, it has physical meaning. After adding the necessary terms for damping, the complete equation of motion for a vibrating plate under inplane loads is:

$$\begin{aligned}
&\rho h\frac{\partial^2 w}{\partial t^2}+D\left(\frac{\partial}{\partial x^2}\left(\frac{\partial^2 w}{\partial x^2}+\upsilon\frac{\partial^2 w}{\partial y^2}\right)\right)+D\left(\frac{\partial^2}{\partial y^2}\left(\frac{\partial^2 w}{\partial y^2}+\upsilon\frac{\partial^2 w}{\partial x^2}\right)\right)\\
&+2G\frac{\partial^2}{\partial x\partial y}\left(\frac{\partial^2 w}{\partial x\partial y}\right)+2G\frac{\partial^2}{\partial y\partial x}\left(\frac{\partial^2 w}{\partial y\partial x}\right)+D_\delta\left(\frac{\partial^2}{\partial x^2}\left(\frac{\partial^2}{\partial x^2}\left(\frac{\partial w}{\partial t}\right)+\upsilon\frac{\partial^2}{\partial y^2}\left(\frac{\partial w}{\partial t}\right)\right)\right)\\
&+D_\delta\left(\frac{\partial^2}{\partial y^2}\left(\frac{\partial^2}{\partial y^2}\left(\frac{\partial w}{\partial t}\right)+\upsilon\frac{\partial^2}{\partial x^2}\left(\frac{\partial w}{\partial t}\right)\right)\right)+2G_\delta\frac{\partial^2}{\partial x\partial y}\left(\frac{\partial^2}{\partial x\partial y}\left(\frac{\partial w}{\partial t}\right)\right)\\
&+2G_\delta\frac{\partial^2}{\partial y\partial x}\left(\frac{\partial^2}{\partial y\partial x}\left(\frac{\partial w}{\partial t}\right)\right)+\left(N_x\right)\frac{\partial^2 w}{\partial x^2}+\left(N_y\right)\frac{\partial^2 w}{\partial y^2}=f
\end{aligned} \tag{3.2.32}$$

$$D_\delta=\frac{\delta h^3}{12\left(1-\upsilon^2\right)},\quad G_\delta=\frac{\delta h^3}{24\left(1+\upsilon\right)} \tag{3.2.33}$$

$$w(x,y,0)=w_0 \qquad \frac{\partial w}{\partial t}w(x,y,0)=0 \tag{3.2.34}$$

$$w(x,y,t)=\frac{\partial w(x,y,t)}{\partial n}=0 \qquad on \qquad \partial\Omega \tag{3.2.35}$$

Here, D_δ and G_δ represent Kelvin-Voigt damping terms, δ is the Kelvin-Voigt damping coefficient. Ω is the domain of the plate, $\partial\Omega$ is the boundary of the plate and Equ. (3.2.34) and Equ. (3.2.35) describe the initial and boundary conditions. ∂n represents the derivative in the normal direction.

3.2.3 Membranes with Piezoelectric Actuators

One of the biggest difficulties of controlling distributed structures is trying to control flexible sheet-like structures that are quite different than rigid bodies. Discovery of piezoelectric materials and its application as actuators are the most important development in technology that allows us to actively control distributed structures using distributed actuators. Especially in aerospace applications, usage of distributed actuators provide lighter and deployable designs. These are very crucial criteria from performance, endurance, and financial aspects. Smart materials and their integration to distributed structures are studied in the following subsections.

3.2.3.1 Smart Materials and Structures

The discovery of smart materials is one of the advent developments in aerospace technology. Smart materials can also be named as multifunctional materials. When an external electrical or thermal effect is applied, they have the capacity to change their structural characteristics, such as stiffness, damping and viscosity, as well as morphing their shape [93]. Smart structures are passively or actively controlled with smart materials. The main components of a smart structure are sensors and actuators made of smarts materials [94]. The inspiration for smart structures comes from the nature, as the motion of living beings depend on the shape change of muscles and tendons without an external device. This allows a smart structure to be aerodynamically feasible and very light. These features are the most crucial characteristics that define the effectiveness of aerospace applications. As a result, the one area that is constantly trying to improve the understanding of smart materials and increase the usage of them is the aerospace industry.

Smart materials were first discovered by Pierre and Jacques Curie in the 1880s [94, 95]. They observed and hypnotized that some crystals such as quartz and tourmaline show very unusual relation between mechanical strain and electric field around the material. When these materials are under mechanical strain, they generate an electric field around them. This characteristics of the material is named as piezoelectricity from Greek root *piezo* that means pressure. More precisely, this effect is named direct piezoelectric effect. Several years later from the first discovery of direct piezoelectric effect, Curie brothers discovered that the same materials show mechanical strain if an external electric field is applied. This phenomena is named converse piezoelectric effect (or inverse piezoelectric effect).

The piezoelectric effect of crystals remained mostly as a pure academic interest until mid-20th century. The biggest reason was the amount of electricity needed to obtain considerable strain for technological applications. Another difficulty postponed the development and applications of smart materials was the technological state of the instruments used to measure the electric and the strain outputs. With existing technology, it was not possible to have precise measurement. The first application of smart materials was carried out during World War I. Paul Langevin and his co-workers used quartz crystals to develop a detector for submarines [96]. After this, piezoelectric materials started being used in more areas in electronics such as

oscillators and filters. However, the interest in smart materials increased during World War II with the invention of synthetic piezoelectric materials. These materials are not piezoelectric in nature; however, they can be altered with poling. They have much higher piezoelectric capacity and can be produced in bulk and different shapes. This advancement in material science increased the motivation to study smart materials in various areas.

Historically, the first conceptualization of smart materials is carried out by Clauser in 1968 [95]. However, the development and application of smart materials became very popular starting the 1990s. Today most commonly used piezoelectric materials are lead zirconate titanate (PZT) for actuators and polyvinylidene fluoride (PVDF) for sensors. Most of the improvement in smart structures are carried out by aerospace industry in areas such as shape control and vibration suppression of large flexible structures. Even though smart structures still need a lot of improvement to be considered as an alternative to conventional control design, nowadays smart structures are used in wide range of areas such as biomedical, civil engineering, electronics, automotive, robotics, naval architecture and energy harvesting. The fundamental classification of control of structures and the placement of smart structures in this classification can be outlined as in Fig. 3.8. [95].

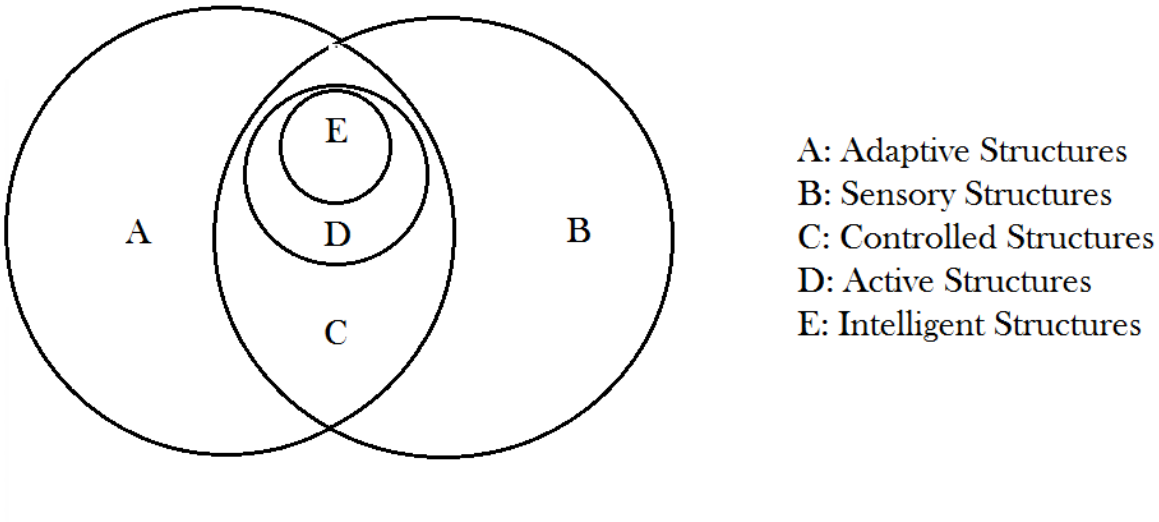

Figure 3.8: Classification of smart structures. (Used under fair use, Ref. [95])

Adaptive structures are conventionally controlled structures with an external input. They have distributed actuators, they do not need to have sensors. Flaps and ailerons are good

examples of this. Sensory structures measure the desired parameters of the structures with distributed sensors. These parameters can be strain, temperature, electric field etc. Controlled structures are both adaptive and sensory structures. They have actuators, sensors and a processor for a feedback control. Active structures are controlled structures with embedded actuators and sensors that have structural function such as load carrying. Smart structures are active structures with a programmed and integrated control logic and processors.

Smart materials belong to one of four class of materials. They are metals and alloys, polymers, ceramics and composites. Piezoelectric materials are the first types of smart materials discovered; however, today we have many different kinds of smart materials, that are being produced and widely used in various areas, in addition to piezoelectric materials. The more widely used ones are Shape Memory Alloys (SMAs), electrostrictives, magnetostrictives, electrorheological (ER) fluids, and magnetorheological (MR) fluids.

Shape memory alloys are thermomechanical materials that change their shape under heat [95]. SMAs have the capability to remember their shape after being deformed. When it is cool or under certain temperature, it stays deformed. When the temperature rises to a certain level, it recovers to the predeformed shape. The first discovery of SMAs was in 1932. Arne Olander observed this effect in a gold-cadmium alloy [93]. After that, some other SMA materials were discovered. However, the first commercially developed SMA was discovered in 1965; Nitinol (nickel-titanium alloy) was developed by Buehler and Wiley.

Electrostrictives are materials that undergo deformation under an applied electric field [94]. This effect exists in almost all materials; however, it is very small and negligible in most materials. The electro-mechanical coupling is quadratic unlike piezoelectric effect which is linear. The most common piezorestrictive material is lead magnesium niobate with lead titanate (PMN-PT).

Magnetorstrictives are ferromagnetic materials that induce strain when a magnetic field is applied or vice versa [93]. The first discovery of magnetostrictives was made by James Joule in 1942 observing the behavior of iron under magnetic effect [94]. Iron (Fe), nickel (Ni) and cobalt (Co) are early magnetostrictives with very low capacity. Terfenol-D and Galfenol are discovered later on and have much higher magnetostrictive capacity.

Electrorheological fluids can be described as colloidal consistent fluid that changes its viscosity under electric field [93]. It was first discovered in the 1940s [94]. They can turn into solids in a very short time forming a strong columns under electrical forces. The viscosity of colloidal fluids or the structure of the solid that is being formed depend on the magnitude of the electric field being applied. Similarly, magnetorheological fluids are described as fluid undergoing viscosity changes when a magnetic field is applied. Discovery of MR fluids were at the same times as ER fluids; however, the focus was more on ER fluids due to their availability.

3.2.3.2 Piezoelectric Actuators

Among many types of smart materials, piezoelectric materials are one of the most widely used smart materials for actuators due its feasibility as actuators. Especially, suppression of the vibration of structures are managed with distributed piezoelectric actuators. Thus, in this dissertation, bimorph piezoelectric actuators are used for control implementation.

As briefly described in the previous section, piezoelectric materials induce strain under an electric effect, and an electric field is generated when a mechanical strain is applied. Piezoelectric crystals in nature has a polarity in their molecular structure, and they are inherently anisotropic. One example for a natural piezoelectric material is quartz crystal as seen in Fig. 3.9.

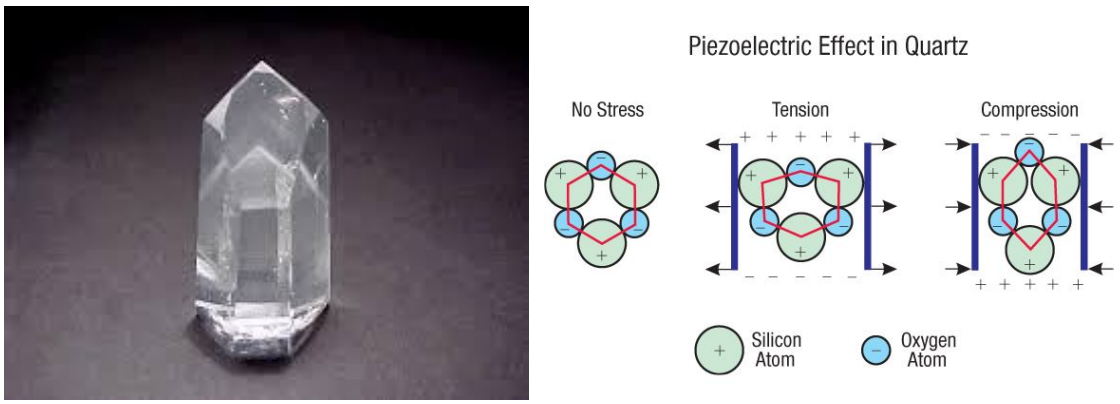

Figure 3.9: Crystal quartz and its molecular structure under mechanical strain.

When a mechanical strain is applied, the anisotropic molecule will generate an electric charge. This phenomena that is known as direct piezoelectric effect, is shown in Fig 3.10 [97].

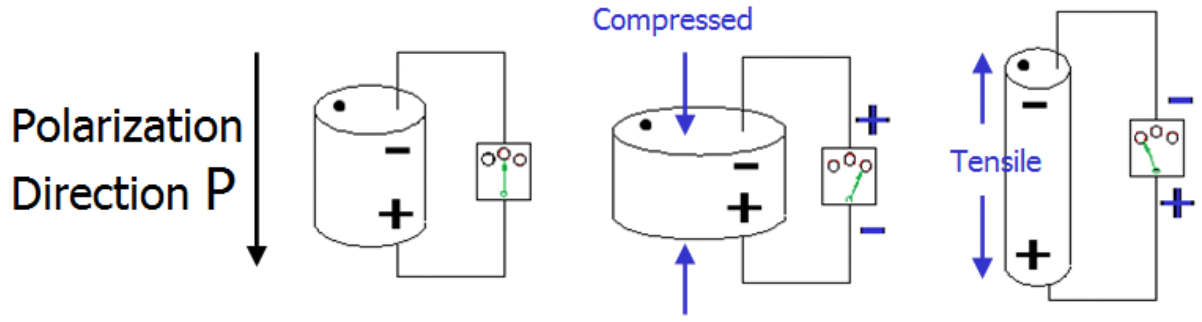

Figure 3.10: Electric charge generated by strain in a crystal quartz.
(Used under fair use, Ref. [97], 2015)

Similarly, when an electric field is applied, the quartz crystal will induce a mechanical strain depending on the direction of the polarization as seen in Fig. 3.11.

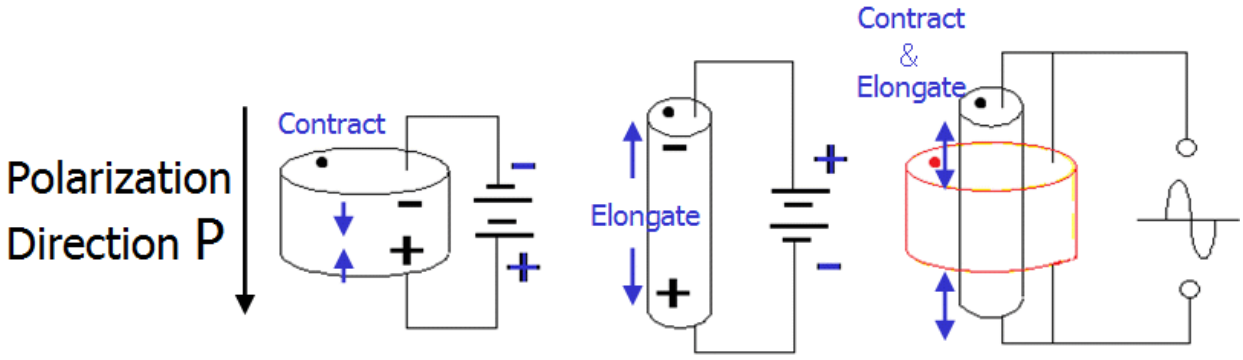

Figure 3.11: Strain induced by an electric field in a crystal quartz.
(Used under fair use, Ref. [97], 2015)

Natural piezoelectric crystals have a very low capacity to generate electric charges and require a very high voltage of electric current to obtain considerable mechanical strain to be used in most industrial applications. However, synthetic piezoelectric materials have a very high capacity, and are easy to manufacture in bulk and various shapes. These materials are not piezoelectric at first. They are inherently isotropic materials. However, under high electric

applications, they become anisotropic and alter to piezoelectric materials permanently. The process of applying a required electric filed to polarize a material is called poling [94]. This is part of the manufacturing process. It can be inversed applying the opposite sign of the electric field, and this inversion process is called depoling. The poling process is demonstrated in Fig 3.12.

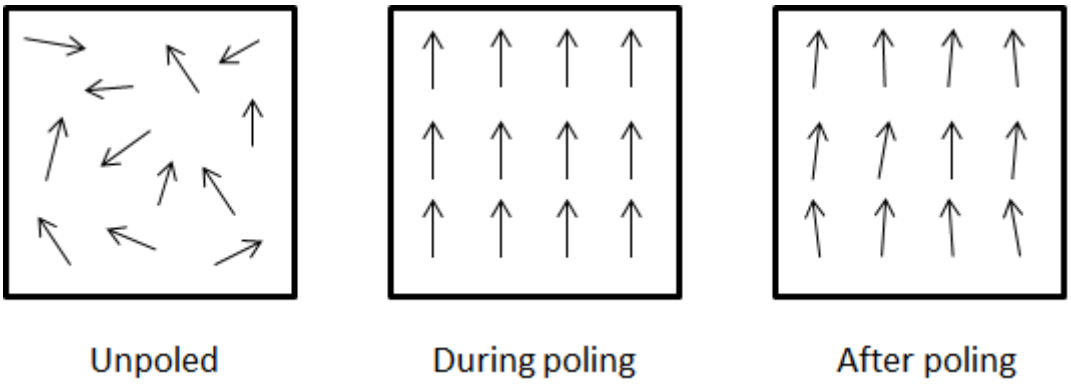

Figure 3.12: Poling process of a piezoelectric material.

The ability to manufacture piezoelectric materials allows us to have a desired shape and characteristics of a piezoelectric actuator within certain limits. Today, there are a few different types of piezoelectric actuators commercially available for different uses. The most common ones are piezoelectric sheets seen in Fig. 3.13 [98]. These are plate-like structures that are considered two dimensional. They can be stacked as multiple layers for different uses, and are called piezostack actuators. Each layer adds more capacity. They can be used as unimorph or bimorph. While unimorph actuators are mostly used for extension or contraction, bimorph actuators are used more commonly for effective bending. We can also use two unimorph actuators attached to both sides of the structures forming a bimorph actuator.

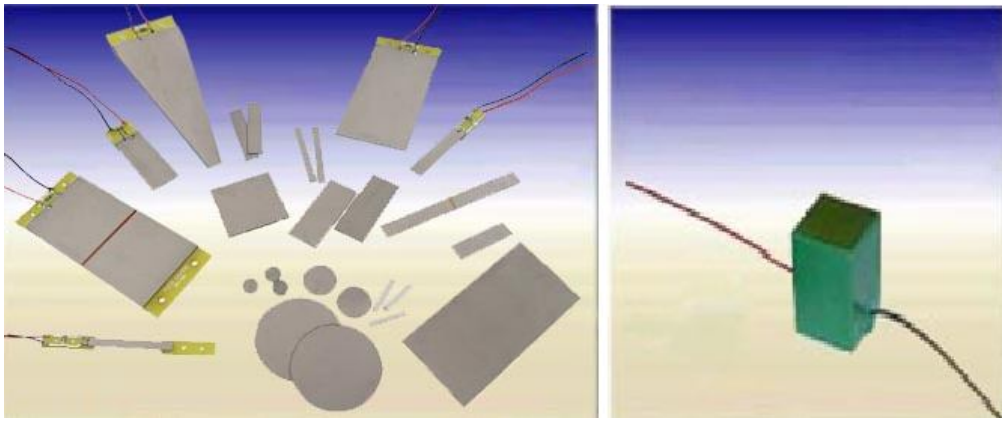

Figure 3.13: Piezoelectric sheets and stacks.
(Used under fair use, Ref. [98], 2015)

Since piezoelectric materials respond to electric field different than conventional isotropic materials, the mathematical modeling should include the terms that are going to capture the behavior of the material under an electric field. The convenient way is formulating mechanical and electrical effects as separate variables. The constitutive equation for a piezoelectric material, that is shown in Fig. 3.14, is defined with Equ. (3.2.36).

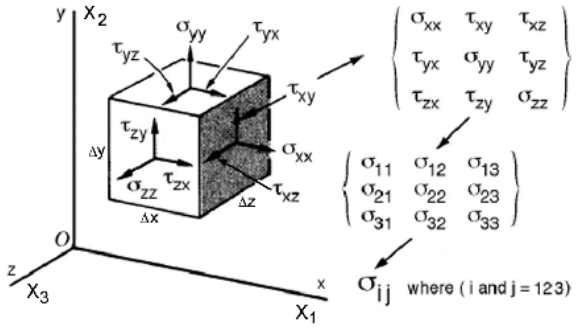

Figure 3.14: Strains on a 3-D piezoelectric material.

$$S_{ij} = s^{\mathrm{E}}_{ijkl} T_{kl} + d_{kij} \mathrm{E}_k \tag{3.2.36}$$

where S_{ij} is the mechanical strain tensor, T_{kl} is the mechanical stress tensor, s^{E}_{ijkl} is the compliance tensor, and d_{kij} is the piezoelectric coefficient tensor where the indices $i, j = 1,2,3$ and $k, l = 1,2,3$. The superscript E defines that the corresponding quantities are measured under constant electric field. This relation is assumed to be linear for low electrical and mechanical

effects. If the material is subject to a higher electric field or mechanical strain, the constitutive relation becomes highly nonlinear.

The constitutive relation can be rewritten using engineering notation to simplify the subscripts as follows:

$$\varepsilon_i = s_{ij}^{\mathrm{E}} \sigma_j + d_{ik} \mathrm{E}_k \tag{3.2.37}$$

$$\varepsilon = \begin{bmatrix} \varepsilon_1 \\ \varepsilon_2 \\ \varepsilon_3 \\ \varepsilon_4 \\ \varepsilon_5 \\ \varepsilon_6 \end{bmatrix} = \begin{bmatrix} \varepsilon_1 \\ \varepsilon_2 \\ \varepsilon_3 \\ \gamma_{23} \\ \gamma_{31} \\ \gamma_{12} \end{bmatrix} \tag{3.2.38}$$

where ε_1, ε_2 and ε_3, are direct strains and γ_{23}, γ_{31}, and γ_{12} are shear strains.

$$\sigma = \begin{bmatrix} \sigma_1 \\ \sigma_2 \\ \sigma_3 \\ \sigma_4 \\ \sigma_5 \\ \sigma_6 \end{bmatrix} = \begin{bmatrix} \sigma_1 \\ \sigma_2 \\ \sigma_3 \\ \tau_{23} \\ \tau_{31} \\ \tau_{12} \end{bmatrix} \tag{3.2.39}$$

Similarly, where σ_1, σ_2 and σ_3 are direct stresses and τ_{23}, τ_{31}, and τ_{12} are shear stresses.

$$s^{\mathrm{E}} = \begin{bmatrix} s_{11}^{\mathrm{E}} & s_{12}^{\mathrm{E}} & s_{13}^{\mathrm{E}} & s_{14}^{\mathrm{E}} & s_{15}^{\mathrm{E}} & s_{16}^{\mathrm{E}} \\ s_{21}^{\mathrm{E}} & s_{22}^{\mathrm{E}} & s_{23}^{\mathrm{E}} & s_{24}^{\mathrm{E}} & s_{25}^{\mathrm{E}} & s_{26}^{\mathrm{E}} \\ s_{31}^{\mathrm{E}} & s_{32}^{\mathrm{E}} & s_{33}^{\mathrm{E}} & s_{34}^{\mathrm{E}} & s_{35}^{\mathrm{E}} & s_{36}^{\mathrm{E}} \\ s_{41}^{\mathrm{E}} & s_{42}^{\mathrm{E}} & s_{43}^{\mathrm{E}} & s_{44}^{\mathrm{E}} & s_{45}^{\mathrm{E}} & s_{46}^{\mathrm{E}} \\ s_{51}^{\mathrm{E}} & s_{52}^{\mathrm{E}} & s_{53}^{\mathrm{E}} & s_{54}^{\mathrm{E}} & s_{55}^{\mathrm{E}} & s_{56}^{\mathrm{E}} \\ s_{61}^{\mathrm{E}} & s_{62}^{\mathrm{E}} & s_{63}^{\mathrm{E}} & s_{64}^{\mathrm{E}} & s_{65}^{\mathrm{E}} & s_{66}^{\mathrm{E}} \end{bmatrix} \tag{3.2.40}$$

The compliance matrix is a symmetric matrix as $s_{ij}^{\mathrm{E}} = s_{ji}^{\mathrm{E}}$, thus there are 21 constants. The electric field vector $\mathbf{E}$ and piezoelectric coefficient matrix $\mathbf{d}$ are defined as:

$$\mathbf{E} = \begin{bmatrix} E_1 \\ E_2 \\ E_3 \end{bmatrix} \tag{3.2.41}$$

$$\mathbf{d} = \begin{bmatrix} d_{11} & d_{21} & d_{31} \\ d_{12} & d_{22} & d_{32} \\ d_{13} & d_{23} & d_{33} \\ d_{14} & d_{24} & d_{34} \\ d_{15} & d_{25} & d_{35} \\ d_{16} & d_{26} & d_{36} \end{bmatrix} \tag{3.2.42}$$

Piezoelectric actuators can be poled in many desired directions. For example a piezoelectric sheet usually is poled in the direction normal to the plane as seen in Fig. 3.15.

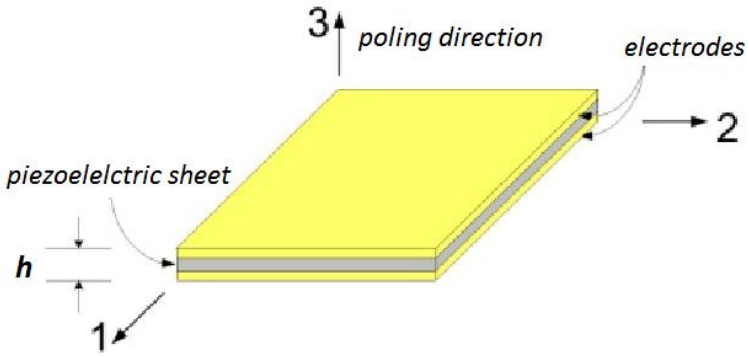

Figure 3.15: Poling direction for a piezoelectric actuator.

Once a piezoelectric sheet is poled, it is anisotropic in the poled direction and isotropic in the directions perpendicular to the poling direction. As a result, material characteristics will change depending on the poling direction. A piezoelectric actuator poled along its thickness is anisotropic in the direction 3, and isotropic in the 1-2 plane.

3.2.3.3 Modeling of Plates with Smart Materials

In this case, bimorph actuators are being used. Voltages of opposite sign are applied to create expansion in one layer and contraction in another as seen in Fig. 3.16.

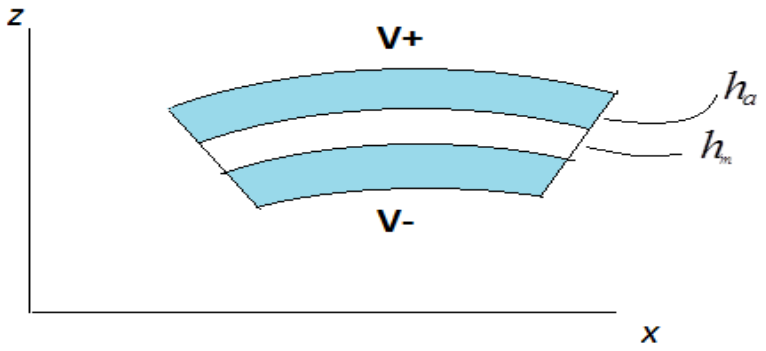

Figure 3.16: The bimorph piezoelectric actuator system

The moment generated by the actuators is implicitly being included in the f term in Equ. (3.2.32). Also, since the thickness and mass of the actuators are not negligible when the membrane-actuator system is considered, the mass, stiffness and damping effects of the actuators need to be considered in the equation of motion of the heterogeneous system composed of the membrane and actuators. Once the actuators added, the equation of motion can be rewritten for the system shown in Fig. 3.17, and this equation has the same structure as Equ. (3.2.32). However, the coefficients are defined differently to include the actuator effects.

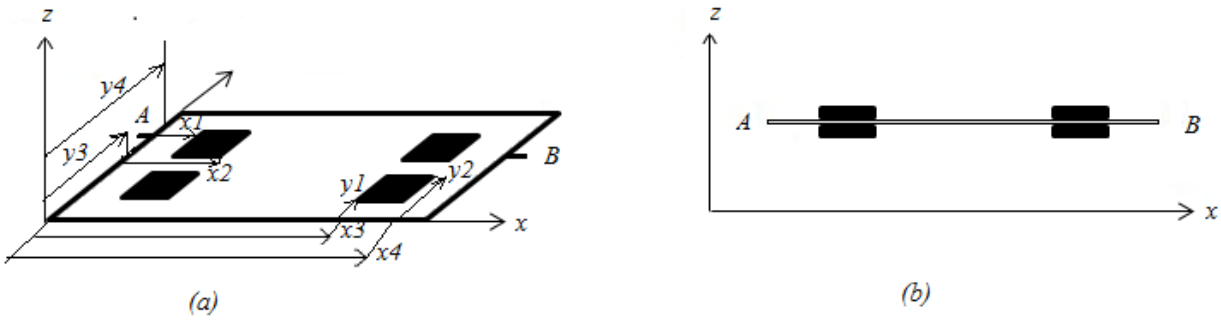

Figure 3.17: (a) The membrane system with four bimorph actuators, (b) A-B intersection of the System

The moment due to the actuator's deflection can be evaluated for a pure bending case, which is uncoupled in terms of extension and bending, such that:

$$\begin{aligned} M_x &= 2\int_{h_m/2}^{h_m/2+h_a} \frac{E_a}{1-\upsilon_a{}^2}\left(-z\left(\frac{\partial^2 w}{\partial x^2}+\upsilon_a\frac{\partial^2 w}{\partial y^2}\right)\right)zdz \\ &= \frac{2E_a}{1-\upsilon_a{}^2}\left[-\frac{1}{3}\left(\frac{\partial^2 w}{\partial x^2}+\upsilon_a\frac{\partial^2 w}{\partial y^2}\right)z^3\Big|_{h_m/2}^{h_m/2+h_a}\right] \\ &= -\frac{2E_a}{3\left(1-\upsilon_a{}^2\right)}\left(\left(\frac{h_m}{2}+h_a\right)^3-\left(\frac{h_m}{2}\right)^3\right)\left(\frac{\partial^2 w}{\partial x^2}+\upsilon_a\frac{\partial^2 w}{\partial y^2}\right) \end{aligned} \tag{3.2.43}$$

$$\begin{aligned} M_y &= 2\int_{h_m/2}^{h_m/2+h_a} \frac{E_a}{1-\upsilon_a{}^2}\left(-z\left(\frac{\partial^2 w}{\partial y^2}+\upsilon_a\frac{\partial^2 w}{\partial x^2}\right)\right)zdz \\ &= \frac{2E_a}{1-\upsilon_a{}^2}\left[-\frac{1}{3}\left(\frac{\partial^2 w}{\partial y^2}+\upsilon_a\frac{\partial^2 w}{\partial x^2}\right)z^3\Big|_{h_m/2}^{h_m/2+h_a}\right] \\ &= -\frac{2E}{3\left(1-\upsilon_a{}^2\right)}\left(\left(\frac{h_m}{2}+h_a\right)^3-\left(\frac{h_m}{2}\right)^3\right)\left(\frac{\partial^2 w}{\partial y^2}+\upsilon_a\frac{\partial^2 w}{\partial x^2}\right) \end{aligned} \tag{3.2.44}$$

$$\begin{aligned} M_{xy} &= 2\int_{h_m/2}^{h_m/2+h_a} \frac{E_a}{2\left(1+\upsilon_a\right)}\left(-2z\left(\frac{\partial^2 w}{\partial x\partial y}\right)\right)zdz \\ &= \frac{2E_a}{\left(1+\upsilon\right)}\left[-\frac{1}{3}\left(\frac{\partial^2 w}{\partial x\partial y}\right)z^3\Big|_{h_m/2}^{h_m/2+h_a}\right] \\ &= -\frac{2E_a}{3\left(1+\upsilon_a\right)}\left(\left(\frac{h_m}{2}+h_a\right)^3-\left(\frac{h_m}{2}\right)^3\right)\left(\frac{\partial^2 w}{\partial x\partial y}\right) \end{aligned} \tag{3.2.45}$$

Here, subscript *"a"* in the E, υ, and h terms represents the bimorph actuator values, and m represents the membrane values. The only external force being applied is the moment force induced by the actuator bending and can be formulated as:

$$f = -\left(\frac{\partial^2 M_x}{\partial x^2}+\frac{\partial^2 M_y}{\partial y^2}\right) \tag{3.2.46}$$

Similar to the steps taken previously, the moment expressions can be derived as:

$$M_x = \int_{h_m/2}^{h_m/2+h_a} \sigma_x z dz \tag{3.2.47}$$

$$M_y = \int_{h_m/2}^{h_m/2+h_a} \sigma_y z dz \tag{3.2.48}$$

where σ_x, and σ_y are defined as:

$$\sigma_x = \frac{E_a}{1-\upsilon_a}\frac{d_{31}}{h_a}V \tag{3.2.49}$$

$$\sigma_y = \frac{E_a}{1-\upsilon_a}\frac{d_{31}}{h_a}V \tag{3.2.50}$$

Here, V is the applied voltage. Substituting Equ. (3.2.49)-(3.2.50) into Equ. (3.2.47)–(3.2.48), the moments induced by actuators are obtained as:

$$\begin{aligned}\left(M_x\right)_i &= 2\int_{h_m/2}^{h_m/2+h_a} \frac{E_a}{1-\upsilon_a}\frac{d_{31}}{h_a}V_i z dz \\ &= \frac{E_a}{1-\upsilon_a}\frac{d_{31}}{h_a}V_i z^2\Big|_{h_m/2}^{h_m/2+h_a} = \frac{E_a}{1-\upsilon_a}\frac{d_{31}}{h_a}V_i\left(\left(\frac{h_m}{2}+h_a\right)^2-\left(\frac{h_m}{2}\right)^2\right) \\ &= \frac{E_a d_{31}}{1-\upsilon_a}\left(h_m+h_a\right)V_i\end{aligned} \tag{3.2.51}$$

$$\begin{aligned}\left(M_y\right)_i &= 2\int_{h_m/2}^{h_m/2+h_a} \frac{E_a}{1-\upsilon_a}\frac{d_{31}}{h_a}V_i z dz \\ &= \frac{E_a}{1-\upsilon_a}\frac{d_{31}}{h_a}V_i z^2\Big|_{h_m/2}^{h_m/2+h_a} = \frac{E_a}{1-\upsilon_a}\frac{d_{31}}{h_a}V_i\left(\left(\frac{h_m}{2}+h_a\right)^2-\left(\frac{h_m}{2}\right)^2\right) \\ &= \frac{E_a d_{31}}{1-\upsilon_a}\left(h_m+h_a\right)V_i\end{aligned} \tag{3.2.52}$$

where V_i is the externally applied voltage to the i^{th} actuator, and $i=1,\ldots,k$, where k is the number of actuators, in this case k=4. Similar to Equ. (3.2.32), the equation of motion for a plate with piezoelectric actuators attached to it is obtained in the form:

$$\begin{aligned}
&\rho h\frac{\partial^2 w}{\partial t^2}+D\left(\frac{\partial^2}{\partial x^2}\left(\frac{\partial^2 w}{\partial x^2}\right)+\frac{\partial^2}{\partial y^2}\left(\frac{\partial^2 w}{\partial y^2}\right)\right)+D_\upsilon\left(\frac{\partial^2}{\partial y^2}\left(\frac{\partial^2 w}{\partial x^2}\right)+\frac{\partial^2}{\partial x^2}\left(\frac{\partial^2 w}{\partial y^2}\right)\right)\\
&+2G\frac{\partial^2}{\partial x\partial y}\left(\frac{\partial^2 w}{\partial x\partial y}\right)+2G\frac{\partial^2}{\partial y\partial x}\left(\frac{\partial^2 w}{\partial y\partial x}\right)+D_\delta\left(\frac{\partial^2}{\partial x^2}\left(\frac{\partial^2}{\partial x^2}\left(\frac{\partial w}{\partial t}\right)\right)+\frac{\partial^2}{\partial y^2}\left(\frac{\partial^2}{\partial y^2}\left(\frac{\partial w}{\partial t}\right)\right)\right)\\
&+D_{\delta\upsilon}\left(\frac{\partial^2}{\partial y^2}\left(\frac{\partial^2}{\partial x^2}\left(\frac{\partial w}{\partial t}\right)\right)+\frac{\partial^2}{\partial x^2}\left(\frac{\partial^2}{\partial y^2}\left(\frac{\partial w}{\partial t}\right)\right)\right)+2G_\delta\frac{\partial^2}{\partial x\partial y}\left(\frac{\partial^2}{\partial x\partial y}\left(\frac{\partial w}{\partial t}\right)\right)\\
&+2G_\delta\frac{\partial^2}{\partial y\partial x}\left(\frac{\partial^2}{\partial y\partial x}\left(\frac{\partial w}{\partial t}\right)\right)+\left(N_x\right)\frac{\partial^2 w}{\partial x^2}+\left(N_y\right)\frac{\partial^2 w}{\partial y^2}=f
\end{aligned} \tag{3.2.53}$$

where the coefficients are defined differently than Equ. (3.2.32). These new definitions include the actuator effects as follows:

$$\rho h=\rho_m h_m+2\rho_a h_a\chi\left(x,y\right) \tag{3.2.54}$$

$$D=\frac{E_m h_m^3}{12\left(1-\upsilon_m^2\right)}+\frac{2E_a}{3\left(1-\upsilon_a^2\right)}\left(\left(\frac{h_m}{2}+h_a\right)^3-\left(\frac{h_m}{2}\right)^3\right)\chi\left(x,y\right) \tag{3.2.55}$$

$$D_\upsilon=\frac{\upsilon_m E_m h_m^3}{12\left(1-\upsilon_m^2\right)}+\frac{2\upsilon_a E_a}{3\left(1-\upsilon_a^2\right)}\left(\left(\frac{h_m}{2}+h_a\right)^3-\left(\frac{h_m}{2}\right)^3\right)\chi\left(x,y\right) \tag{3.2.56}$$

$$G=\frac{E_m h_m^3}{24\left(1+\upsilon_m\right)}+\frac{2E_a}{3\left(1+\upsilon_a\right)}\left(\left(\frac{h_m}{2}+h_a\right)^3-\left(\frac{h_m}{2}\right)^3\right)\chi\left(x,y\right) \tag{3.2.57}$$

$$D_\delta=\frac{\delta_m h_m^3}{12\left(1-\upsilon_m^2\right)}+\frac{2\delta_a}{3\left(1-\upsilon_a^2\right)}\left(\left(\frac{h_m}{2}+h_a\right)^3-\left(\frac{h_m}{2}\right)^3\right)\chi\left(x,y\right) \tag{3.2.58}$$

$$D_{\delta\upsilon}=\frac{\upsilon_m\delta_m h_m^3}{12\left(1-\upsilon_m^2\right)}+\frac{2\upsilon_a\delta_a}{3\left(1-\upsilon_a^2\right)}\left(\left(\frac{h_m}{2}+h_a\right)^3-\left(\frac{h_m}{2}\right)^3\right)\chi\left(x,y\right) \tag{3.2.59}$$

$$G_\delta = \frac{\delta_m h_m^3}{24\left(1+\upsilon_m\right)} + \frac{2\delta_a}{3\left(1+\upsilon_a\right)}\left(\left(\frac{h_m}{2}+h_a\right)^3 - \left(\frac{h_m}{2}\right)^3\right)\chi\left(x,y\right) \tag{3.2.60}$$

Here, the $\chi(x,y)$ function has value "1" when it is being evaluated in the region where actuators attached, and otherwise it has value "0". The boundary conditions are defined the same way:

$$w(x,y,0) = w_0 \qquad \frac{\partial w}{\partial t} w(x,y,0) = 0 \tag{3.2.61}$$

$$w(x,y,t) = \frac{\partial w(x,y,t)}{\partial n} = 0 \qquad on \qquad \partial\Omega \tag{3.2.62}$$

3.3 Finite Element Modeling

In order to create models appropriate for numerical analysis and control design, the Finite Element Method (FEM) is applied to transform the equation of motion for heterogeneous membrane systems, which is an infinite dimensional, partial differential equation, into the finite dimensional systems of ordinary differential equations (ODEs). At the end of this process, a systems of linear time invariant second order differential equations are generated. To select an appropriate number of elements in the FEM procedure, the variations of the first fundamental frequencies of the systems and of the mode shapes with the number of elements are monitored. This number is chosen based on satisfactory convergence of these dynamic features. Such an approach is justified by the desire to accurately capture essential dynamic system features that are crucial in control design.

3.3.1 Weak Form Finite Element Formulation

The equation of motion of the system is rewritten in the linear second order time invariant form by generating the coefficient matrices using the weak form Finite Element Method [99] as:

$$M\ddot{q} + C\dot{q} + Kq = F, \quad M > 0, \quad K = K_m + K_g > 0, \quad C \geq 0 \tag{3.3.1}$$

where M is the mass matrix, C is the damping matrix, and $K = K_m + K_g$ is the tangent stiffness matrix partitioned as material (K_m) and geometric (K_g) stiffness matrices. Also, F is the external force vector that can be written as $\bar{F}u$, where u is the control vector and $\bar{F}$ is the control matrix. Where q is the vector of generalized coordinates. To derive the weak form FEM, the displacement is defined in an approximate form as:

$$w(x, y, t) = \sum_{i=1}^{N} q_i(t)\psi_i(x, y) \tag{3.3.2}$$

where ψ_i is a complete third order orthogonal polynomial basis function for the finite element. Substituting this approximation into the equation of motion of the membrane defined in Equ. (3.2.56), the following expression is obtained as:

$$\begin{aligned}
&\sum_{i=1}^{N}\left\{\rho h\ddot{q}_i\psi_i + Dq_i\left(\frac{\partial^2}{\partial x^2}\left(\frac{\partial^2\psi_i}{\partial x^2}\right)\right) + D_\upsilon q_i\left(\frac{\partial^2}{\partial y^2}\left(\frac{\partial^2\psi_i}{\partial x^2}\right)\right)\right. \\
&+2Gq_i\frac{\partial^2}{\partial x\partial y}\left(\frac{\partial^2\psi_i}{\partial x\partial y}\right) + 2Gq_i\frac{\partial^2}{\partial y\partial x}\left(\frac{\partial^2\psi_i}{\partial y\partial x}\right) + D_\delta\dot{q}_i\left(\frac{\partial^2}{\partial x^2}\left(\frac{\partial^2\psi_i}{\partial x^2}\right)\right) \\
&+D_{\delta\upsilon}\dot{q}_i\left(\frac{\partial^2}{\partial y^2}\left(\frac{\partial^2\psi_i}{\partial x^2}\right)\right) + 2G_\delta\dot{q}_i\frac{\partial^2}{\partial x\partial y}\left(\frac{\partial^2\psi_i}{\partial x\partial y}\right) + +2G_\delta\dot{q}_i\frac{\partial^2}{\partial y\partial x}\left(\frac{\partial^2\psi_i}{\partial y\partial x}\right) \\
&\left.+(N_x)q_i\frac{\partial^2\psi_i}{\partial x^2} + (N_y)q_i\frac{\partial^2\psi_i}{\partial y^2}\right\} = f
\end{aligned} \tag{3.3.3}$$

Multiplying Equ (3.3.2) with ψ_j and integrating over the domain of the membrane, Ω, another expression is obtained as:

$$\sum_{i=1}^{N}\int_{\Omega}\left\{\left[\rho h\psi_i\psi_j\right]\ddot{q}_i+\left[D_\delta\left(\frac{\partial^2}{\partial x^2}\left(\frac{\partial^2\psi_i}{\partial x^2}\right)\right)\psi_j+D_{\delta\upsilon}\left(\frac{\partial^2}{\partial y^2}\left(\frac{\partial^2\psi_i}{\partial x^2}\right)\right)\psi_j\right.\right.$$
$$+2G_\delta\frac{\partial^2}{\partial x\partial y}\left(\frac{\partial^2\psi_i}{\partial x\partial y}\right)\psi_j+2G_\delta\frac{\partial^2}{\partial y\partial x}\left(\frac{\partial^2\psi_i}{\partial y\partial x}\right)\psi_j\Bigg]\dot{q}_i+\Bigg[D\left(\frac{\partial^2}{\partial x^2}\left(\frac{\partial^2\psi_i}{\partial x^2}\right)\right)\psi_j$$
$$+D_\upsilon\left(\frac{\partial^2}{\partial y^2}\left(\frac{\partial^2\psi_i}{\partial x^2}\right)\right)\psi_j+2G\frac{\partial^2}{\partial x\partial y}\left(\frac{\partial^2\psi_i}{\partial x\partial y}\right)\psi_j+2G\frac{\partial^2}{\partial y\partial x}\left(\frac{\partial^2\psi_i}{\partial y\partial x}\right)\psi_j$$
$$\left.\left.+\left(N_x\right)\frac{\partial^2\psi_i}{\partial x^2}\psi_j+\left(N_y\right)\frac{\partial^2\psi_i}{\partial y^2}\psi_j\Bigg]q_i\right\}d\Omega=\int_{\Omega}f\psi_j d\Omega \tag{3.3.4}$$

This equation is in the form of Equ. (3.3.1). The increment of the domain of the membrane is defined as $d\Omega=dxdy$. To reduce the order of the spatial derivatives, the integration is carried out using Divergence Theorem that is defined as:

$$\int_{\Omega}\frac{\partial}{\partial x}\left(w\Lambda\right)dxdy=\int_{\partial\Omega}w\Lambda n_x ds \tag{3.3.5}$$

$$\int_{\Omega}\frac{\partial}{\partial y}\left(w\Lambda\right)dxdy=\int_{\partial\Omega}w\Lambda n_y ds \tag{3.3.6}$$

Here, Λ is a function, n_x and n_y are the components of the unit normal vector. Applying Divergence theorem to each term in Equ. (3.3.4), the coefficient matrices are obtained as follow:

$$\int_{\Omega}D_\delta\left(\frac{\partial^2}{\partial x^2}\left(\frac{\partial^2\psi_i}{\partial x^2}\right)\right)\psi_j dxdy=\int_{\partial\Omega}D_\delta\left(\frac{\partial}{\partial x}\left(\frac{\partial^2\psi_i}{\partial x^2}\right)\right)\psi_j dy-\int_{\partial\Omega}D_\delta\left(\frac{\partial^2\psi_i}{\partial x^2}\right)\frac{\partial\psi_j}{\partial x}dy$$
$$+\int_{\Omega}D_\delta\left(\frac{\partial^2\psi_i}{\partial x^2}\right)\frac{\partial^2\psi_j}{\partial x^2}dxdy \tag{3.3.7}$$

$$\int_{\Omega}D_{\delta\upsilon}\left(\frac{\partial^2}{\partial y^2}\left(\frac{\partial^2\psi_i}{\partial x^2}\right)\right)\psi_j dxdy=\int_{\partial\Omega}D_{\delta\upsilon}\left(\frac{\partial}{\partial y}\left(\frac{\partial^2\psi_i}{\partial x^2}\right)\right)\psi_j dx-\int_{\partial\Omega}D_{\delta\upsilon}\left(\frac{\partial^2\psi_i}{\partial x^2}\right)\frac{\partial\psi_j}{\partial y}dx$$
$$+\int_{\Omega}D_{\delta\upsilon}\left(\frac{\partial^2\psi_i}{\partial x^2}\right)\frac{\partial^2\psi_j}{\partial y^2}dxdy \tag{3.3.8}$$

$$\int_{\Omega} 2G_{\delta}\left(\frac{\partial^2}{\partial x\partial y}\left(\frac{\partial^2\psi_i}{\partial x\partial y}\right)\right)\psi_j dxdy = \int_{\partial\Omega} 2G_{\delta}\left(\frac{\partial}{\partial y}\left(\frac{\partial^2\psi_i}{\partial x\partial y}\right)\right)\psi_j dy - \int_{\partial\Omega} 2G_{\delta}\left(\frac{\partial^2\psi_i}{\partial x\partial y}\right)\frac{\partial\psi_j}{\partial x}dx + \int_{\Omega} 2G_{\delta}\left(\frac{\partial^2\psi_i}{\partial x\partial y}\right)\frac{\partial^2\psi_j}{\partial x\partial y}dxdy \tag{3.3.9}$$

$$\int_{\Omega} 2G_{\delta}\left(\frac{\partial^2}{\partial y\partial x}\left(\frac{\partial^2\psi_i}{\partial y\partial x}\right)\right)\psi_j dxdy = \int_{\partial\Omega} 2G_{\delta}\left(\frac{\partial}{\partial x}\left(\frac{\partial^2\psi_i}{\partial y\partial x}\right)\right)\psi_j dx - \int_{\partial\Omega} 2G_{\delta}\left(\frac{\partial^2\psi_i}{\partial y\partial x}\right)\frac{\partial\psi_j}{\partial y}dy + \int_{\Omega} 2G_{\delta}\left(\frac{\partial^2\psi_i}{\partial y\partial x}\right)\frac{\partial^2\psi_j}{\partial y\partial x}dxdy \tag{3.3.10}$$

$$\int_{\Omega} D\left(\frac{\partial^2}{\partial x^2}\left(\frac{\partial^2\psi_i}{\partial x^2}\right)\right)\psi_j dxdy = \int_{\partial\Omega} D_{\delta}\left(\frac{\partial}{\partial x}\left(\frac{\partial^2\psi_i}{\partial x^2}\right)\right)\psi_j dy - \int_{\partial\Omega} D_{\delta}\left(\frac{\partial^2\psi_i}{\partial x^2}\right)\frac{\partial\psi_j}{\partial x}dy + \int_{\Omega} D_{\delta}\left(\frac{\partial^2\psi_i}{\partial x^2}\right)\frac{\partial^2\psi_j}{\partial x^2}dxdy \tag{3.3.11}$$

$$\int_{\Omega} D_{\upsilon}\left(\frac{\partial^2}{\partial y^2}\left(\frac{\partial^2\psi_i}{\partial x^2}\right)\right)\psi_j dxdy = \int_{\partial\Omega} D_{\upsilon}\left(\frac{\partial}{\partial y}\left(\frac{\partial^2\psi_i}{\partial x^2}\right)\right)\psi_j dx - \int_{\partial\Omega} D_{\upsilon}\left(\frac{\partial^2\psi_i}{\partial x^2}\right)\frac{\partial\psi_j}{\partial y}dx + \int_{\Omega} D_{\upsilon}\left(\frac{\partial^2\psi_i}{\partial x^2}\right)\frac{\partial^2\psi_j}{\partial y^2}dxdy \tag{3.3.12}$$

$$\int_{\Omega} 2G\left(\frac{\partial^2}{\partial x\partial y}\left(\frac{\partial^2\psi_i}{\partial x\partial y}\right)\right)\psi_j dxdy = \int_{\partial\Omega} 2G\left(\frac{\partial}{\partial y}\left(\frac{\partial^2\psi_i}{\partial x\partial y}\right)\right)\psi_j dy - \int_{\partial\Omega} 2G\left(\frac{\partial^2\psi_i}{\partial x\partial y}\right)\frac{\partial\psi_j}{\partial x}dx + \int_{\Omega} 2G\left(\frac{\partial^2\psi_i}{\partial x\partial y}\right)\frac{\partial^2\psi_j}{\partial x\partial y}dxdy \tag{3.3.13}$$

$$\int_{\Omega} 2G\left(\frac{\partial^2}{\partial y\partial x}\left(\frac{\partial^2\psi_i}{\partial y\partial x}\right)\right)\psi_j dxdy = \int_{\partial\Omega} 2G\left(\frac{\partial}{\partial x}\left(\frac{\partial^2\psi_i}{\partial y\partial x}\right)\right)\psi_j dx - \int_{\partial\Omega} 2G\left(\frac{\partial^2\psi_i}{\partial y\partial x}\right)\frac{\partial\psi_j}{\partial y}dy + \int_{\Omega} 2G\left(\frac{\partial^2\psi_i}{\partial y\partial x}\right)\frac{\partial^2\psi_j}{\partial y\partial x}dxdy \tag{3.3.14}$$

$$\int_{\Omega} N_x \frac{\partial^2 \psi_i}{\partial x^2} \psi_j dxdy = \int_{\partial\Omega} N_x \frac{\partial \psi_i}{\partial x} \psi_j dy - \int_{\Omega} N_x \frac{\partial \psi_i}{\partial x} \frac{\partial \psi_j}{\partial x} dxdy \tag{3.3.15}$$

$$\int_{\Omega} N_y \frac{\partial^2 \psi_i}{\partial y^2} \psi_j dxdy = \int_{\partial\Omega} N_y \frac{\partial \psi_i}{\partial y} \psi_j dx - \int_{\Omega} N_y \frac{\partial \psi_i}{\partial y} \frac{\partial \psi_j}{\partial y} dxdy \tag{3.3.16}$$

Adding the terms and applying the boundary conditions, components of the mass, stiffness, damping and force matrices in Equ (3.3.1) are derived as:

$$M_{ij} = \int_{\Omega_e} \rho h \psi_i \psi_j dxdy \tag{3.3.17}$$

$$\begin{aligned} C_{ij} = \int_{\Omega_e} \Bigg[& D_\delta \left(\left(\frac{\partial^2 \psi_i}{\partial x^2} \right) \frac{\partial^2 \psi_j}{\partial x^2} + \left(\frac{\partial^2 \psi_i}{\partial y^2} \right) \frac{\partial^2 \psi_j}{\partial y^2} \right) + D_{\delta\upsilon} \left(\left(\frac{\partial^2 \psi_i}{\partial x^2} \right) \frac{\partial^2 \psi_j}{\partial y^2} + \left(\frac{\partial^2 \psi_i}{\partial y^2} \right) \frac{\partial^2 \psi_j}{\partial x^2} \right) \\ & + 2G_\delta \left(\frac{\partial^2 \psi_i}{\partial x \partial y} \right) \frac{\partial^2 \psi_j}{\partial x \partial y} + 2G_\delta \left(\frac{\partial^2 \psi_i}{\partial y \partial x} \right) \frac{\partial^2 \psi_j}{\partial y \partial x} \Bigg] dxdy \end{aligned} \tag{3.3.18}$$

$$\begin{aligned} K_{m_{ij}} = \int_{\Omega_e} \Bigg[& D \left(\left(\frac{\partial^2 \psi_i}{\partial x^2} \right) \frac{\partial^2 \psi_j}{\partial x^2} + \left(\frac{\partial^2 \psi_i}{\partial y^2} \right) \frac{\partial^2 \psi_j}{\partial y^2} \right) + D_\upsilon \left(\left(\frac{\partial^2 \psi_i}{\partial x^2} \right) \frac{\partial^2 \psi_j}{\partial y^2} + \left(\frac{\partial^2 \psi_i}{\partial y^2} \right) \frac{\partial^2 \psi_j}{\partial x^2} \right) \\ & + 2G \left(\frac{\partial^2 \psi_i}{\partial x \partial y} \right) \frac{\partial^2 \psi_j}{\partial x \partial y} + 2G \left(\frac{\partial^2 \psi_i}{\partial y \partial x} \right) \frac{\partial^2 \psi_j}{\partial y \partial x} \Bigg] dxdy \end{aligned} \tag{3.3.19}$$

$$K_{g_{ij}} = \int_{\Omega_e} \left[N_x \frac{\partial \psi_i}{\partial x} \frac{\partial \psi_j}{\partial x} + N_y \frac{\partial \psi_i}{\partial y} \frac{\partial \psi_j}{\partial y} \right] dxdy \tag{3.3.20}$$

$$F_j = \int_{\Omega_e} f \psi_j dxdy \tag{3.3.21}$$

where Ω_e is the domain of one finite element, while M_{ij} and K_{ij} and C_{ij} are the ij^{th} element of the mass, stiffness and damping matrices of the finite element, respectively. Similarly, F_j is the j^{th} element of the force vector of the finite element. Since the membrane is square, the rectangular plate element is selected for convenience. The plate element that is used has 12

degrees of freedom. A crucial issue when building a finite element model is to appropriately select the number of finite elements. Too many elements may lead to numerical errors and difficulties whereas too few elements may not accurately capture the essential properties of the system. This issue is tackled in the next section.

3.3.2 Convergence of the FEM Solution

To find the appropriate number of finite elements, the number of element being used is increased gradually, and the convergence of parameters that are critical for dynamics and control design are monitored. Specifically, the convergence of the natural frequencies and mode shapes are checked to select an appropriate number of elements used for the FEM. The advantage of using dynamic characteristics, such as natural frequencies and mode shapes, instead of conventional static characteristics, such as displacements, strains or stresses, is crucial. In static analysis we use only the stiffness matrix, while in order to calculate natural frequencies and mode shapes we need both stiffness and mass matrices. Guaranteeing natural frequencies and mode shapes are correctly captured is a necessary criterion to carry on a dynamic analysis. Another advantage when monitoring these dynamic characteristics is that we do not need to solve for the displacement each time when we remesh the system. The analysis is carried out to find out the feasible number for convergence for two different systems as seen in Figs. 3.18 and 3.19, each with four bimorph actuators attached to the membrane, symmetrically with respect to the center of the membrane. System I is designed to have an equal actuation effect all over the domain of the membrane placing the actuators in the mid locations. System II is designed to have a larger homogenous area in the center to have a more efficient reflector. In this section, structural effects of the actuator placements are demonstrated. For System I and System II, the actuator locations are defined in Table 3.1.

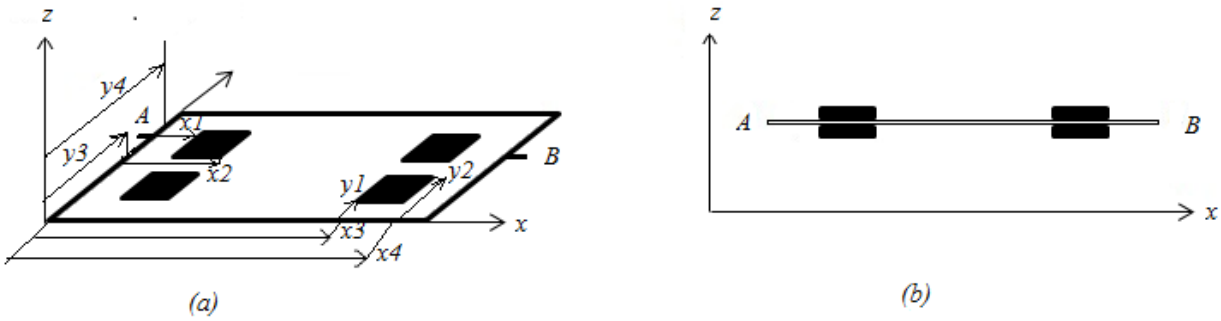

Figure 3.18: (a) System I. The membrane with four bimorph actuators away from the corrners, (b) A-B intersection of System I

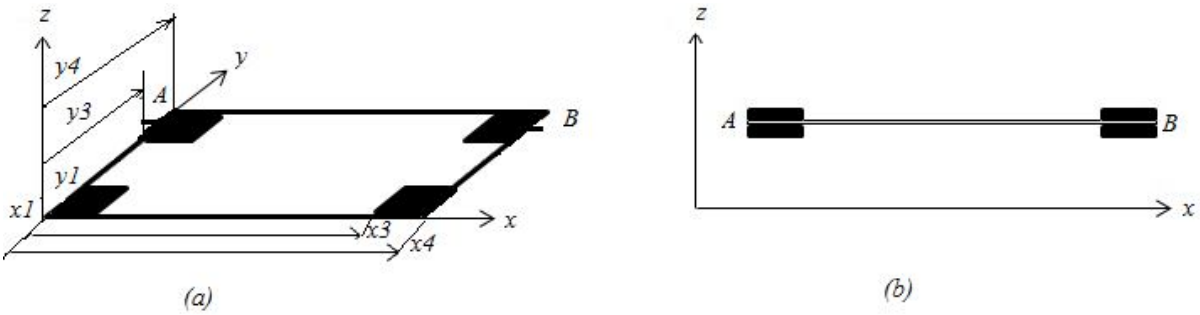

Figure 3.19: (a) System II. The membrane with four bimorph actuators at the corners, (b) A-B intersection of System II

Table 3.1: Actuator locations for the Systems

	System I	System II
$x1$ (m)	0.025	0
$x2$ (m)	0.050	0.025
$x3$ (m)	0.075	0.100
$x4$ (m)	0.100	0.125
$y1$ (m)	0.025	0
$y3$ (m)	0.050	0.025
$y3$ (m)	0.075	0.100
$y4$ (m)	0.100	0.125

For membrane material Kapton membrane is chosen as the material; because, it is one of the most used materials in aerospace applications [3]. It is largely available and inexpensive. For piezoelectric actuators the most common material is PZT due its effectiveness as an actuator. PVDF is another option to have a more compliant structure, but it is mostly used as sensors since it generates less force. Intuitively PVDF would be more suitable for Kapton membrane; however, a higher control force is more desired for this work. PZT actuators can also vibrate at higher frequencies, and this is another important property of PZT actuators for active control of reflectors. To find the optimal material for the actuator, both PZT and PVDF actuators are implemented. Also, PZT actuators with different thicknesses are used to choose a more feasible actuator. In this section, the convergence analysis is carried out for the PZT actuator that is selected for control application after trying different actuators in Chapter 6. The prestress is $40N/m$ and homogenous in both *x* and *y* directions. Material properties are defined in Table 3.2.

Table 3.2: Material properties and geometric characteristics of the membrane actuator systems

		Kapton Membrane	Bimorph Actuator
Young's Modulus	$E(Pa)$	165×10^{6}	62×10^{9}
Poisson' Ratio	υ	0.34	0.31
Material density	$\rho(kg/m^{3})$	1400	7800
Thickness	$h(m)$	51×10^{-6}	267×10^{-6}
Length	$L(m)$	0.125	0.025
Width	$W(m)$	0.125	0.025
Kelvin-Voigt Coefficient	(kg/ ms)	5.2495×10^{5}	2.5536×10^{3}
Coupling Coefficient $d_{31}(pmV^{-1})$		-	320

To compute the natural frequencies and mode shapes, the well-known formula,

$$(K - \omega_l^2 M)\phi_l = 0 \tag{3.3.22}$$

is used. Here, ω_l is the l^{th} natural frequency of the system, and ϕ_l is the corresponding eigenvector called "mode shape". Discretizing process is started with a very coarse mesh of 25 elements, and the number of elements is gradually increased until 900 elements. For each mesh, the natural frequencies and mode shapes are calculated. For convergence, the first 6 natural frequencies of both systems, considered the fundamental frequencies, are monitored. It is observed that, when the number of elements is gradually increased up to 900 elements, the natural frequencies converge to certain values. This pattern is clearly illustrated in Figs. 3.20 and 3.21. Table 3.3 also shows the corresponding minimum and maximum natural frequencies for each number of elements for System I and System II. The value of the minimum natural frequencies are stabilized to certain values with 0.008 and 0.006 relative error for System I and System II, respectively, for 400 elements. When the elements number is increased, the relative errors are 0.005 and 0.003 for System I and System II, respectively, for 625 elements, 0.003 and 0.002 for System I and System II, respectively, for 900 elements. Depending on the desired accuracy, the number of elements can be the selected for the material and geometry. However, it should be noted that changing the material or thickness will affect the convergence rate.

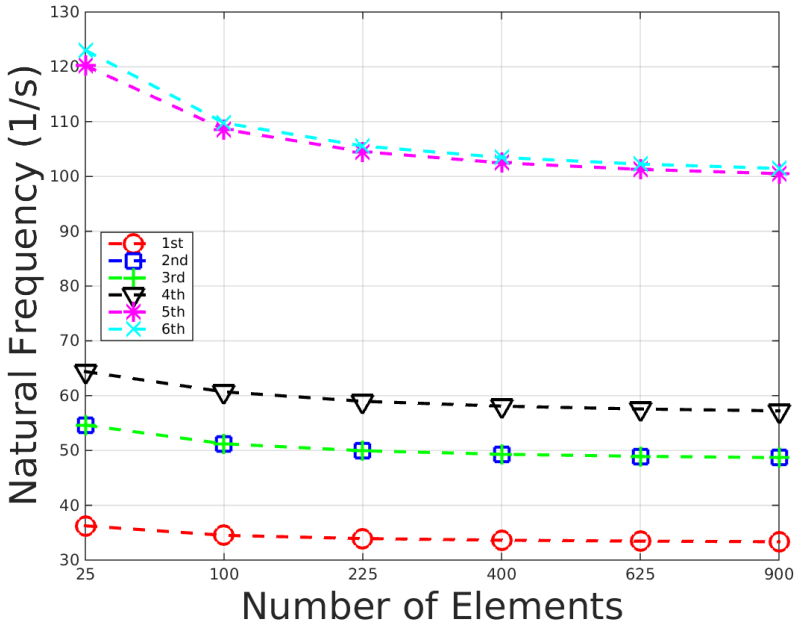

Figure 3.20: Convergence of the natural frequencies for System I.

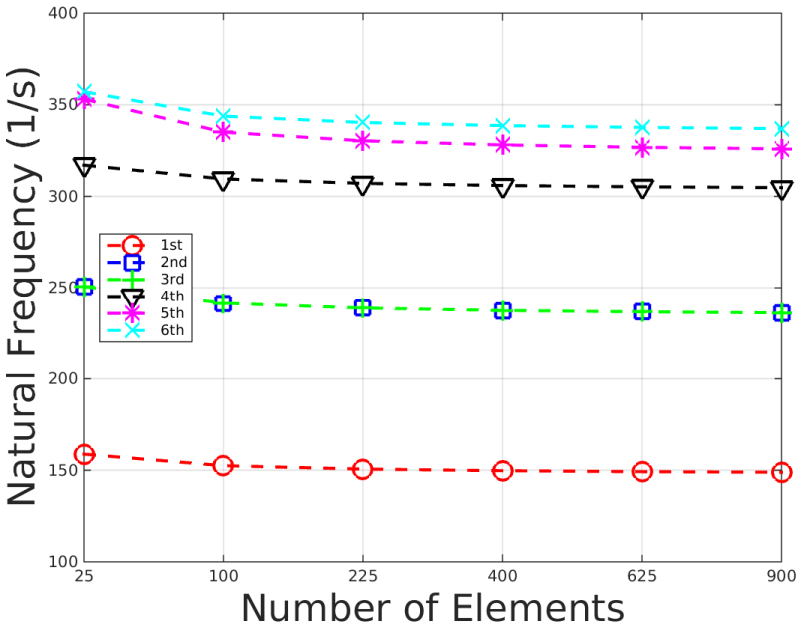

Figure 3.21: Convergence of the natural frequencies for System II.

Table 3.3: Convergence of the natural frequencies for System I and System II.

		System I		System II	
NE	n	Max. ω_l	Min. ω_l	Max. ω_l	Min. ω_l
25	48	1.14E+4	36.25	5.52E+3	158.80
100	243	4.11E+4	34.52	3.21E+4	152.49
225	588	8.97E+4	33.92	8.08E+4	150.63
400	1083	1.55E+5	33.63	1.48E+5	149.75
625	1728	2.42E+5	33.46	2.34E+5	149.23
900	2523	3.45E+5	33.35	3.40E+5	148.90

Once it is understood how the natural frequencies converge depending on the number of elements used, the convergence of the mode shapes respect to increased number of elements is analyzed. Mode shapes correspond to displacement of the system, and the biggest influence on displacement comes from the 1st mode. Therefore, the focus is on the 1st mode while analyzing the convergence of mode shapes. Using Equ. (3.3.22), the mode shapes of the two systems (i.e. System I and II) for the 1st natural frequency are obtained. Since the expected maximum displacement is at the center of the membrane for the 1st mode, an intersection that passes through the center of the membrane and is parallel to the x axis is taken for convergence analysis. Figs. 3.22 and 3.23 show these intersections corresponding to each number of elements (listed in the Figure legends) for System I and System II, respectively. Note that also in these Figures, the "zoomed in" areas, represented by dotted rectangles, better visualize the mode shape convergence.

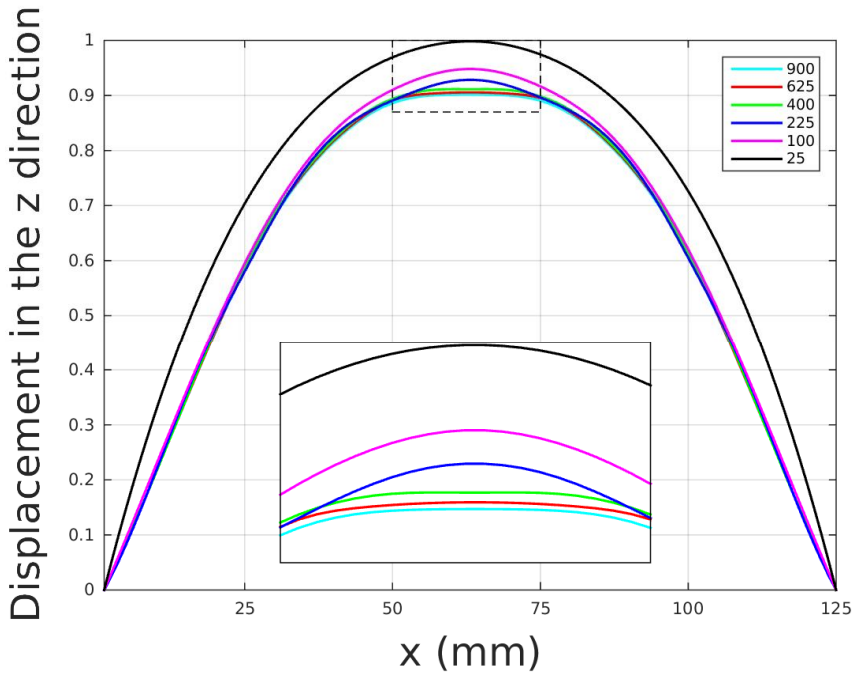

Figure 3.22: Convergence of the 1st mode at the center of System I

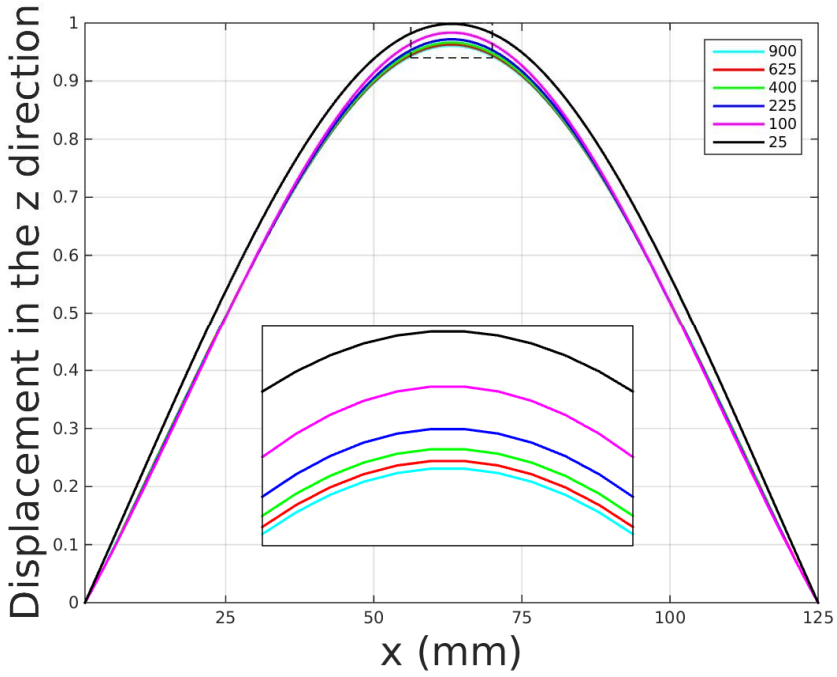

Figure 3.23: Convergence of the 1st mode at the center of System II

To better visualize the mode shape convergence in Figs. 3.24 and 3.25, the displacements in the z direction at the center of the membrane for 1st mode, that is obtained for each number of elements, are plotted respect to number of elements.

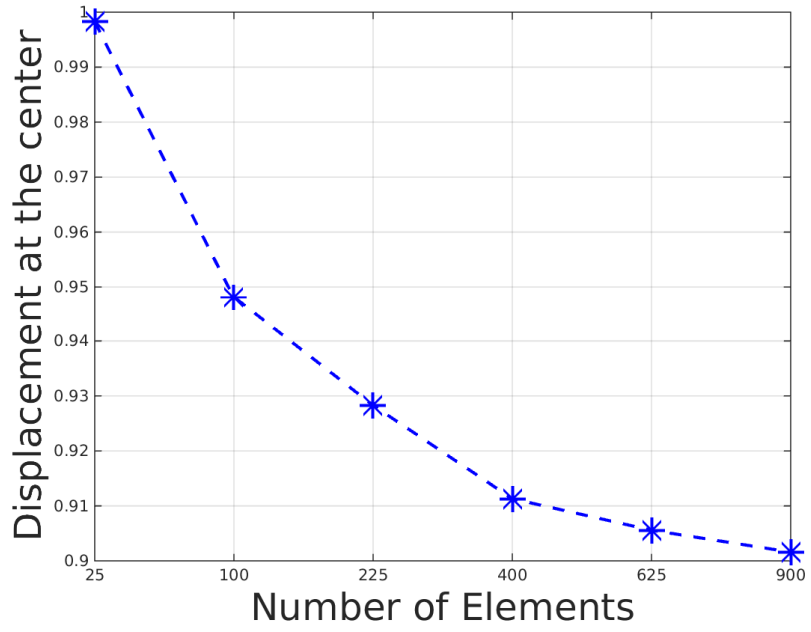

Figure 3.24: Displacement at the center of System I

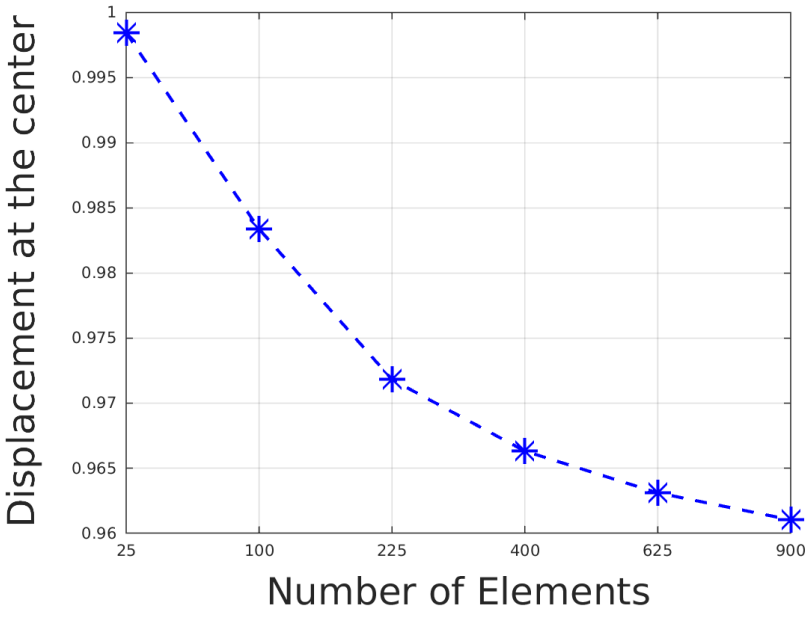

Figure 3.25: Displacement at the center of System II

From Figs. 3.22 and 3.24 it is seen that the displacement is converging to a certain value as the number of elements is increasing. For System II, from Figs. 3.23 and 3.25, a convergence is observed as the number of elements is increased. Thus, the appropriate number of elements can be determined according to the convergence rate that is acceptable for structural and control purposes. In order to satisfy the requirements, the appropriate number of elements can be determined as 400 for both System I and System II. This number can be increased if desired; however, it should be noted that this may lead to computational difficulties.

After determining the number of elements for the two systems, the first 6 mode shapes of both systems are obtained in order to observe how the actuator locations influence the structural behavior of the two systems. Figures 3.26 and 3.27 show the first 6 mode shapes of System I and System II, respectively.

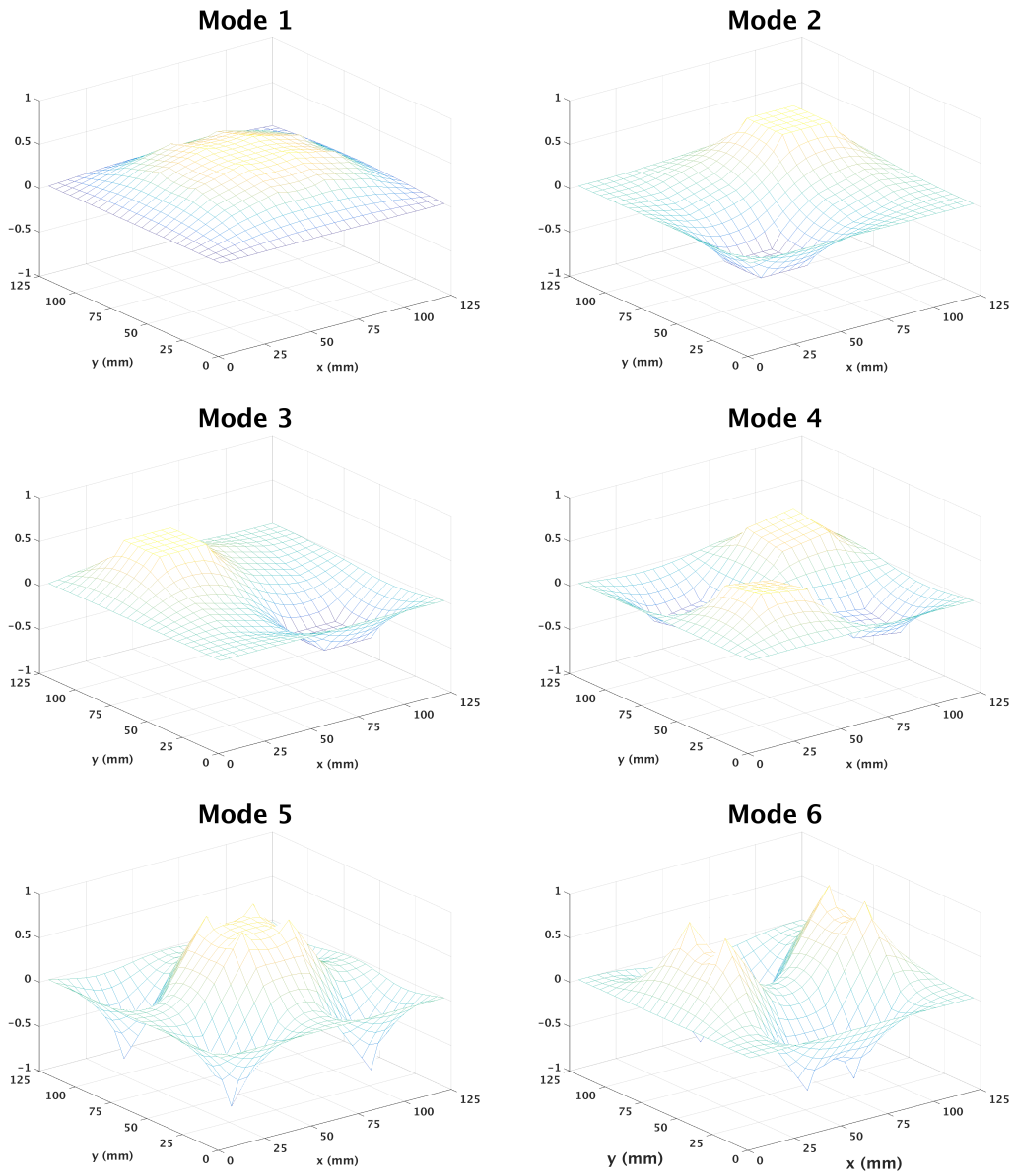

Figure 3.26: Mode shapes of System I

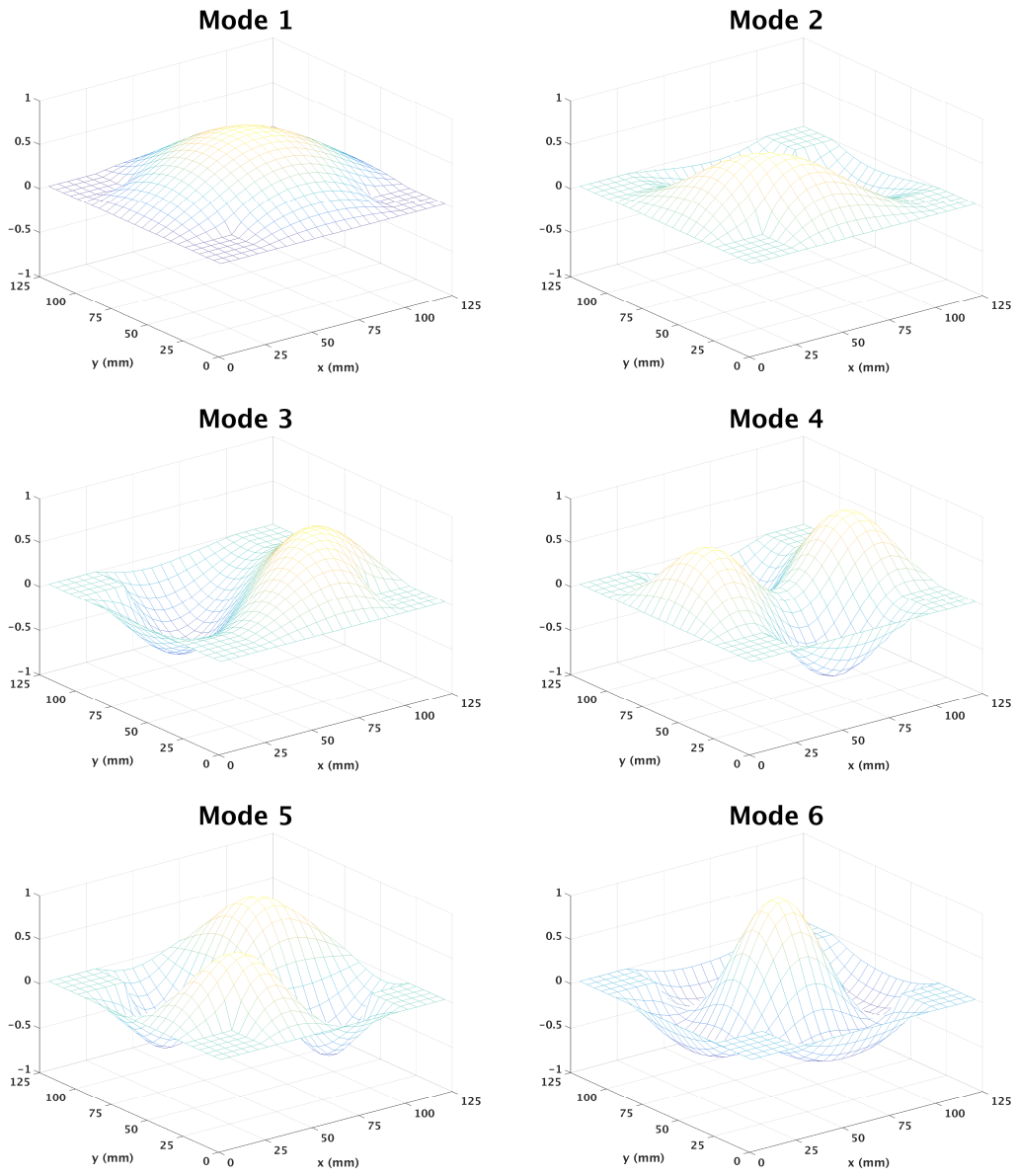

Figure 3.27: Mode shapes of System II

It is seen from Fig. 3.26 that for System I, the actuators away from the boundary of the membrane behave like lumped masses and cause the spatial derivative of the displacement to be apparently discontinuous at the boundary of the actuators, towards the central domain of the membrane. This behavior can be easily explained by the heterogeneity of the system; specifically, the membrane is very thin and light compared to the bimorph actuators. However, for System II, such drastic discontinuities in the spatial derivatives of the displacement are not

observed. They are confined to more restricted domains, i.e. near the membrane edges, away from the central domain of the membrane (Fig. 3.27), the actuators appear to behave like boundary constraints.

These issues can be solved using more compliant actuators (PVDF, MFC) or thinner actuators. However, this will also affect the control efficiency as demonstrated in Chapter 6. To be able see the structural effects of the actuator selection, the first two modes of membrane actuator systems, with different materials and actuator thickness, are demonstrated in Figs. 3.28-3.37.

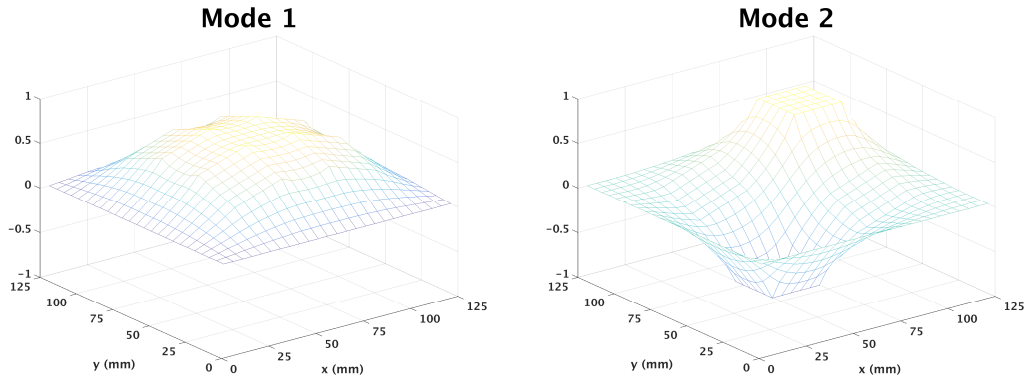

Figure 3.28: Mode shapes of System I for PZT actuator with $h = 534\mu m$

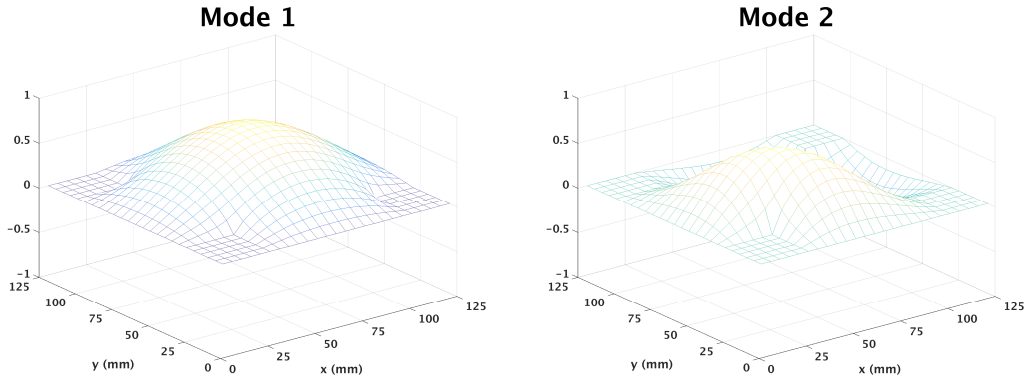

Figure 3.29: Mode shapes of System II for PZT actuator with $h = 534\mu m$

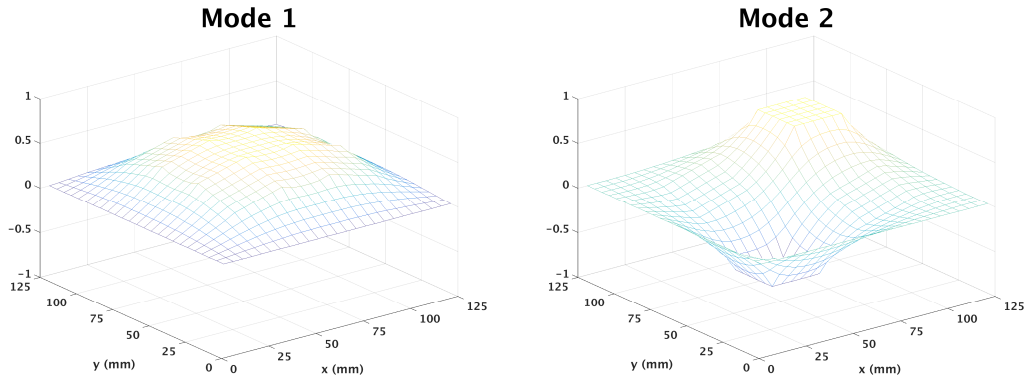

Figure 3.30: Mode shapes of System I for PZT actuator with $h = 191\mu m$

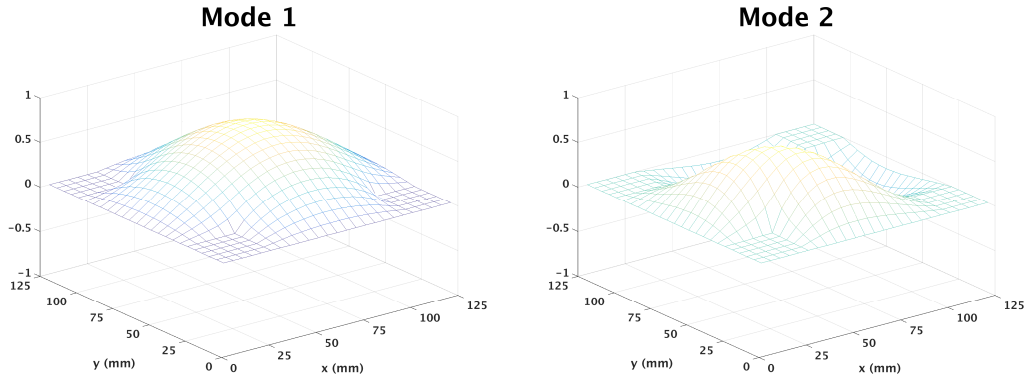

Figure 3.31: Mode shapes of System II for PZT actuator with $h = 191\mu m$

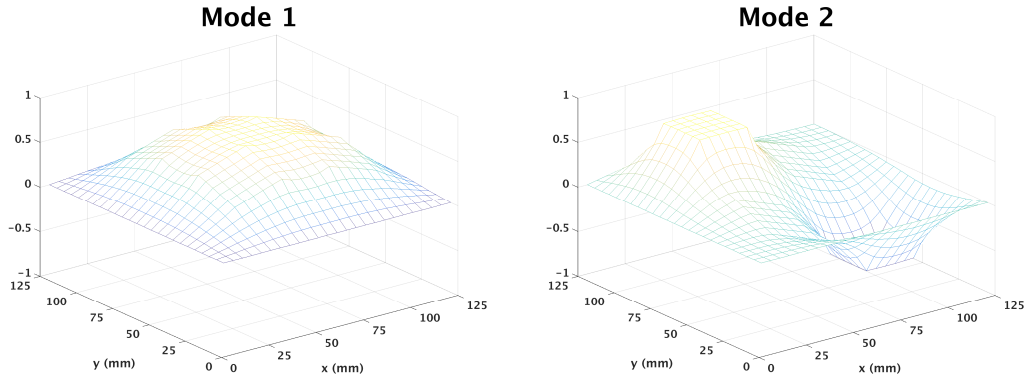

Figure 3.32: Mode shapes of System I for PZT actuator with $h = 127\mu m$

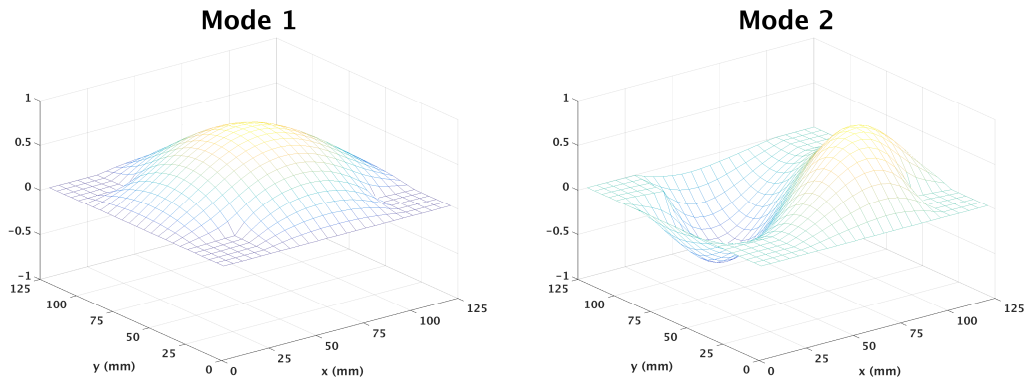

Figure 3.33: Mode shapes of System II for PZT actuator with $h = 127\mu m$

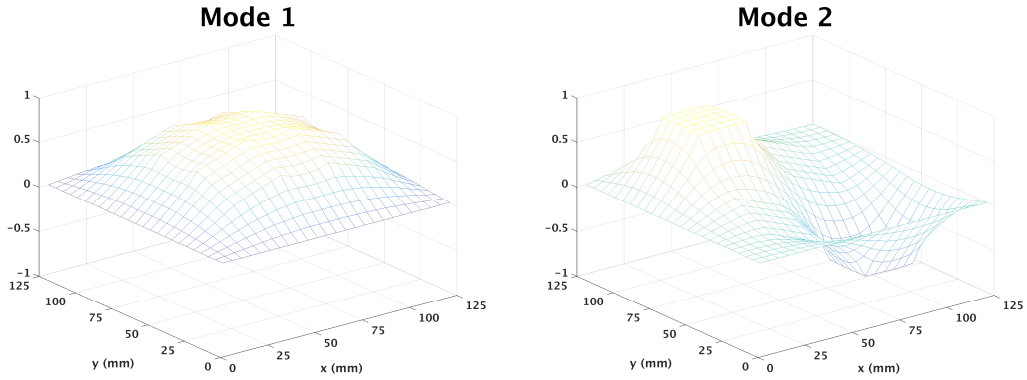

Figure 3.34: Mode shapes of System I for MFC actuator

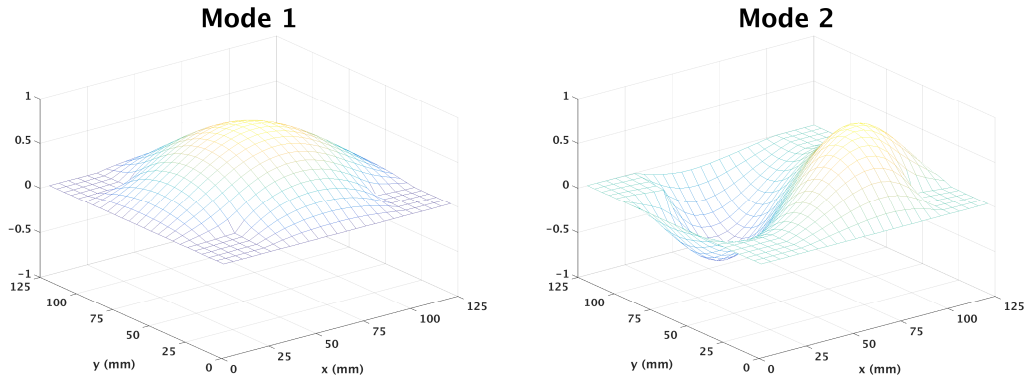

Figure 3.35: Mode shapes of System II for MFC actuator

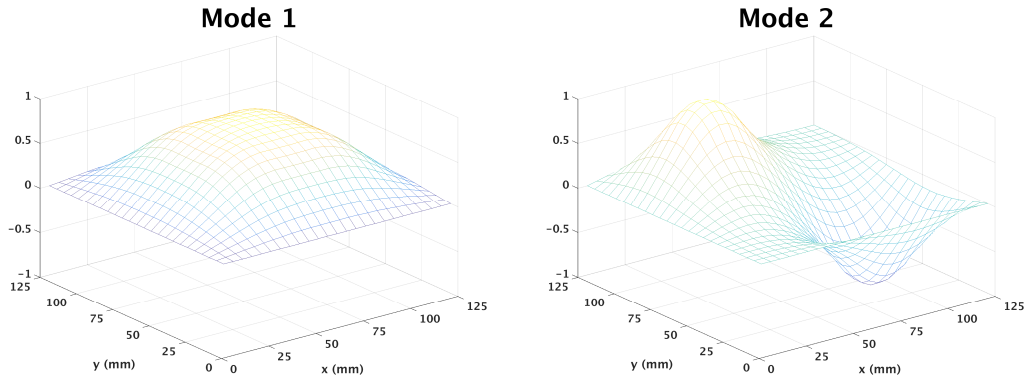

Figure 3.36: Mode shapes of System I for PVDF actuator

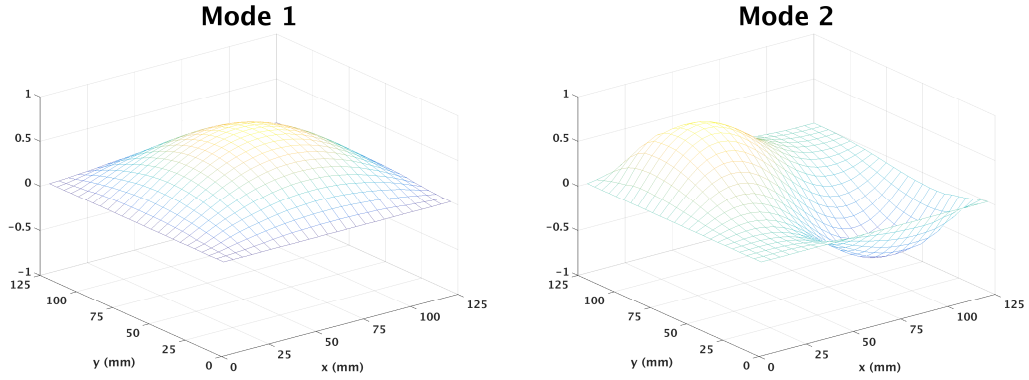

Figure 3.37: Mode shapes of System II for PVDF actuator

As seen from Fig. 3.28-3.37, PVDF eliminates the singularity issues due to its more compliant nature. However, reducing the thickness of the PZT actuator or using MFC do not have much structural effect on the system.

3.4 Chapter Summary

Modeling a system can be considered as one of the most important stages of analyzing and controlling a system, because any decision during modeling will affect the later stages. As it was emphasized before, the first step of modeling a system is having a clear understanding of what is being required from the model. In this case, a membrane structure with piezoelectric bimorph actuators attached to it is being modeled. The goal is suppressing the vibration of the membrane to have a feasible reflector. This requires to have a model that has enough detail to

apply an active control to a distributed system and that can be approximated to be able to carry out numerical evaluations.

For his purpose the system is approached as a thin plate that can be controlled under moment effects. As it is demonstrated in Section 3.2.1, modeling the system as membranes would not permit the usage of piezoelectric actuators as bending actuators. In Section 3.2.2, it is demonstrated that a plate has a bending resistance and creating a bending effect is considered as externally applied moment. In addition, the derivation of equation of motion for a plate shows that plates can also carry inplane loads that contribute the transverse displacement of the plate.

The invention, history and development of smart materials are reviewed in Section 3.2.3. The importance of smart materials in aerospace technology and structural control is tremendous as it enables us to control distributed systems using distributed actuators. The mechanism of how smart materials work has a crucial importance in modeling the membrane bimorph actuator system as it is carried out in detail in Section 3.2.3.

Analytical solution for a partial differential equation is not always possible, especially for complex geometries and heterogeneous systems. Therefore, the FEM is selected to approximate the system to be able to apply a numerical solution. One important criteria when applying a numerical solution is the convergence of the desired parameters. The closer the approximation is, the more accurate the solution is. However, the trade-off between the accuracy of the results and computational efficiency needs to be considered for practical applications. The derivation of the FEM and convergence check are carried out in Section 3.3.

Chapter 4

SYSTEM ANALSYS

4.1 Introduction

Since knowing the characteristics of the system accurately is crucial for developing a more appropriate control law, system characteristics such as stability, controllability and observability need to be analyzed thoroughly. This will determine if a working control law can be developed for the system, and what the performance of the control system will be. Developing and applying a control law without really knowing the system characteristics is a trial and error process that can be very time consuming, inefficient and non-optimal.

Conventional methods for analyzing characteristics of a system are based on the first order form of the equations of motion. When the dynamics of a system is obtained in vector second order form, first it needs to be converted to vector first order form to be able to analyze the system. However, the dynamics of most physical systems in mechanics is derived directly in vector second order form due to the physical characteristics. This means that most of the time the system needs to be converted to vector first order form by reducing the order of the equations of motion, which doubles the number of equations and loses the matrix characteristics. For high dimensional systems, like those describing the motion of heterogeneous membrane structures, this approach results in many difficulties ranging from numerical errors and numerically unstable algorithms, to difficult control design.

The most common remedy that is studied to overcome these problems is reducing the dimension of the system with Model Order Reduction (MOR) techniques. This method focuses on analyzing the system for only certain modes and frequencies and ignores the others. Even though this method works on many cases, reliability strongly depends on each case. However, model order reduction never gives full understanding of the system because of its inherent nature

which ignores many modes. Another drawback is controller and observer spillover effects. Due to the very flexible and lightly damped nature of the membrane structures, residual modes might lead to instabilities [9]. Therefore, vector second order form approaches were advocated by some researchers. Even though there are not many control design methods for vector second order form, there are methods already developed for system analysis such as stability, controllability and observability.

In the vector second order form approach, the system matrices, which are obtained directly from the equation of motion, do not need to be converted to vector first order form. The big advantage in this case is that we work directly in the generalized coordinate space so the dimensions of all the matrices are significantly smaller. Furthermore, inversion of potentially ill conditioned matrices is avoided, and symmetric matrices are predominantly used. The superiority of this approach is both improved numerical accuracy and reliability due to lower dimensions of the matrices and effective modern control designs [72, 73].

In this chapter, the system is analyzed using both conventional approach (vector first order form) and alternative approach (vector second order form). Stability of the system is analyzed in Section 4.2 using both methods. Section 4.3 shows the controllability tests and results of both methods. Observability of the system is analyzed in Section 4.4. Section 4.5 summarizes this chapter.

4.2 Stability

Stability of a system is the ability of the system to stay in the equilibrium condition after exposed to a disturbance. Another way to define stability is the total energy of the system such that if the energy of the system is increasing it is unstable, if it is decreasing it is stable, and if it is constant it is stable. To analyze a systems stability is very crucial to develop an effective control law. Sometimes, we may not be able to control all the modes of the system; thus, we need to make sure that the uncontrolled modes are stable. Or sometimes it can be redundant to try to control an already stable mode. There are a few methods developed to check the stability of a system. The most powerful method that covers a very large class of system is Lyapunov Stability Theory. The most general definition of Lyapunov stability states that an equilibrium point is stable if all solutions starting close to an equilibrium stays in that region, if they

converge to the equilibrium point it is asymptotically stable, if they do not stay in the region it is unstable [100]. This theorem gives sufficient condition for stability. The most general approach is proposing a positive definite Lyapunov function and checking its time derivative. For autonomous and linear systems, there are more specific techniques that are used in Section 4.2.1 and Section 4.2.2

4.2.1 Vector First Order Form

A typical equation of a motion of an LTI system in vector second order form for a dynamic system is showed in Equ. (4.2.1), which is derived in Chapter 3.

$$M\ddot{q} + C\dot{q} + Kq = F, \quad M > 0, \quad K = K_m + K_g > 0, \quad C \geq 0 \tag{4.2.1}$$

where M is the mass matrix, C is the damping matrix, and $K = K_m + K_g$ is the tangent stiffness matrix partitioned as material (K_m) and geometric (K_g) stiffness matrices. Also, F is the external force vector that can be written as $\bar{F}u$, where u is the control vector and $\bar{F}$ is the control matrix, whereas q is the vector of generalized coordinates. In the traditional approach of system analysis and control, a first order system of linear ordinary differential equations is obtained by converting the second order system of ordinary differential equations. This is easily achieved by defining the state vector as:

$$x = \begin{bmatrix} q \\ \dot{q} \end{bmatrix}, \quad q = \begin{bmatrix} q_1 \\ \vdots \\ q_n \end{bmatrix} \tag{4.2.2}$$

and writing it in the vector first order form as:

$$\dot{x} = Ax + Bu, \quad A = \begin{bmatrix} 0 & I \\ -M^{-1}K & -M^{-1}C \end{bmatrix}, \quad B = \begin{bmatrix} 0 \\ M^{-1}\bar{F} \end{bmatrix}, \qquad x(0)=x_0 \tag{4.2.3}$$

Here, A and B are called state and control matrices respectively, x is the state vector, u is the control vector, $\bar{F}$ is the control matrix for the vector second order system, n is the number of generalized coordinates, and m is the number of control inputs. It should be noted that the

equation of motion of a system can be obtained in vector first order form using Hamilton's principle. The generalized velocities are used as auxiliary dependent variables to generalized coordinates and *2n* dimensional state vector is obtained. Applying Hamilton's principle, the equation of motion in vector first order form is obtained as Hamilton's canonical equations [101]. This method preserves more physical insight than Newtonian method.

The stability tests for LTI systems in the first order state space form are performed using the eigenvalues of the state matrix. This is also called Lyapunov's indirect method [100]. An LTI system in the form of Equ. (4.2.3) is exponentially stable if and only if

$$\mathrm{Re}(\lambda_l) < 0, \;\; l = 1,...,2n \qquad \textit{for} \quad \textit{all} \quad \lambda_l \tag{4.2.4}$$

where λ_l is any eigenvalue of the state matrix, *A*. This test is very popular due to its generality (i.e. it applies to any first order system, not necessarily obtained from a vector second order form). The system is unstable if

$$\mathrm{Re}(\lambda_l) > 0, \;\; l = 1,...,2n \qquad \textit{for} \quad \textit{any} \quad \lambda_l \tag{4.2.5}$$

The unstable condition is valid if any of the eigenvalue satisfies Equ. (4.2.5), while to be stable all of the eigenvalues must satisfy Equ. (4.2.4). These cases are considered as having significant behaviors [101]. The third case is when the system has critical behavior, which is some or all eigenvalues of the state matrix have zero real part while the remaining eigenvalues have strictly negative real part.

4.2.2 Vector Second Order Form

When a vector second order system in the form of Equ. (4.2.1) is available to describe the system's linearized dynamics, a stability test can be carried out using directly this form. Specifically, an LTI system expressed in vector second order form is exponentially stable if and only if [71],

$$rank\begin{bmatrix} \omega_l^2 M - K \\ C \end{bmatrix} = n, \;\; l = 1,...,n \tag{4.2.6}$$

where n is the number of generalized coordinates and ω_l is natural frequencies of the system. The results obtained using both methods in Matlab are shown in Table 4.1. and 4.2.

Table 4.1: Stability analysis for System I

		Vector First Order Form		Vector Second Order Form	
NE	n	Undamped	Damped	Undamped	Damped
100	243	No	Yes	No	Yes
225	588	No	Yes	No	Yes
400	1083	No	Yes	No	Yes
625	1728	No	Yes	No	Yes

Table 4.2: Stability analysis for System II

		Vector First Order Form		Vector Second Order Form	
NE	n	Undamped	Damped	Undamped	Damped
100	243	No	Yes	No	Yes
225	588	No	Yes	No	Yes
400	1083	No	Yes	No	Yes
625	1728	No	Yes	No	Yes

In these tables, NE is the number of finite element and n is the degree of freedom. As seen in these tables, the systems are reported as not exponentially stable for the undamped cases and reported as exponentially stable for the damped cases, as expected. Note that the two tests give identical information for the stability. Here, the number of eigenvalues, λ_l, is twice the number of natural frequencies, ω_l. Also creation of the state matrix, A, requires inversion of the mass matrix, which might lead to numerical errors for ill conditioned, high dimensional systems.

In contrast, the test in Equ. (4.2.1) does not require inversion of any matrices, all matrices are symmetric, and of smaller size than the state matrix, *A*.

4.3 Controllability

Controllability of a system can be simply defined as: "a system is controllable if a control $u(t)$ exist such that any response requirement can be met" [71]. Therefore, knowing if a system is controllable or not is very important before we start designing a control law. A controller designed for an uncontrollable system may not give feasible results. The desired performance of the system also cannot be achieved with systematic approach. It is more trial and error method which is unreliable and inefficient.

Another importance of checking the controllability of the system is being able to optimize the actuator numbers and locations [8]. Actuators themselves can have a great impact on the system's dynamics. Having more than necessary actuators can have undesired financial and structural results. This might affect the performance of the systems, as well as the range of practical application.

The methods for checking controllability of a system were developed mostly in vector first order form. These method require the use of higher dimensions as well as the calculation of rank of a very large matrix. Therefore, having a method that uses vector second order form directly is more reliable and computationally efficient. These methods are described in the following Subsections 4.3.1 and 4.3.2.

4.3.1 Vector First Order Form

The mathematical expression of a system's controllability is defined as: a system (Equ. (4.2.3)) is controllable at the initial time (t_0) if there exist a control $u(t)$ that can take the arbitrary initial state $x(t_0)$ to a desired final state $x(t_f)$ in a finite time [71]. The standard test for the controllability of LTI systems uses the vector first order form and states that a system in the form of Equ. (4.3.1) is controllable if and only if [71]

$$rank(\mathbb{C}(A,B)) = 2n \tag{4.3.1}$$

where $\mathbb{C}(A,B)$ is the controllability matrix defined as:

$$\mathbb{C}(A,B) = [B \quad AB \quad A^2B \quad ... \quad A^{2n-1}B] \tag{4.3.2}$$

Even though apparently very simple, there are several issues with this test. First, since the power of matrix A increases as the number of generalized coordinates (n) increases, any numerical error will accumulate rapidly and computation of the rank of the controllability matrix $\mathbb{C}(A,B)$ will be increasingly unreliable. Also, the size of the controllability matrix is $2n \times 2nm$ so the number of columns increases with the number of actuators, which is an additional source of numerical errors. Lastly, this is a global controllability test, which, in case it yields a negative result, does not provide immediate information about the uncontrollable modes.

From this last perspective, a better controllability test is the Popov-Hautus-Rosenbrock (PHR) test [102]. The PHR test uses the vector first order form of the equations of motion and the eigenvalues of matrix A: an LTI system in the form of Equ. (4.2.3) is controllable if and only if

$$rank\left[\left(\lambda_l I - A\right) \;\; B\right] = 2n, \;\; l = 1,...,2n \tag{4.3.3}$$

for all eigenvalues, λ_l, of matrix A; and I is the identity matrix. Clearly, the PHR test immediately identifies the uncontrollable modes and the expected accumulated numerical error is less than the error resulted when calculating the rank of the controllability matrix because the matrices involved in Equ. (4.3.3) have smaller dimensions, i.e. $2n \times 2(n+m)$. However, the PHR test requires calculation of the rank of matrices which may still have high dimensions.

4.3.2 Vector Second Order Form

A system in the form of Equ. (4.2.1) is controllable if and only if [71]

$$rank\left[\lambda_l^2 M + \lambda_l C + K \quad \bar{F}\right] = n, \;\; l = 1,...,2n \tag{4.3.4}$$

where λ_l is any eigenvalue of matrix A. Remark that for this test we do not need to take powers of any matrices, like in the standard test. Also, the dimensions of the matrices involved in this test (i.e. $n\times(n+m)$) are significantly smaller than the dimension of the controllability matrix and the ones used in the PHR test. It should also be noted that this is a modal controllability test, indicating specifically which mode is not controllable. The specific features of the test (Equ. (4.3.4)) allows the computation of the rank much more efficiently and reliably. This is revealed in Tables 4.3-4.6 which show the results obtained using all three methods (i.e. Equ. (4.3.1), (4.3.3) and (4.3.4)) in Matlab. In these tables, NA stands for "Not Available".

Table 4.3: Controllability analysis for undamped System I

		Vector First Order Form		Vector Second Order Form
NE	*n*	Rank of Cont. Matrix	Rank of PHR Matrix	Controllability
100	243	NA	No	Yes
225	588	NA	No	Yes
400	1083	NA	No	Yes
625	1728	NA	No	Yes

Table 4.4: Controllability analysis for damped System I

		Vector First Order Form		Vector Second Order Form
NE	*n*	Rank of Cont. Matrix	Rank of PHR Matrix	Controllability
100	243	NA	No	Yes
225	588	NA	No	Yes
400	1083	NA	No	Yes
625	1728	NA	No	Yes

Table 4.5: Controllability analysis for undamped System II

		Vector First Order Form		Vector Second Order Form
NE	*n*	Rank of Cont. Matrix	Rank of PHR Matrix	Controllability
100	243	NA	No	Yes
225	588	NA	No	Yes
400	1083	NA	No	Yes
625	1728	NA	No	Yes

Table 4.6: Controllability analysis for damped System II

		Vector First Order Form		Vector Second Order Form
NE	*n*	Rank of Cont. Matrix	Rank of PHR Matrix	Controllability
100	243	NA	No	Yes
225	588	NA	No	Yes
400	1083	NA	No	Yes
625	1728	NA	No	Yes

Compared to the stability analysis, different results for the controllability are obtained depending on the method that is used. The controllability check using the controllability matrix for the vector first order form did not give *any* results for large number of elements due to numerical problems. The controllability matrix consists of very large or small numbers, reported by Matlab as infinite/NaN numbers; thus, the rank cannot be calculated. This is an important problem because as discussed before, in order to correctly capture many natural frequencies of the system (or eigenvalues of matrix *A*), a large number of elements must be used. However, this leads to unreliable controllability tests if the vector first order form is used. On the other hand, the PHR test reported both systems not controllable. However, the test that uses the second order form did not raise any issues and both systems were clearly identified as controllable. As it is neen in Chapter 6, both system are controllable and the controllers, that are developed, suppress the vibrations effectively. One reason for PHR test to give results as not controllable might be the values of *A* matrix that are close to singular values.

4.4 Observability

Similar to concept of the controllability, observability is simply described as the ability to estimate the system's state with the existing measurements. As a results, knowing if a system is observable or not, has similar importance as knowing a system's controllability. Without knowing the state variables of the system, we cannot know if the controller is affecting the system the way we desire.

Again in a similar way, knowing the observability of a system allows us to optimize the number and placement of the sensors [8]. Sensors, like actuators, have structural impact on the system. Having redundant sensors can affect the system's performance as well as the cost of the system. Furthermore, the practical applicability of having many sensors might not be possible for many structures.

Similar to controllability, the methods for checking the observability of a system were developed mostly for vector first order form. This method requires the use of higher dimensions as well as the calculation of rank of a very large matrix. The methods developed for directly vector second order form can help remedy this issue and have more reliable and computationally efficient system analysis. These methods are carried out in the following Subsections 4.4.1 and 4.4.2.

4.4.1 Vector First Order Form

Similar to the standard test for controllability of LTI systems, the observability test uses the first order form and states that a system in the form of Equ. (4.2.3) and with an output as:

$$y = H_1 q + H_2 \dot{q} = Hx \tag{4.4.1}$$

is observable if and only if [102]

$$rank(\mathrm{O}(A, H)) = 2n \tag{4.4.2}$$

where $\mathrm{O}(A, H)$ is the observability matrix defined as:

$$\mathrm{O}(A,H)=\begin{bmatrix} H \\ HA \\ HA^2 \\ \vdots \\ HA^{2n-1} \end{bmatrix} \tag{4.4.3}$$

Similar to controllability test, there are several issues with this test too. The power of matrix A increases as the number of generalized coordinates (n) increases, any numerical error will accumulate rapidly and computation of the rank of the observability matrix $\mathrm{O}(A,H)$ will be increasingly unreliable. Lastly, this is a global observability test, which, in case it yields a negative result, does not provide immediate information about the uncontrollable modes. In addition to checking the observability of a system calculating the rank of the observability matrix, the PHR test can be used to check the observability of the system in a similar way to the controllability check.

4.4.2 Vector Second Order Form

A system in the form of Equ. (4.2.1) and Eq.(4.4.1) is observable if and only if [71]

$$rank\begin{bmatrix} \lambda_l^2 M+\lambda_l C+K \\ H_1+\lambda_l H_2 \end{bmatrix}=n,\quad l=1,\ldots,2n \tag{4.4.4}$$

where λ_l is any eigenvalue of matrix A. Similar to controllability test, for this test we do not need to take powers of any matrices, like in the standard test. Also the dimensions of the matrices involved in this test (i.e. $(n+m)\times n$ for the case $H=\bar{F}^T$) are significantly smaller than the dimension of the observability matrix. This is a modal observability test, indicating specifically which mode is not observable. The specific features of the test (Equ. (4.4.4)) allow the computation of the rank much more efficiently and reliably.

The observability tests are carried out for the systems with an output vector defined in Equ. (4.4.5). The sensors were assumed to have negligible effect on the system's dynamics.

$$y = \bar{F}^T q + \bar{F}^T \dot{q} \tag{4.4.5}$$

The results, obtained using both method for undamped and damped systems, are summarized in the Tables 4.7-4.10.

Table 4.7: Observability analysis for undamped System I

		Vector First Order Form	Vector Second Order Form
NE	*n*	Rank of Obsv. Matrix	Observability
100	243	NA	Yes
225	588	NA	Yes
400	1083	NA	Yes
625	1728	NA	Yes

Table 4.8: Observability analysis for damped System I

		Vector First Order Form	Vector Second Order Form
NE	*n*	Rank of Obsv. Matrix	Observability
100	243	NA	Yes
225	588	NA	Yes
400	1083	NA	Yes
625	1728	NA	Yes

Table 4.9: Observability analysis for undamped System II

		Vector First Order Form	Vector Second Order Form
NE	*n*	Rank of Obsv. Matrix	Observability
100	243	NA	Yes
225	588	NA	Yes
400	1083	NA	Yes
625	1728	NA	Yes

Table 4.10: Observability analysis for damped System II

NE	*n*	Vector First Order Form	Vector Second Order Form
		Rank of Obsv. Matrix	Observability
100	243	NA	Yes
225	588	NA	Yes
400	1083	NA	Yes
625	1728	NA	Yes

The same way with the controllability results, observability check using the observability matrix for the vector first order form did not give *any* result for large number of elements due to numerical problems. The observability matrix consists of very large or small numbers, reported by Matlab as infinite/NaN numbers, thus the rank cannot be calculated. On the other hand, the test that uses the vector second order form did not raise any issues, and both systems were clearly identified as observable. This clearly shows the advantages of the vector second order form test.

4.5 Chapter Summary

Analyzing a system is the first step to develop a controller for the system as we cannot know how the system will react to any control being applied. This puts more emphasis on the accuracy of the system analysis. The conventional methods to analyze a system's control characteristic such as the stability, controllability and observability are grouped under the vector first order form. These methods are used by most of the engineers and scientists as they are common and well established in control research area. However, the developing technology and the new inventions require us to work with high dimensional systems with higher accuracy demand. One alternative to this is using the methods developed directly by vector second order form. This immediately reduces the number of equations, that needs to be solved, to half. Furthermore, this approach allows us to omit the steps required to reduce the order of the system as well as the matrices can be kept the way they are derived in the equation of motion. This gives further numerical advantages as the mass, damping and stiffness matrices are usually symmetric and positive definite.

As demonstrated in Section 4.2, stability analysis is mostly depend on the eigenvalues of the system so similar results are obtained for both vector first order and vector second order forms. However, when there are very high dimensional matrices with elements close to singular values, Matlab is not able to calculate the rank of the controllability or the observability matrices. The results, that are obtained using vector second order form, are shown in detail in Sections 4.3 and 4.4. As this step is very crucial before any control attempt, it can clearly be stated that the methods developed using vector second order form are more superior to vector first order form.

Chapter 5

CONTROLLER DEVELOPMENT

5.1 Introduction

Control of structures has become a very important area of research in the last few decades due to technological developments such as the invention of smart materials and the high computational capacity of computers. The early attempts of structural control were mostly passive control, in which the output did not have an effect on the input. For example, to suppress the vibration of space structures, extra layers were added to the structures to dampen the system, which lead to heavy sluggish systems. With the invention of piezoelectric materials, we are able implement active control, which enables us to have a lighter and more efficient system.

Vibration on a mechanical system can have detrimental effects on the system such as failure, comfort, and operation of precision devices. For a feasible membrane system that is being used as a reflector, the critical requirement for control system design should be that it effectively eliminates the vibrations. Furthermore, the control energy used for this purpose should be small in order to limit the size of the power supply system (e.g., batteries). To account for both requirements, a cost function that combines vibration and control energy measures can be used. Its minimization via feedback control design will result in small control energy *and* small vibrations. Because multi-input multi-output (MIMO) LTI models for the membrane dynamics are available, this control design task is facilitated by modern control theory such as Linear Quadratic Regulator (LQR). In LQR design, a quadratic cost function that combines both control energy and state measures is minimized via state feedback control, so it is appropriate for simultaneous reduction of vibrations and control energy. Further advantages of LQR consist of its guaranteed strong robustness properties and the low computational cost.

However, the fundamental issue with the LQR theory is it assumes that all the states are available for feedback, which is often not the case; in practice only some measurements are available, not the entire state vector. Moreover, these measurements, as well as the system, are affected by disturbances. If these disturbances cannot be neglected, we have to consider their effect on the system and the measurements when designing controllers. Therefore, we need to estimate the state of the system. For Linear Time Invariant (LTI) systems, this is accomplished by the Kalman filter. Then, based on the state estimates a controller can be designed. This is the essence of Linear Quadratic Gaussian (LQG) control theory, in which disturbances are assumed to be zero-mean Gaussian white noises. Most of the time, disturbances in a real environment can be classified as Gaussian signals. Therefore, LQG control is very useful in many cases. One drawback is that LQG control does not always guarantee stability robustness [103]. However, we can still check the stability limits numerically via parameter sensitivity analysis.

In this chapter, the controller development for the membrane actuator system is studied. Section 5.2 derives the two conventional optimal controllers which are Linear Quadratic Regulator (LQR) and Linear Quadratic Gaussian (LQG) control using the vector first order form. The alternative approach of developing LQR and LQG controller using vector second order form is carried out in Section 5.3. One way to achieve this is to obtain a reduced Algebraic Riccati Equation and the other is by using a variational calculus based on the Hamiltonian Approach. These methods are derived in detail in Subsections 5.3.1-5.3.2, respectively. The summary of the chapter is given in Section 5.4.

5.2 Conventional Optimal Control

Control theories and control engineering were developed mostly by mathematicians and physicists in the first half of the twentieth century [8]. Control of mechanical systems has become a more important area of research for engineers and researchers in mechanics during the 1960s. As a result, most control theories have been developed using vector first order form. These theories are well established and largely being implemented in industry. Therefore, they are very popular among control researchers today even though they require an extra step to convert vector second order systems to the vector first order form. The following subsection will summarize the LQR and LQG controller development in vector first order form.

5.2.1 LQR

Let *x*, *y* and *u* denote the state, output and input (i.e. control) vectors, respectively. Output and input vectors are related to the system's state vector, *x*, via linear relationships [71] as:

$$\dot{x} = Ax + Bu, \qquad x(0)=x_0 \tag{5.2.1}$$

$$y = Hx = H_1 q + H_2 \dot{q} \tag{5.2.2}$$

$$u = Gx \tag{5.2.3}$$

where *A* and *B* are called state and control matrices respectively. The infinite time horizon LQR problem consists of designing the linear state feedback controller, $u = Gx$, that drives the system to equilibrium from nonzero initial states, while minimizing an integral quadratic cost function, *V*. Formally, the LQR problem is stated as:

$$\begin{aligned} &\textit{minimize} && V = \int_0^\infty \left(y^T Q y + u^T R u \right) dt \\ &\textit{subject to} && \dot{x} = Ax + Bu \\ & && y = Hx \end{aligned} \tag{5.2.4}$$

Here, $Q \geq 0$ and $R > 0$ are semi positive definite and positive definite matrices called state and control penalties (weights), respectively. The traditional LQR approach is using states to penalize the energy due to displacement assuming that we can measure all the states. However, this is not usually realistic since we may not measure all the states; therefore, the output vector is penalized instead of the state vector.

Under fairly general conditions (e.g., stabilizability of the (*A*,*B*) pair and detectability of the $(A, H^T Q^{1/2})$ pair), the feedback gain matrix *G* is easily obtained after solving a matrix Riccati equation:

$$\Sigma A + A^T \Sigma - \Sigma B R^{-1} B^T \Sigma + H^T Q H = 0, \quad G = -R^{-1} B^T \Sigma \tag{5.2.5}$$

where Σ is the positive semidefinite solution to the Algebraic Riccati Equation. The minimum cost is calculated as:

$$V_{\min} = x_0^T \Sigma x_0 \tag{5.2.6}$$

This solution is clearly straightforward and numerically very reliable for small sized systems. However, as it is already seen in the previous chapter, the first order form may be inadequate for large dimensional systems because of significant numerical difficulties. One solution to this issue addressed by Massioni et al. is a simple approximate solution of Algebraic Riccati Equation for the discrete time low voice measurement case [104]. However, this is only for a specific case.

5.2.2 LQG

A system under Gaussian white noise is defined in first order form as:

$$\dot{x} = Ax + Bu + Lw_p, \qquad x(0) = x_0 \tag{5.2.7}$$

$$y = Hx + v_p \tag{5.2.8}$$

where A and B are called state and control matrices respectively, L is the disturbance input matrix, x is the state vector, u is the control vector, y is the measurement, w_p and v_p are stationary, zero mean, un-correlated Gaussian white noise processes with power spectral density W_p and V_p, respectively.

The LQG problem is stated as follows [105]: Find a dynamic feedback controller for the system Equ. (5.2.7)-(5.2.8) which minimizes:

$$\lim_{t\to\infty} E\left\{y^T Q y + u^T R u\right\} \tag{5.2.9}$$

Here, "E" represents the expected value of X defined as $E\{\mathrm{X}\} = \int_{-\infty}^{+\infty} \mathrm{X} p(\mathrm{X}) d\mathrm{X}$, where $p(\mathrm{X})$ is the probability density function of X, and X is a random distribution. Matrices $R > 0$ and $Q \geq 0$ represent "input" and "state" penalty matrices, respectively.

The approach to solve this problem is to use the "separation principle". First develop an LQR by solving the system without an external disturbance as derived in Section 5.2.1. Next, determine the steady-state observer gain T for the state observer using Kalman filtering. The linear system, which constructs an optimal estimate for the state called $\hat{x}$ is:

$$\dot{\hat{x}} = A\hat{x} + Bu + T\left(y - H\hat{x}\right) \tag{5.1.10}$$

$$T = \bar{\Sigma} H^T V^{-1} \tag{5.2.11}$$

The estimation is optimal because it minimizes the estimation error,

$$\lim_{t\to\infty} E\left\{\left(x - \hat{x}\right)^T \left(x - \hat{x}\right)\right\} \tag{5.2.12}$$

where $\bar{\Sigma}$ is the unique positive semidefinite solution to the Algebraic Riccati Equation defined below, assuming $\left(A, LW_p^{1/2}\right)$ is stabilizable and (A,H) is detectable:

$$\bar{\Sigma}A^T + A\bar{\Sigma} - \bar{\Sigma}H^T V^{-1} H\bar{\Sigma} + LW_p L^T = 0 \tag{5.2.13}$$

After obtaining the optimal control gain G, it can be used to obtain the optimal control $\left(u^* = G\hat{x}\right)$ in terms of estimated state vector, $\hat{x}$; and rewriting Equ. (5.2.7) and Equ. (5.2.10), the following expression are obtained as:

$$\dot{x} = Ax + B\left(G\hat{x}\right) + Lw_p \tag{5.2.14}$$

$$\dot{\hat{x}} = A\hat{x} + B\left(G\hat{x}\right) + T\left(y - H\hat{x}\right) \tag{5.2.15}$$

Defining $e = x - \hat{x}$ as a state error vector, the dynamics for the error below can be writes as follows:

$$\dot{e} = \left(A - TH\right)e + Lw_p - Tv_p \tag{5.2.16}$$

Equ. (5.2.14) can be rewritten in terms of x and e as:

$$\dot{x} = Ax + BG(x - e) + Lw_p \tag{5.2.17}$$

Combining Equ. (5.2.16) and Equ. (5.2.17), the closed loop system is obtained as follows:

$$\begin{pmatrix} \dot{x} \\ \dot{e} \end{pmatrix} = \begin{pmatrix} A + BG & BG \\ 0 & A - TH \end{pmatrix} \begin{pmatrix} x \\ e \end{pmatrix} + \begin{pmatrix} Lw_p \\ Lw_p - Tv_p \end{pmatrix} \tag{5.2.18}$$

5.3 Vector Second Order Forms

Since the most reliable tests for the controllability, observability, and stability proved to be those that use the vector second order form, it is natural to attempt feedback control design using this formulation of the equations of motion instead of the vector first order form that is traditionally used in control design. One approach to develop optimal control is by partitioning the solution of the Algebraic Riccati Equation and substituting it the Algebraic Riccati Equation to obtain a direct result from the system's dynamics in vector second order form. Another approach uses variational calculus techniques (e.g., the Hamiltonian method) to develop the LQR solution for systems expressed in vector second order form.

5.3.1 LQR and LQG using Reduced Algebraic Riccati Equation

LQR problem for vector second order form is defined as:

$$\begin{aligned} &\textit{minimize} && V = \int_0^\infty \left(y^T Q y + u^T R u \right) dt \\ &\textit{subject to} && M\ddot{q} + C\dot{q} + Kq = \bar{F}u \\ & && y = H_1 q + H_2 \dot{q} \end{aligned} \tag{5.3.1}$$

When we use the first order system to develop the LQR for the system that is defined by Equ. (5.2.1), assuming the (A,B) pair is at least stabilizable and $(A, H^T Q^{1/2})$ is at least detectable, there is a unique positive semidefinite solution Σ to the Algebraic Riccati Equation as derived in Section 5.2.1. In order to use the vector second order form and LQR formulation, the matrix

solution matrix (Σ) is partitioned and substituted into the Algebraic Riccati Equation (Equ. (5.2.5)) to obtain the following sets of results. Let

$$\Sigma = \begin{bmatrix} P & S \\ S^T & U \end{bmatrix} \geq 0 \tag{5.3.2}$$

After substitution of Equ. (5.3.2) into Equ. (5.2.5), the following set of equations are derived as:

$$-SM^{-1}K - \left(M^{-1}K\right)^T S^T - SM^{-1}\bar{F}R^{-1}\left(M^{-1}\bar{F}\right)^T S^T + H_1^T Q H_1 = 0 \tag{5.3.3}$$

$$S^T - UM^{-1}C + S - \left(M^{-1}C\right)^T U - UM^{-1}\bar{F}R^{-1}\left(M^{-1}\bar{F}\right)^T U + H_2^T Q H_2 = 0 \tag{5.3.4}$$

$$P - SM^{-1}C - \left(M^{-1}K\right)^T U - SM^{-1}\bar{F}R^{-1}\left(M^{-1}\bar{F}\right)^T U + H_1^T Q H_2 = 0 \tag{5.3.5}$$

In addition, the optimal control law can be written as:

$$u = G_1 q + G_2 \dot{q}, \quad G_1 = -R^{-1}\bar{F}^T S, \quad G_2 = -R^{-1}\bar{F}^T U \tag{5.3.6}$$

In general, Equ. (5.3.3-5.3.5) cannot be easily solved; however, if the problem is relaxed by assuming that $S = S^T$, Equ. (5.3.3) becomes an Algebraic Riccati Equation that can be solved immediately. Since the equations are decoupled, the equations can be solved one by one in the order of: Equ. (5.3.3) for *S*, Equ. (5.3.4) for *U*, and Equ. (5.3.5) for *P*. Note that the assumption $S = S^T$ might not lead to the optimal solution if the requirements on $\sum$ are not met; however, the computational advantages are tremendous. In practice, one implements the controller if satisfactory results are obtained.

Similar to the vector first order form, an LQG control problem for vector second order form is described for a system under Gaussian white noise defined in vector second order form as:

$$M\ddot{q} + C\dot{q} + Kq = \bar{F}u + \ell w_p \qquad q(0) = q_0, \qquad \dot{q}(0) = \dot{q}_0, \tag{5.3.7}$$

$$y = H_1 q + H_2 \dot{q} + v_p = Hx + v_p \tag{5.3.8}$$

where ℓ is the disturbance input matrix, w_p and v_p are stationary, zero mean, un-correlated Gaussian white noise processes with power spectral density W_p and V_p, respectively. The LQG problem is stated similar to the vector first order form. Find a dynamic feedback controller for the system (Equ. (5.3.7)-(5.3.8)) which minimizes:

$$\lim_{t\to\infty} E\left\{y^T Q y + u^T R u\right\} \tag{5.3.9}$$

Here, "E" represents the expected value of X defined as $E\{\mathrm{X}\} = \int_{-\infty}^{+\infty} \mathrm{X} p(\mathrm{X}) d\mathrm{X}$, where p(X) is the probability density function of X, and X is a some random distribution. Matrices $R > 0$ and $Q \geq 0$ represent "input" and "state" penalty matrices, similar to the vector first order form.

The approach to solve this problem is also the same approach used in the vector first order form, which is to use the "separation principle", first develop an LQR by solving the LQR problem, and then developing a Kalman filtering to estimate the state. The LQR problem is developed previously for vector second order form. In the same way, to develop the Kalman filtering, the solution matrix $\left(\bar{\Sigma}\right)$ is partitioned and substituted it into the Algebraic Riccati Equation (Equ. (5.2.13)) such that:

$$\bar{\Sigma} = \begin{bmatrix} \bar{P} & \bar{S} \\ \bar{S}^T & \bar{U} \end{bmatrix} \geq 0 \tag{5.3.10}$$

After substituting Equ. (5.3.10) into Equ. (5.2.13), the following sets of equations are derived as:

$$\bar{S} + \bar{S}^T - (H_1\bar{P} + H_2\bar{S}^T)^T V^{-1}(H_1\bar{P} + H_2\bar{S}^T) = 0 \tag{5.3.11}$$

$$-\bar{P}\left(M^{-1}K\right)^T - \bar{S}\left(M^{-1}C\right)^T + \bar{U} - (H_1\bar{P} + H_2\bar{S}^T)^T V^{-1}(H_1\bar{S} + H_2\bar{U}) = 0 \tag{5.3.12}$$

$$\begin{aligned} &-\bar{S}^T\left(M^{-1}K\right)^T - \bar{U}\left(M^{-1}C\right)^T - M^{-1}K\bar{S} - M^{-1}C\bar{U} \\ &-(H_1\bar{S} + H_2\bar{U})^T V^{-1}(H_1\bar{S} + H_2\bar{U}) + M^{-1}\ell W(M^{-1}\ell)^T = 0 \end{aligned} \tag{5.3.13}$$

These equations cannot be solved independently in sequence since they are highly coupled. The only approach would be applying numerical solutions. However, under special

circumstances, these equations can take the form of Algebraic Riccati Equations and can be solved with existing methods. To obtain the observer gain in vector second order form, Equ. (5.3.10) is substituted into Equ (5.2.15), and the expression for the Kalman filtering is derived such that:

$$\begin{bmatrix}\dot{\hat{q}}\\ \ddot{\hat{q}}\end{bmatrix}=\begin{bmatrix}0 & I\\ -M^{-1}K & -M^{-1}C\end{bmatrix}\begin{bmatrix}\hat{q}\\ \dot{\hat{q}}\end{bmatrix}+\begin{bmatrix}0\\ M^{-1}F'\end{bmatrix}u+\begin{bmatrix}\bar{P} & \bar{S}\\ \bar{S}^T & \bar{U}\end{bmatrix}\begin{bmatrix}H_1\\ H_2\end{bmatrix}V^{-1}\underbrace{(y-H\hat{x})}_{\tilde{y}}$$

$$\begin{bmatrix}\dot{\hat{q}}\\ \ddot{\hat{q}}\end{bmatrix}=\begin{bmatrix}\dot{\hat{q}}\\ -M^{-1}K\hat{q}-M^{-1}C\dot{\hat{q}}\end{bmatrix}+\begin{bmatrix}0\\ M^{-1}F'u\end{bmatrix}+\begin{bmatrix}\left(\bar{P}H_1+\bar{S}H_2\right)V^{-1}\tilde{y}\\ \left(\bar{S}^TH_1+\bar{U}H_2\right)V^{-1}\tilde{y}\end{bmatrix} \tag{5.3.14}$$

$$\dot{\hat{q}}=\dot{\hat{q}}+\left(\bar{P}H_1+\bar{S}H_2\right)V^{-1}y \tag{5.3.15}$$

$$\begin{aligned}\ddot{\hat{q}}&=-M^{-1}K\hat{q}-M^{-1}C\dot{\hat{q}}+M^{-1}Fu+\left(\bar{S}^TH_1+\bar{U}H_2\right)V^{-1}\tilde{y}\\ \ddot{\hat{q}}+M^{-1}C\dot{\hat{q}}+M^{-1}K\hat{q}&=M^{-1}Fu+\underbrace{\left(\bar{S}^TH_1+\bar{U}H_2\right)V^{-1}}_{\zeta}\tilde{y}\end{aligned} \tag{5.3.16}$$

The Kalman gain is given by

$$\zeta=\left(\bar{S}^TH_1+\bar{U}H_2\right)V^{-1}\tilde{y} \tag{5.3.17}$$

5.3.1.1 Specials Solutions

As demonstrated before, the Equ. (5.3.3-5.3.5) and Equ. (5.3.11-5.3.13) do not have analytical solutions. However, under many special situations certain terms will be zero and the new expressions will have simple solutions. These situations can be no damping situations, special sensor or actuator placements, or non-physical phenomena such as financial systems etc. Some special cases are carried out as following.

A Simple LQR Case

One of the most feasible situation for LQR application is undamped collocated actuator sensor system. Consider a system that has no damping and is expressed in vector second order form. The traditional approach to LQR design is to convert the system to vector first order form as in Equ. (5.2.1) and to apply Equ. (5.2.5). However, there is an important practical situation when this is not necessary and the LQR problem can be directly solved using the vector second order form. This situation is when sensors and actuators are collocated, i.e. the actuators and sensors are placed at the same location and the sensors measure the velocities. For such a system, an analytical solution to the LQR problem exists and is formulated directly using the vector second order form. Specifically for a stabilizable and detectable system given as:

$$\begin{aligned} &M\ddot{q} + Kq = \bar{F}u, \qquad q(0) = q_0, \;\; \dot{q}(0) = \dot{q}_0 \\ &y = \bar{F}^T \dot{q} \end{aligned} \tag{5.3.18}$$

The state feedback optimal control which minimizes the cost function

$$V = \int_0^\infty \left(\alpha^2 y^T \beta y + u^T \beta^{-1} u \right) dt, \tag{5.3.19}$$

is

$$u = -\alpha \beta y \tag{5.3.20}$$

where $\alpha > 0$ is a positive scalar, and $\beta > 0$ is a positive definite matrix. Note that here, $Q = \alpha^2 \beta$, $R = \beta^{-1}$ and $H_2 = \bar{F}^T$. The proof of this result is given in [71]. Note that in this situation, the solution of an Algebraic Riccati Equation is not necessary, which makes the implementation of the controller for high dimensional systems immediate, as it will be illustrated in Chapter 6.

Simple Kalman Filtering Cases

When we are faced with certain situations such as undamped, special outputs or situations that lead to no stiffness (can be financial or quantum systems), we can easily solve the kalman filtering problem. Some simple cases are shown as follows:

Case 1) When there is an undamped system with sensors that only measure the generalized coordinates, Equ. (5.3.11)-(5.3.13) can be solved approaching them as Algebraic Riccati Equations. Under the following assumptions:

$$\bar{S} = \bar{S}^T \tag{5.3.21}$$

$$\begin{aligned} &ZZ^T = M^{-1}\ell W (M^{-1}\ell)^T \\ &(-M^{-1}K, H_1) \rightarrow Detectable \\ &(-M^{-1}K, Z) \rightarrow Stabilizable \end{aligned} \tag{5.3.22}$$

Equ. (5.3.11), (5.3.12), and (5.3.13) can be rewritten as:

$$2\bar{S} - \bar{P}H_1^T V^{-1} H_1 \bar{P} = 0 \tag{5.3.23}$$

$$-\bar{P}\left(M^{-1}K\right)^T + \bar{U} - \bar{P}H_1^T V^{-1} H_1 \bar{S} = 0 \tag{5.3.24}$$

$$-\bar{S}\left(M^{-1}K\right)^T - M^{-1}K\bar{S} - \bar{S}H_1^T V^{-1} H_1 \bar{S} + M^{-1}L'W(M^{-1}L')^T = 0 \tag{5.3.25}$$

Equ. (5.3.25) is an Algebraic Riccati Equation and can be solved for $\bar{S}$. Equ. (5.3.23) can be used to find $\bar{P}$. $\bar{P}$ matrix needs to be checked with Equ. (5.3.15) such that:

$$\dot{\hat{q}} = \dot{\hat{q}} + \underbrace{\left(\bar{P}H_1\right)}_{0} V^{-1} \underbrace{\tilde{y}}_{0} \tag{5.3.26}$$

According to Equ. (5.3.26), one of the two situations may be possible such that:

i) $\tilde{y} = 0 \Rightarrow \bar{P}H_1 \neq 0$

ii) $\tilde{y} \neq 0 \Rightarrow \bar{P}H_1 = 0$

Even though any of these situations are mathematically possible, situation i) does not have any physical meaning as it suggest $\bar{S}$ to be singular. If $\bar{S}$ is singular, the mass matrix needs to be zero and this would violate the definition of the system. Once obtaining $\bar{S}$ and $\bar{P}$ matrices, Equ. (5.3.24) can be solved for $\bar{U}$ and the Kalman gain can be obtained using Equ. (5.3.17).

Case 2) Similar to Case 1, when there is an undamped system with sensors that only measure the generalized coordinates, Equ. (5.3.11)-(5.3.13) can be solved using an analytical approach. The difference between Case 1 and Case 2 is that there is no restriction on $\bar{S}$ matrix such that $\bar{S} \neq \bar{S}^T$ is possible. For this situation, Equ. (5.3.11), (5.3.12), and (5.3.13) can be rewritten as:

$$\bar{S} + \bar{S}^T - \bar{P}H_1^T V^{-1} H_1 \bar{P} = 0 \tag{5.3.27}$$

$$-\bar{P}\left(M^{-1}K\right)^T + \bar{U} - \bar{P}H_1^T V^{-1} H_1 \bar{S} = 0 \tag{5.3.28}$$

$$-\bar{S}\left(M^{-1}K\right)^T - M^{-1}K\bar{S}^T - \bar{S}^T H_1^T V^{-1} H_1 \bar{S} + M^{-1}\ell W (M^{-1}\ell)^T = 0 \tag{5.3.29}$$

There is an analytical solution for the following math expression such that:

$$\textbf{Equation :} \qquad (AX + B)R(AX + B)^T = 0 \tag{5.3.30}$$

$$\textbf{Solution :} \qquad \zeta = \left(\bar{S}^T H_1 + \bar{U}H_2\right)V^{-1}\tilde{y} \tag{5.3.31}$$

Assuming $A=I$ and rewriting Equ. (5.53), the following expression is obtained as:

$$BRX^T + XRB^T + XRX^T + BRB^T = 0 \tag{5.3.32}$$

There is an analogy between Equ. (5.3.29) and Equ. (5.3.32) under the following assumptions:

$$X = \bar{S}^T \tag{5.3.33}$$

$$R = -H_1 V^{-1} H_1 \tag{5.3.34}$$

$$RB^T = -M^{-1}K \Rightarrow B = \left(M^{-1}K\right)^T \left[\left(H_1 V^{-1} H_1\right)^{-1}\right]^T \tag{5.3.35}$$

$$BRB^T = -M^{-1}\ell W(M^{-1}\ell)^T = M^{-1}K\left[\left(H_1V^{-1}H_1\right)^{-1}\right]^T(M^{-1}K)^T \tag{5.3.36}$$

Once these conditions are satisfied, the solution for $\bar{S}$ is:

$$\bar{S} = -\left(H_1V^{-1}H_1\right)^{-1}(M^{-1}K) \tag{5.3.37}$$

$\bar{P}$ matrix is obtained by substituting $\bar{S}$ into Equ. (5.3.27) and solving it for $\bar{P}$ matrix. Once $\bar{S}$ and $\bar{P}$ are obtained, Equ. (5.3.28) can be solved for $\bar{U}$ and the Kalman gain can be obtained using Equ. (5.3.17).

5.3.2 The Hamiltonian Approach

As already seen partitioning the solution matrix for an Algebraic Riccati Equation is one way to develop an LQR for the vector second order form [71]. The controller is optimal for the special situation of an undamped case; however, for most cases, the controller is optimal only under very specific conditions. Therefore, in this section, an LQR that is obtained using Euler-Lagrange equations instead of Algebraic Riccati Equations [74, 75]. The LQR problem for vector second order form is defined as [75]:

$$\begin{aligned} &\textit{minimize} && V = \int_0^\infty \left(q^TQ_1q + \dot{q}^TQ_2\dot{q} + u^TRu\right)dt \\ &\textit{subject to} && M\ddot{q} + C\dot{q} + Kq = \bar{F}u \\ & && y = H_1q + H_2\dot{q} \end{aligned} \tag{5.3.38}$$

Here, $Q_1 \geq 0$ and $Q_2 \geq 0$ are semipositive definite matrices, $R > 0$ is positive definite matrix, while *u* is defined as:

$$u = G_1q + G_2\dot{q} \tag{5.3.39}$$

Defining a co-state vector γ and solving the optimization problem using Euler-Lagrange equations, a second order matrix augmented differential equations of the closed loop system is obtained as:

$$\begin{bmatrix} M & 0 \\ 2Q_2 & -M \end{bmatrix}\ddot{z}+\begin{bmatrix} C & 0 \\ 0 & C \end{bmatrix}\dot{z}+\begin{bmatrix} K & -\frac{1}{2}\bar{F}R^{-1}\bar{F}^T \\ 2Q_1 & -K \end{bmatrix}z=0 \tag{5.3.40}$$

where

$$z=\begin{bmatrix} q \\ \gamma \end{bmatrix} \tag{5.3.41}$$

Taking Laplace transform of the closed loop system, the eigenvalue problem of Equ. (5.3.40) is derived such that:

$$\begin{bmatrix} \left(s^2M+sC+K\right) & -\frac{1}{2}\bar{F}R^{-1}\bar{F}^T \\ 2\left(s^2Q_2-Q_1\right) & -\left(s^2M-sC+K\right) \end{bmatrix}\begin{pmatrix} \Lambda \\ \Gamma \end{pmatrix}=0 \tag{5.3.42}$$

where Λ and Γ are the corresponding eigenvectors. Note that, 4*n* eigenvalues, wherein *2n* stable and *2n* unstable, are obtained. For *2n* stable eigenvalues, the solution for Equ. (5.3.40) can be expressed as:

$$q=\sum_{i=1}^{N}a_k e^{s_k t}\Lambda_k \tag{5.3.43}$$

$$\gamma=\sum_{i=1}^{N}a_k e^{s_k t}\Gamma_k \tag{5.3.44}$$

Matrix expression of the generalized coordinates can be written as:

$$q=YD_e\mathbf{a} \tag{5.3.45}$$

$$\gamma=\Psi D_e\mathbf{a} \tag{5.3.46}$$

where

$$D_e = \begin{bmatrix} e^{s_1 t} & 0 & 0 & 0 \\ 0 & e^{s_1 t} & 0 & 0 \\ 0 & 0 & \ddots & 0 \\ 0 & 0 & 0 & e^{s_{2n} t} \end{bmatrix} \tag{5.3.47}$$

$$\mathbf{a} = \begin{bmatrix} a_1 & a_2 & \cdots & a_{2n} \end{bmatrix} \tag{5.3.48}$$

$$Y = \begin{bmatrix} \Lambda_1 & \Lambda_2 & \cdots & \Lambda_{2n} \end{bmatrix} \tag{5.3.49}$$

$$\Psi = \begin{bmatrix} \Gamma_1 & \Gamma_2 & \cdots & \Gamma_{2n} \end{bmatrix} \tag{5.3.50}$$

For *2n* stable eigenvalues and corresponding eigenvectors, the gain matrices are derived as:

$$\begin{bmatrix} G_1 & G_2 \end{bmatrix} \begin{bmatrix} Y \\ Y_s \end{bmatrix} = \frac{1}{2} \Psi^T \bar{F} R^{-1} \tag{5.3.51}$$

where

$$Y_s = \begin{bmatrix} s_1 \Lambda_1 & s_2 \Lambda_2 & \cdots & s_{2n} \Lambda_{2n} \end{bmatrix} \tag{5.3.52}$$

To calculate the minimum cost, the state vector *x* is defined to have a concise expression. Once a state vector is defined, the minimum cost is calculated. Initial conditions are defined as:

$t = 0$

$$\left.\begin{matrix} q(0) = Y\mathbf{a} \\ \dot{q}(0) = Y_s \mathbf{a} \end{matrix}\right\} x(0) = \begin{bmatrix} q(0) \\ \dot{q}(0) \end{bmatrix} \Rightarrow x_0 = \underbrace{\begin{bmatrix} Y \\ Y_s \end{bmatrix}}_{\phi} \mathbf{a} \Rightarrow \mathbf{a} = \phi^{-1} x_0 \tag{5.3.53}$$

$$x = \phi D_e \mathbf{a} = \phi D_e \phi^{-1} x_0 \tag{5.3.54}$$

Optimal control input using state vector is rewritten in the following format such that:

$$u = \begin{bmatrix} G_1 & G_2 \end{bmatrix} \begin{bmatrix} q \\ \dot{q} \end{bmatrix} \Rightarrow u = Kx = \frac{1}{2} R^{-1} F^T \psi \phi^{-1} x = \frac{1}{2} R^{-1} F^T \psi D_e \phi^{-1} x_0 \tag{5.3.55}$$

Substituting the values of state vector and optimal control into Equ. (5.3.38), the minimum cost is evaluated as:

$$
\begin{aligned}
&V_{\min} = \int_0^\infty \left(q^T U q + \dot{q}^T V q + u^T R u \right) dt = \int_0^\infty \left(x^T \begin{bmatrix} U & 0 \\ 0 & V \end{bmatrix} x + u^T R u \right) dt = \int_0^\infty \left(x^T Q x + x^T K^T \right. \\
&\int_0^\infty \left(x_0{}^T \phi^{-1T} D_e{}^T \phi^T Q \phi D_e \phi^{-1} x_0 + \frac{1}{4} x_0{}^T \phi^{-1T} D_e \psi^T F R^{-1} F^T \psi D_e \phi^{-1} x_0 \right) dt = \\
&x_0{}^T \phi^{-1T} \int_0^\infty D_e{}^T \underbrace{\left(\phi^T Q \phi + \frac{1}{4} \psi^T F R^{-1} F^T \psi \right)}_{\hat{T}} D_e dt \phi^{-1} x_0
\end{aligned}
\tag{5.3.56}
$$

An analytical expression of the integral in Equ. (5.3.56) can be derive since D_e is a diagonal matrix of exponential terms. This will reduce the computation time and increase the computational efficiency. The integration is carried out as:

$$
\begin{aligned}
&\int_0^\infty D_e{}^T T D_e dt = \int_0^\infty \begin{bmatrix} e^{\bar{s}_1 t} & & 0 \\ & \ddots & \\ 0 & & e^{\bar{s}_{2n} t} \end{bmatrix} \begin{bmatrix} T_{11} & \cdots & T_{12n} \\ \vdots & \ddots & \vdots \\ T_{2n1} & \cdots & T_{2n2n} \end{bmatrix} \begin{bmatrix} e^{s_1 t} & & 0 \\ & \ddots & \\ 0 & & e^{s_{2n} t} \end{bmatrix} dt = \\
&\int_0^\infty \begin{bmatrix} T_{11} e^{(s_1+\bar{s}_1)t} & T_{12} e^{(s_2+\bar{s}_1)t} & \cdots & T_{12n} e^{(s_{2n}+\bar{s}_1)t} \\ T_{21} e^{(s_1+\bar{s}_2)t} & T_{22} e^{(s_2+\bar{s}_2)t} & \cdots & \vdots \\ \vdots & \vdots & \vdots & \vdots \\ T_{2n1} e^{(s_1+\bar{s}_{2n})t} & T_{22} e^{(s_2+\bar{s}_{2n})t} & \cdots & T_{2n2n} e^{(s_{2n}+\bar{s}_{2n})t} \end{bmatrix} dt = \\
&- \begin{bmatrix} \frac{T_{11}}{s_1+\bar{s}_1} & \frac{T_{12}}{s_2+\bar{s}_1} & \cdots & \frac{T_{12n}}{s_{2n}+\bar{s}_1} \\ \frac{T_{21}}{s_1+\bar{s}_2} & \frac{T_{22}}{s_2+\bar{s}_1} & \cdots & \vdots \\ \vdots & \vdots & \vdots & \vdots \\ \frac{T_{2n1}}{s_1+\bar{s}_{2n}} & \cdots & \cdots & \frac{T_{2n2n}}{s_{2n}+\bar{s}_{2n}} \end{bmatrix} = \\
&- \begin{bmatrix} T_{11} & \cdots & T_{12n} \\ \vdots & \ddots & \vdots \\ T_{2n1} & \cdots & T_{2n2n} \end{bmatrix} \div \begin{bmatrix} s_1+\bar{s}_1 & \cdots & s_{2n}+\bar{s}_1 \\ \vdots & \ddots & \vdots \\ s_1+\bar{s}_{2n} & \cdots & s_{2n}+\bar{s}_{2n} \end{bmatrix} = -(T \div Sm)
\end{aligned}
\tag{5.3.57}
$$

where

$$s = [s_1 \quad s_2 \quad \cdots \quad s_{2n}] \tag{5.3.58}$$

$$Sm_{ij} = \bar{s}_i + s_j \tag{5.3.59}$$

Substituting the algebraic evaluation of the integration, that is obtained in Equ. (5.3.57), into Equ. (5.3.56), the minimum cost is obtained such that:

$$V_{\min} = -x_0^T \phi^{-1T} (T \div Sm) \phi^{-1} x_0 \tag{5.3.60}$$

The biggest difference and superiority of using the Hamiltonian approach to develop an LQR for vector second form is that the controller is always optimal. Another advantage is that there is no need to solve the Algebraic Riccati Equation. It is needed to solve only the eigenvalues and eigenvectors of the system. However, sometimes eigenvalue problems can create numerical difficulties depending on the distribution of eigenvalues.

5.4 Chapter Summary

The biggest issue in structures used as reflectors is the vibration of the system. The vibration can be caused by structural unstabilities or external effects such as thermal changes or disturbance signals. In aerospace applications, suppressing the vibration is not enough to have a feasible system, we also need to be optimal about the usage of power, that is needed to control the system, as the source will be limited in the space. Therefore, an LQR is very well suited to optimize the vibration suppression time and the usage of control power. However, the LQR is designed for theoretically ideal systems. In practice, we cannot always measure all the states and there will always be some disturbance signals that will affect the control implementations and measurements. Since most of the disturbance signals can be modeled as white Gaussian noise, LQG controllers are very useful and more realistic than LQR as demonstrated in Section 5.2.

With the invention of smart materials and developing technology, we are able to control high dimensional distributed systems and obtain high performances. Even though we always improve our computational power, the demand to control with higher accuracy will always increase too. Therefore, a fundamental change on reducing the dimension of the system, is a

crucial issue that needs to be addressed. For this purpose, control methods, that are developed using vector second order form, are proposed in Section 5.3.

Two different approaches to develop control in vector second order form are carried out. One is reducing the dimension of Algebraic Riccati Equation partitioning the solution matrix. The other method is using the Hamiltonian approach directly and obtain the eigenvalue eigenvector problem. It is hard to compare them and draw a conclusion to decide which one is better at this point. They both have certain advantages and drawbacks depending on the system. Thus, a trade-off needs to be considered. Using a reduced Algebraic Riccati Equation does not give optimal results unless certain conditions are satisfied. However, there can be very simple solutions for certain systems. On the other hand, using the Hamiltonian approach always gives an optimal solution, but the reliability of the controller depends on the behavior of the eigenvalues and eigenvectors.

Chapter 6

CONTROL APPLICATION

6.1 Introduction

In this Chapter, the controllers, that are developed in Chapter 5, are applied to the membrane-actuator system. Even though theoretically, the same results should be obtained when the same controller is applied regardless if it is developed using vector first order form or vector second order form, slightly different results are obtained due to numerical errors. In some cases, it is not even possible to compare the results of the control applications in vector first order form and vector second order form; because, the vector first order form controller is not solvable due to numerical difficulties. To be able to compare the results, the same values are used while applying the controllers. The number of finite element can be chosen as 400 or 625 based on the convergence of the FEM solutions in Chapter 3. In this chapter, all the applications carried out for 400 finite elements for both system to be able to compare. Note that, since the membrane actuator system is symmetric, it is expected that the behavior of the central point captures the essence of the system behavior. This is why the displacement of the central point of the membrane is selected for illustrations. Also point P (x= 82.5, y=82.5) is selected to give an example at a non-central point. From structural point of stand, the PVDF actuators are the most compatible for Kapton membrane as seen in Chapter 3. However, the MFC and PZT actuators are much more effective from control aspect. Also, while the thickness increases, the more effective the actuator becomes. However, this means having a stiffer and heavier system over all. Thus, a trade-off between more effective control and a lighter structure needs to be considered. To address this issue, the PVDF, MFC and PZT actuators are compared. It should be noted that, if a higher control ability is desired, a PZT actuator should be used. To minimize the effect of

numerical errors, the comparison of the different materials is carried out for undamped collocated actuator sensor case using the simple LQR result from Chapter 5, Subsection 5.3.1.1.

The Section 6.2 shows the results of the control applications that are obtained using vector first order form. Closed loop simulations of the LQR are demonstrated in the Subsection 6.2.1, while closed loop simulations of the LQG controller and robustness study of the LQG control are shown in the Subsection 6.2.2. The simulations that are obtained using vector second order form are demonstrated in the Section 6.3. The simple solutions that are obtained through Algebraic Riccati Equtaions are demonstrated in the Subsection 6.3.1. The applications of the Hamiltonian derivation for vector second order forms are displayed in Subsection 6.3.2. The Section 6.4 discusses the results and summarizes this chapter.

6.2 Vector First Order Form

As explained in detail in previous chapters, application of vector first order form controllers is very challenging when it is applied to high dimensional systems. Sometimes, it is not even possible to use vector first order form without reducing the order of the model. The other problem is reliability of the results, when the system is larger, the accumulated numerical error is larger.

6.2.1 LQR

Simulation of damped system with no control and the results of the LQR application for values of $Q = \mathrm{I}$ and $R = \mathrm{Ix}10^{8}$, are shown as following in Figs. 6.1-6.6 for both systems. Linear combination of first three mode shapes is used to construct the initial condition.

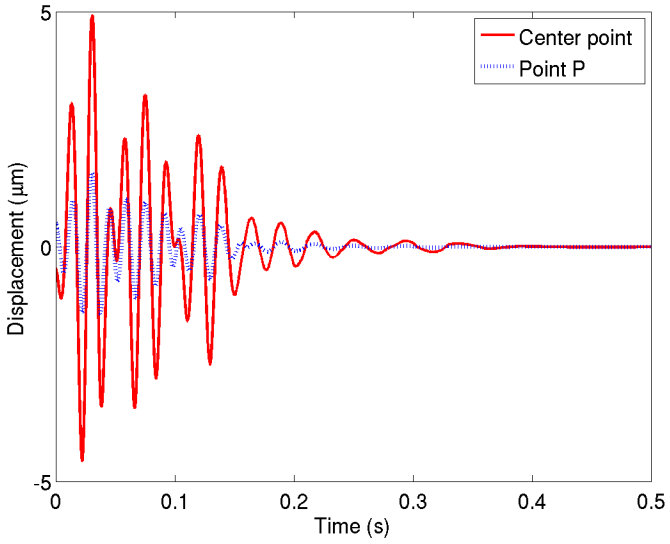

Figure 6.1: Displacement of the membrane versus time for System I with no control.

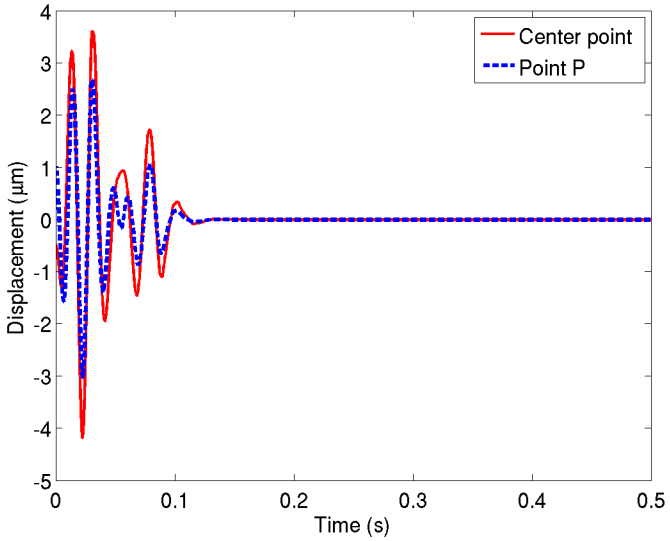

Figure 6.2: Displacement of the membrane versus time for System I using vector first order form LQR.

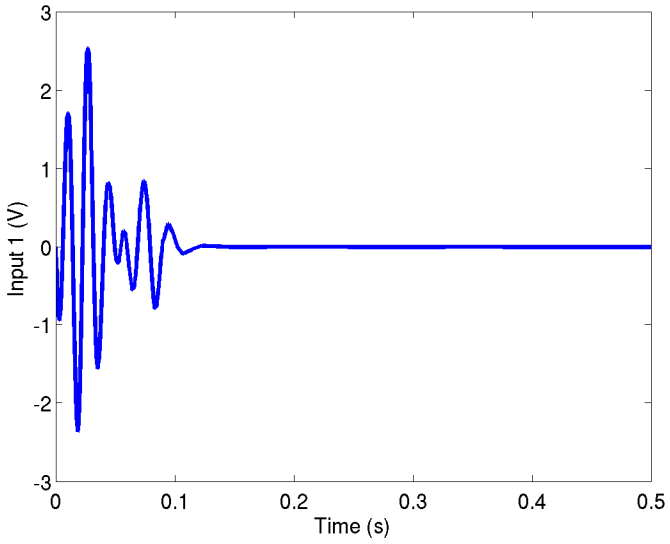

Figure 6.3: Control input versus time for System I using vector first order form LQR.

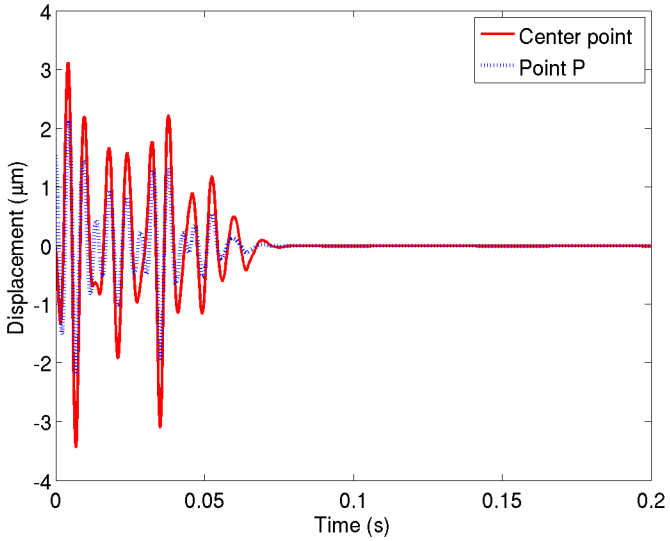

Figure 6.4: Displacement of the membrane versus time for System II with no control.

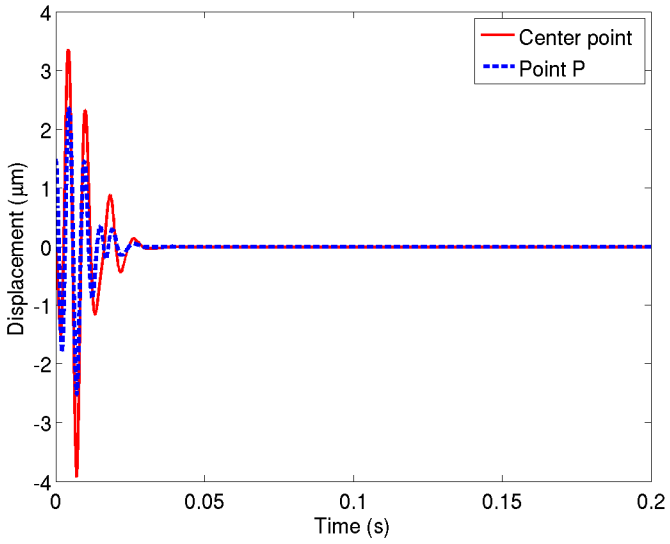

Figure 6.5: Displacement of the membrane versus time for System II using vector first order form LQR.

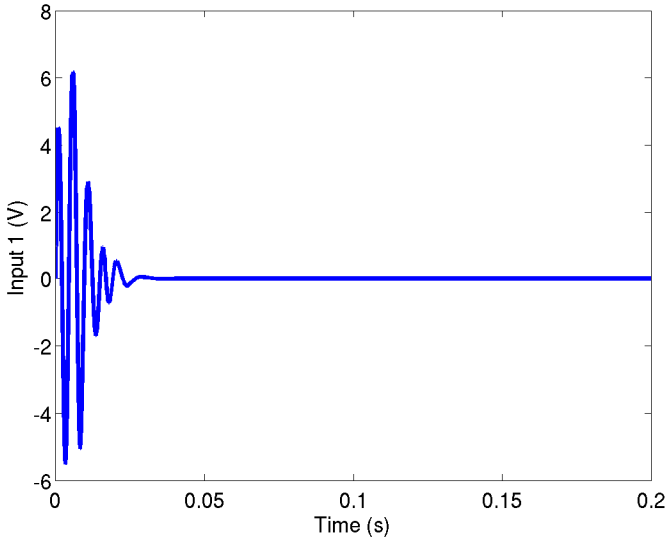

Figure 6.6: Control input versus time for System II using vector first order form LQR.

It is seen from Figs. 6.1-6.6 that the LQR stabilizes the system in an optimal manner. The System I and System II are stabilized in different times for the same gain values in the cost function due to the structural differences.

6.2.2 LQG

Since the mode shapes of System II display a more "natural" and tolerable behavior at the actuator edges that is similar with clamped boundary conditions, in this subsection, System II is selected for LQG control study. An LQG controller is developed using the values of $W_p = 10^2$ and $V_p = 10^2$ for noise intensities and $Q = I \times 10^4$ and $R = I$ for state and input penalty matrices, respectively [45].

Since the LQG control theory does not guarantee stability margins, a complete LQG study should include a robustness analysis. For example, certain parameters, that can have modeling errors inherently from manufacturing process, such as damping, thickness, modulus of elasticity, density, and prestress, can be checked. To perform this study, the control gain (*G*) and steady state observer gain (*T*) matrices are obtained from the values given above. Using these gain matrices, the value of each of these parameters is changed one a time. These perturbations resulted in changed values for the system matrices, *A*, the state matrix, and *B*, the input matrix. New closed loop systems are created using these perturbed system matrices and the fixed control and observer gains. Then, the eigenvalues of these closed loop systems are computed to investigate the stability robustness under these parameter perturbations. The results for System II are shown in Figs. 6.7-6.11. In these figures, only the eigenvalues whose real parts are close zero are illustrated. As predicted by the LQG control theory, the linear closed loop system is exponentially stable (i.e. all closed loop system's eigenvalues have negative real parts). This is one of the key advantages of the LQG control theory: it provides an optimal stabilizing controller in the presence of white noise Gaussian disturbances using optimal state estimates.

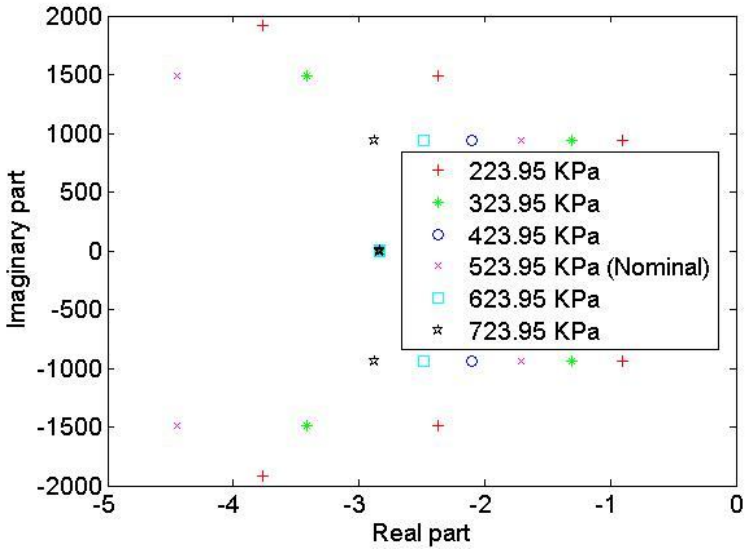

Figure 6.7: Robustness with respect to Kelvin-Voigt damping coefficient

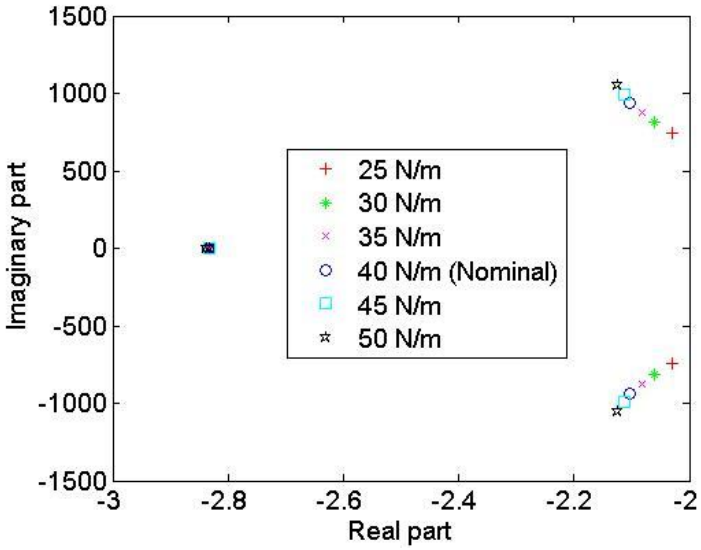

Figure 6.8: Robustness with respect to prestress

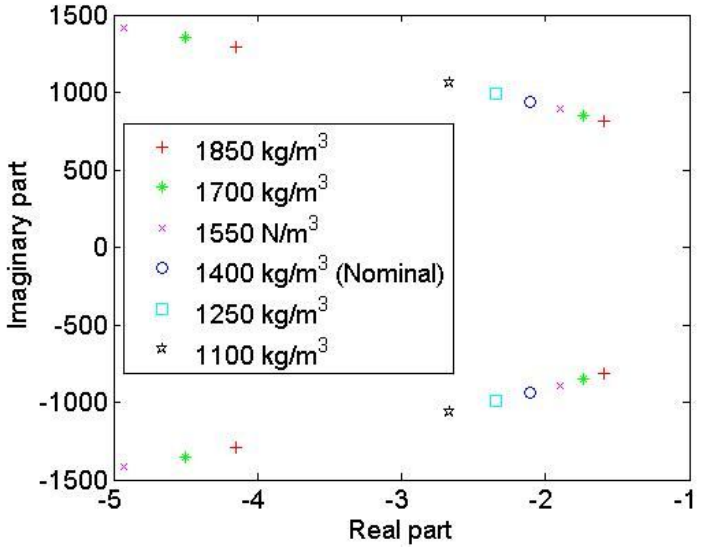

Figure 6.9: Robustness with respect to membrane density

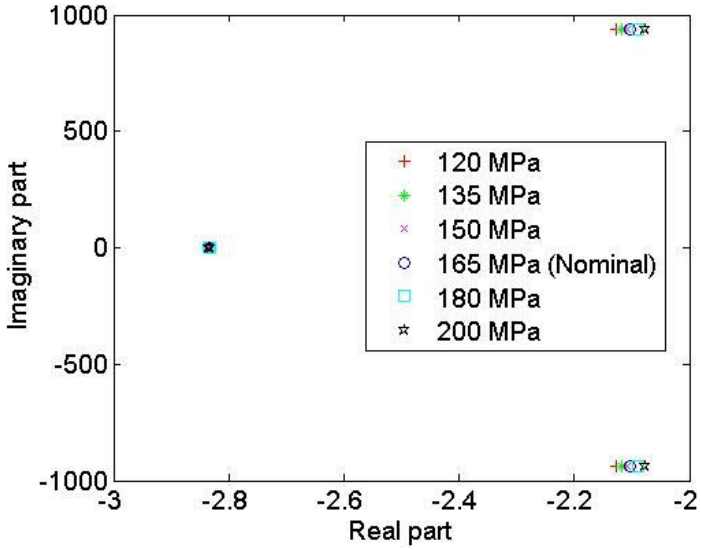

Figure 6.10: Robustness with respect to elasticity modulus

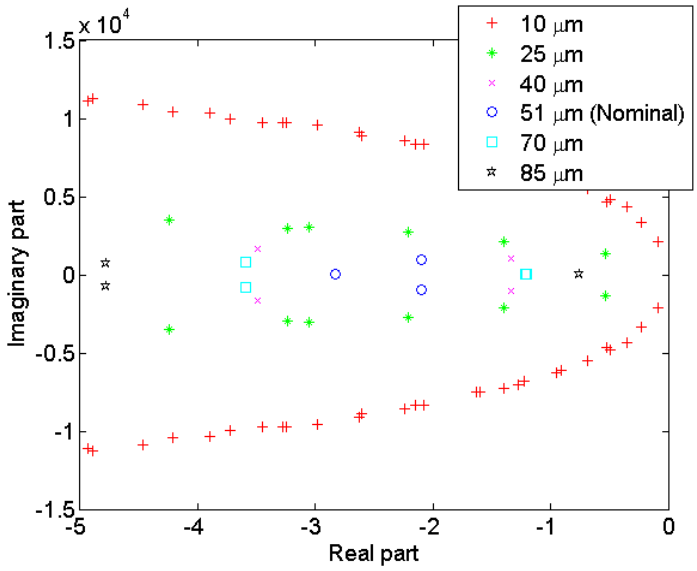

Figure 6.11: Robustness with respect to membrane thickness

It is seen from Figs. 6.7-6.11 that the developed LQG controller is robustly stable (i.e. the closed loop system eigenvalues have negative real part) with respect to some material properties and prestress to a certain extent. Therefore, when there is an individual uncertainties in the ranges shown in Figs. 6.7-6.11, the system will still be exponentially stable under the developed LQG controller. Another important observation is the sensitivity of the closed loop system's eigenvalues to certain parameters. For example, while different values of the prestress and modulus of elasticity of the membrane have very small effect on the stability of the system (Fig. 6.8 and Fig. 6.10 respectively), the changes in the membrane thickness shift the eigenvalues of the closed loop system more drastically (Fig. 6.11).

6.3 Vector Second Order Form

6.3.1 Reduced Algebraic Riccati Equation

The controllers, that are developed in the vector second order form using reduced Algebraic Riccati Equation (RARE), are applied to Systems I and II, both for undamped and damped cases for the same Q and R values of the vector first order form LQR. The linear

combination of first three natural mode of the system is selected as initial conditions. The simulations are presented in Figs. 6.12-15 for System I.

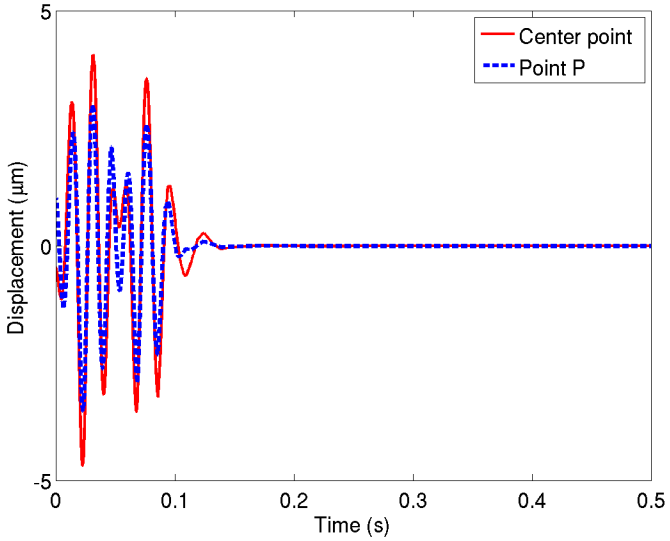

Figure 6.12: Displacement of the membrane versus time for undamped System I using LQR with RARE.

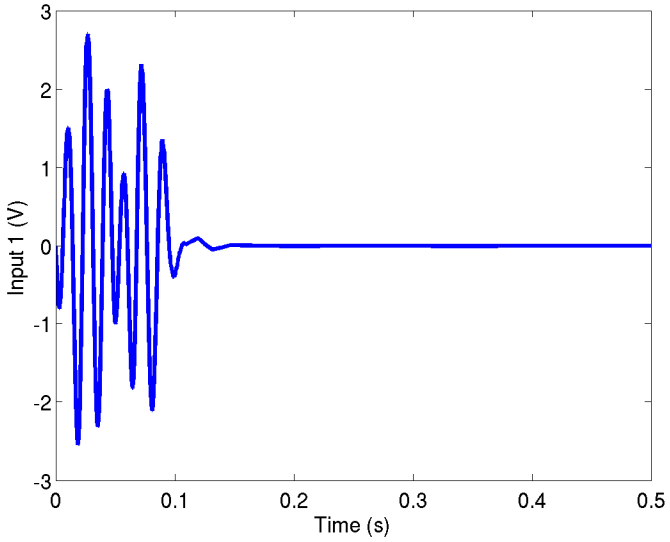

Figure 6.13: Control input versus time for undamped System I using LQR with RARE.

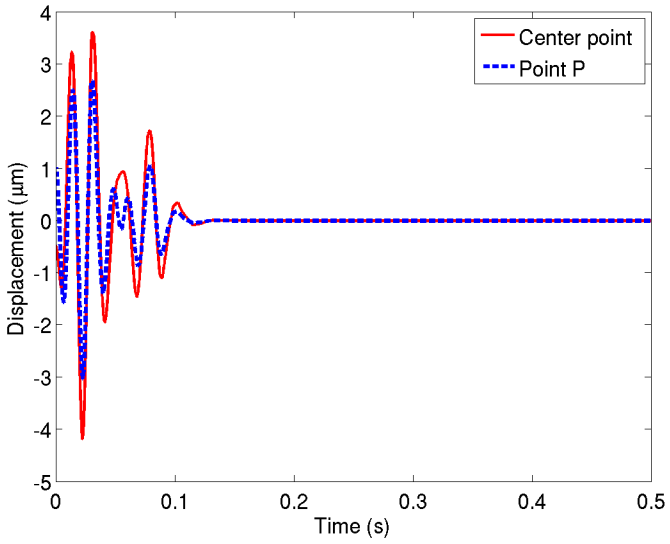

Figure 6.14: Displacement of the membrane versus time for damped System I using LQR with RARE.

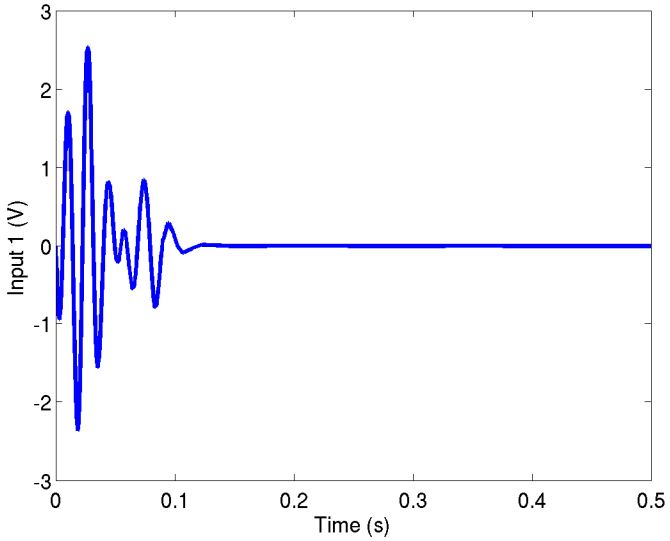

Figure 6.15: Control input versus time for damped System I using LQR with RARE.

The simulations of undamped case with LQR show that the controller drives the states to zero very fast as seen in Fig. 6.12. Thus, the “artificial damping” introduced by the controller is very effective in eliminating membrane vibrations. For the damped case, in Fig. 6.14, it is shown

that the controller reduces the convergence time slightly faster than undamped case. For the same values of cost penalties, the simulations of undamped System II are presented in Figs. 6.16-6.21. This time, the PZT actuator is compared to the MFC and PVDF actuators.

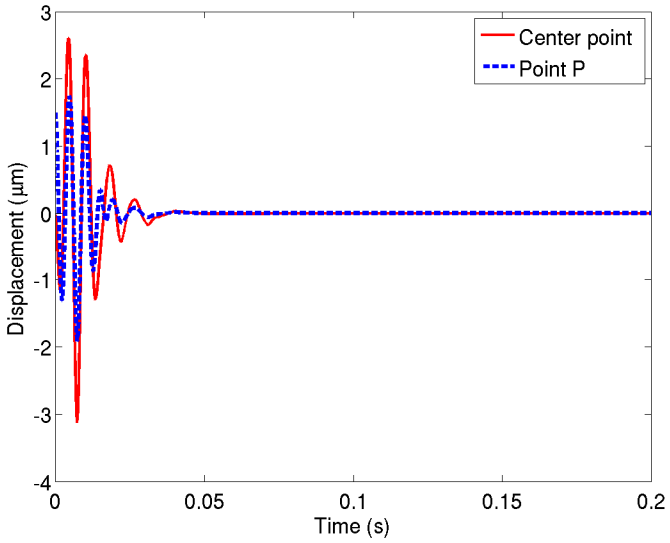

Figure 6.16: Displacement of the membrane versus time for undamped System II using LQR with RARE for PZT actuator.

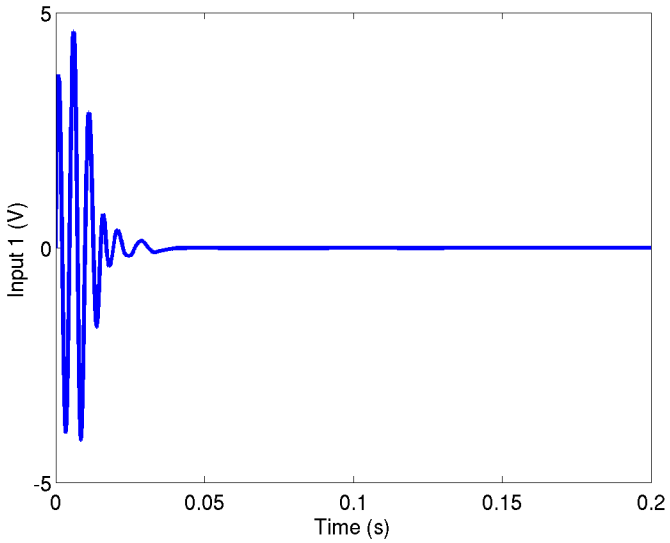

Figure 6.17: Control input versus time for undamped System II using LQR with RARE for PZT actuator.

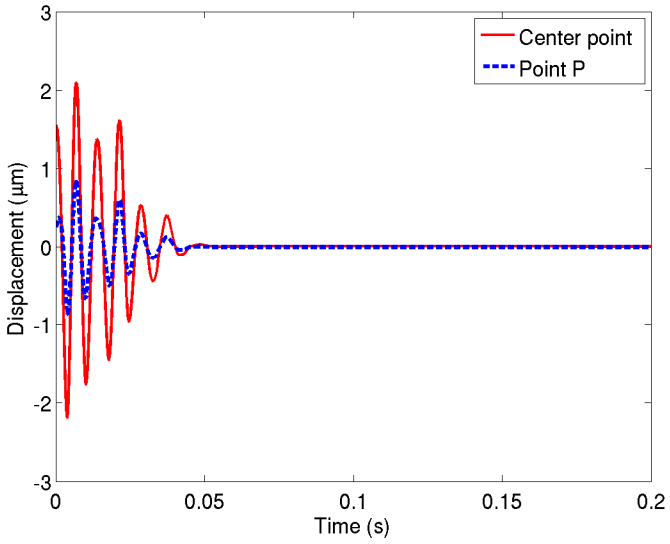

Figure 6.18: Displacement of the membrane versus time for damped System II using LQR with RARE for MFC actuator.

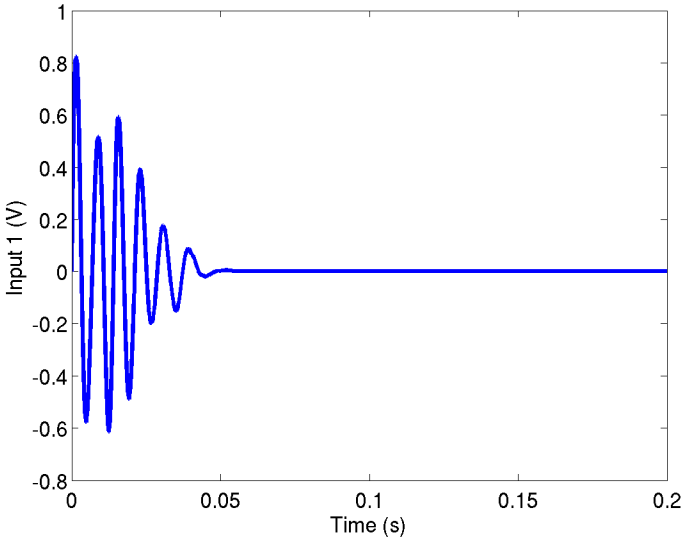

Figure 6.19: Control input versus time for damped System II using LQR with RARE for MFC actuator.

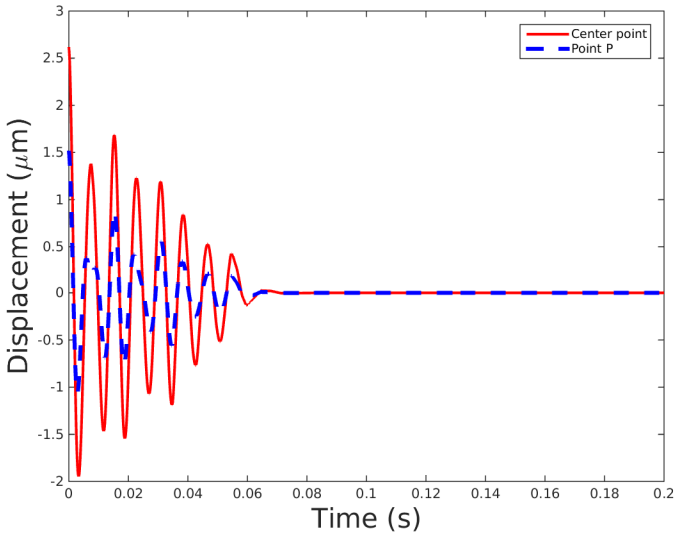

Figure 6.20: Displacement of the membrane versus time for damped System II using LQR with RARE for PVDF actuator.

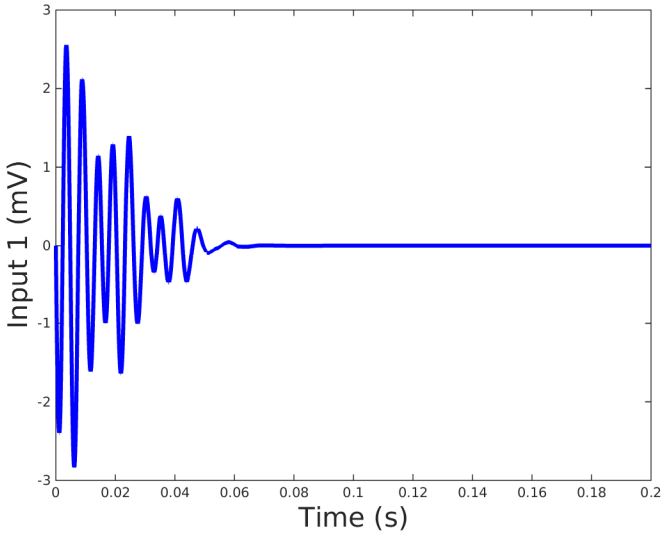

Figure 6.21: Control input versus time for damped System II using LQR with RARE for PVDF actuator.

For the same values of cost penalties, the simulations of damped System II are presented in Figs. 6.22-6.23.

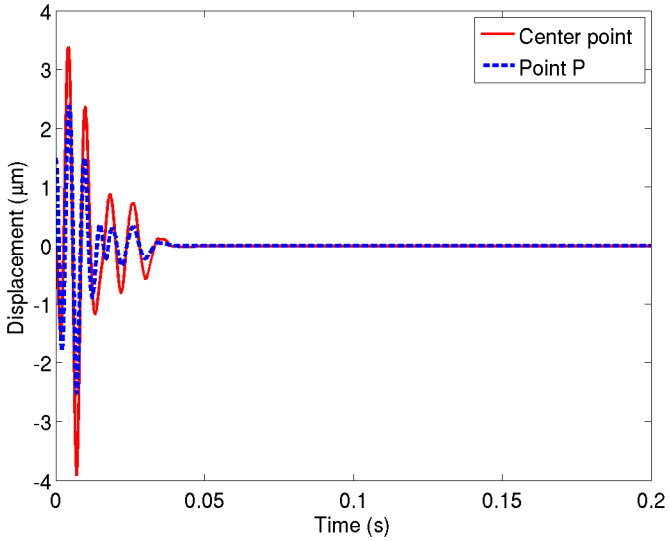

Figure 6.22: Displacement of the membrane versus time for damped System II using LQR with RARE.

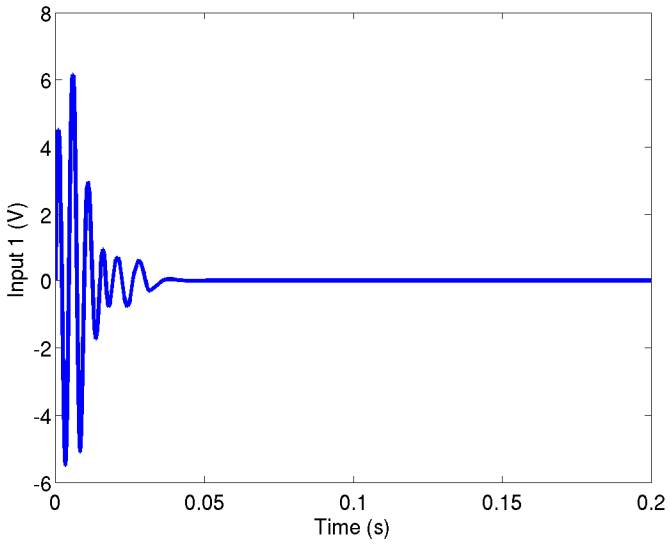

Figure 6.23: Control input versus time for damped System II using LQR with RARE.

The effect of the controller on the System II is similar to System I for undamped and damped cases for the PZT actuator, as seen in Figs. 6.16 -6.17 and Figs. 6.22-6.23. When the

PZT actuator is compared to the PVDF and MFC actuators, there is not much difference between the PZT and MFC actuators; however, the PZT actuator is definitely more effective. On the other hand, it takes much longer when the PVDF actuator is used. To have same effect with the PZT actuator, the PVDF and MFC actuators would require a higher voltage which is not feasible in space application where the source is limited. PVDF actuators are inherently good for being used as sensors as explained in Chapter 3.

6.3.2 The Hamiltonian Approach

For the same penalty values of cost function, the vector second order form LQR, that is developed using the Hamiltonian approach, is applied to both systems for damped cases. The simulation results are shown in Figs. 6.24-6.27.

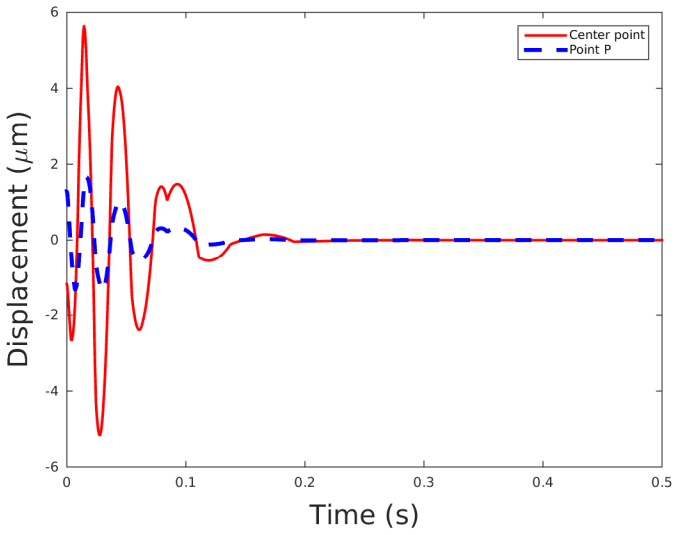

Figure 6.24: Displacement of the membrane versus time for System I using LQR with the Hamiltonian approach.

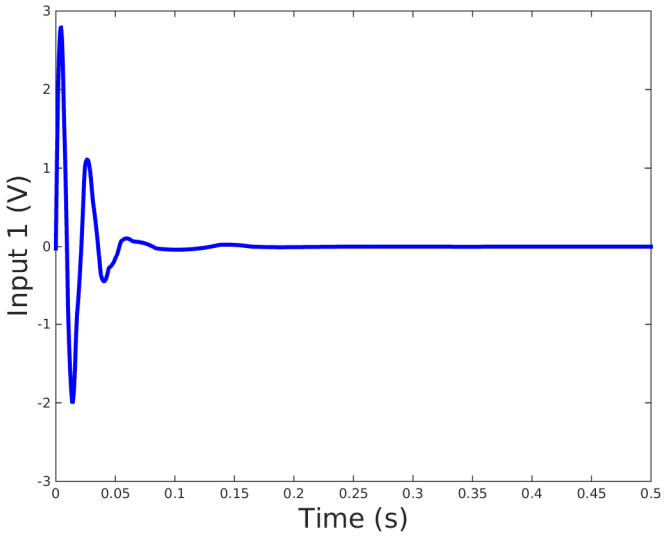

Figure 6.25: Control input versus time for System I using LQR with the Hamiltonian approach.

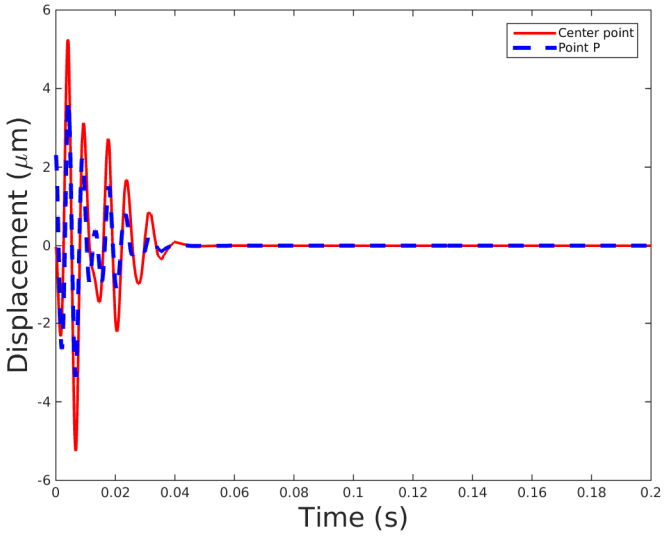

Figure 6.26: Displacement of the membrane versus time for System II using LQR with the Hamiltonian approach.

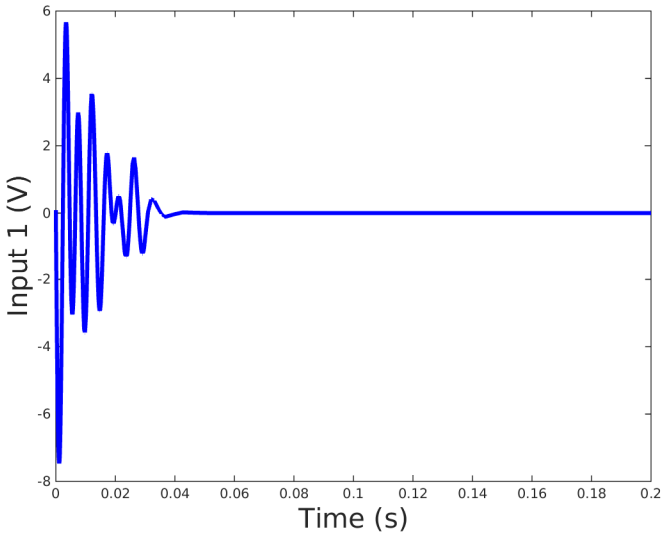

Figure 6.27: Control input versus time for System II using LQR with the Hamiltonian approach.

Figures 6.24-27 show that vibrations are effectively suppressed using the vector second order form LQR. When it is compared to the vector first order form results, it is qualitatively the same with slight difference for System II. However, this difference is more visible for System I.

6.4 Chapter Summary

As it can be seen from the figures, LQR that is developed using both methods are able to stabilize the system effectively. The comparison of vector first order form and vector second order form concludes that they behave qualitatively very similar with some quantitative discrepancies. This shows that vector second order form can be used instead of vector first order form to increase the computational performance.

The robustness study of LQG control demonstrated that the small changes of parameters of the system can result in big differences on the stability of the system. This situation proves the need for a robustness study for real life applications.

Chapter 7

CONCLUSION AND FUTURE WORK

7.1 Summary and Key Contributions

The necessity for light big space structures in aerospace applications is increasing as technology develops and will always be a research interest since scholars in this area never stop exploring new possibilities. The usage of light big space structures introduces structural and control difficulties. These need to be analyzed using large flexible models, which means using distributed models with very high dimensions. One of the biggest difficulties with high dimensional models is the effort required to carry out numerical computations. Sometimes this computation may not even be possible. The super computers available today remedy this issue to a certain extent, but they are not able to completely avoid numerical errors. Furthermore, these computational issues will continue due to the desire to use even bigger and more complex systems.

With this in mind, the objective of this dissertation is to model and develop modern control laws for a membrane structure to suppress the vibration. This membrane structure can be used as a reflector in a space antenna. Distributed piezoelectric actuators are used to control the system because the system is a distributed flexible system. The membrane is modeled as a thin plate due to its behavior under prestress. This modeling allows the use of piezoelectric actuators that generate a bending effect on the membrane for vibration suppression.

The membrane is square with four bimorph smart actuators. For actuator locations, two different approaches are used for different performance motivations. One approach is placing the actuators away from the boundaries of the membrane to have an equal control effect on every region; this is called System I. System II has the actuators at the corners of the membrane to

create a large homogeneous central space for a larger reflecting area. These systems are compared structurally and from control perspective.

The piezoelectric actuators attached to the membrane are relatively thick. Thus, the system is heterogeneous and analytical solution cannot be derived. Due to the heterogeneity of the system, the weak form finite element is used to obtain an approximate solution of the partial differential equation derived as the equation of motion. The structural effects of the actuators cannot be neglected in this case. It is seen from the structural and control results that the actuator's material and thickness have a significant impact on the behavior of the system.

In order to ensure accurate results for the finite element solution, a high number of elements must be used. However, using too many elements can result in computational difficulties as well as divergence. Therefore, a convergence analysis is carried out to address the trade-off between numerical accuracy and computational difficulties and to determine the appropriate number of elements. For the convergence of the solution, dynamic parameters such as natural frequencies and natural modes are analyzed. In control application, these parameters are more crucial than static parameters such as displacements and stresses. The mode shapes of both systems show that System I has singularities at the actuator edges effecting the smoothness of the membrane central area. However, in System II, actuators behave as boundary conditions enabling a large and smooth central area for a reflector.

For system analysis, to determine the control characteristics such as the stability, controllability and observability, the vector second order form is used as well as the vector first order form. The results show the effect of numerical difficulties of a high dimensional system. For the stability analysis both approaches give the same results. However, it should be noted that the dimension of the matrix that needs to be solved for the vector first order form is double the vector second order form. For controllability and observability work, vector first order form is not able to draw a conclusion. The results of the analysis carried out by Matlab show NaN values. This is caused due to a high dimension of the controllability and observability matrices. Also, taking power of the state matrix results in accumulated errors dramatically. On the other hand using vector second order form give the results as controllable and observable for both systems. The biggest advantages of using vector second order form are that it uses half of the dimension of the matrix that needs to be solved in the vector first order form, and keeps the

matrix properties such as symmetry and positive definiteness that help to have an easy modal transformations. These properties help to have more efficient and reliable numerical results.

Once it is determined that the system is controllable and observable, an LQR is developed using vector second order form and vector first order form. Since an LQR does not take into account the external disturbances, an LQG controller is needed for a system that needs to be implemented in a real application rather than just theoretical.

Since no material is perfectly manufactured and it is very hard to generate a prestress for the exact desired value, a robustness study of the system is carried out for parameters that are distributed around nominal values of the parameters. These parameters are the prestress, material density, elasticity modulus, Kelvin-Voigt damping coefficient and thickness of the membrane. The results show that the developed LQG controller is robustly stable to a certain extent. Therefore, when there is an individual uncertainty, at least in the demonstrated ranges, the system will be still exponentially stable under the developed LQG controller. Another important observation is the sensitivity of the closed loop system eigenvalues to certain parameters. For example, while different values of the prestress and modulus of elasticity of the membrane have very small effect on the stability of the system, the changes in the membrane thickness shift the eigenvalues of the closed loop system more drastically.

To develop controllers in vector second order form two different approaches are used. One is reducing the dimension of Algebraic Riccati Equation by partitioning the solution. The other approach is using the Hamiltonian method directly for vector second order systems. With the first approach, a series of Algebraic Riccati Equations with the dimension reduced to half respect to the vector first order form are obtained. This enables much more efficient and reliable computations to take place. However, certain conditions need to be satisfied for an optimal solution. Even though this method works well and stabilizes the system, it cannot always guarantee to be optimal. However, there are very simple solutions for some special cases. For example, when a system is undamped with collocated actuators and sensor, an analytical solution can be derived for the LQR problem. Some other simple solutions for the LQR and Kalman filtering in vector second order form are derived to give examples. When the Hamiltonian method is used to derive an LQR for vector second order form, an optimal result is always obtained. This is the biggest superiority of the Hamiltonian approach compared to the LQR

developed using reduced Algebraic Riccati Equation. The Hamiltonian approach uses only the eigenvalues and eigenvectors of the system. There is no nonlinear equation to be solved. However, it should be noted that using eigenvalues and eigenvectors of a system has its own challenges. If the modal matrix is close to a singular value, the solution may not be very reliable since the inversion of the modal matrix is required to obtain the controller.

The most common smart material used as actuators is piezo ceramics due to their effectiveness. Another material sometimes used for actuators is piezo polymers. They are more suitable for sensor applications. In this work PZT, PVDF and MFC actuators are compared to select a more efficient actuator. As expected, the PZT actuator has the highest control capacity. Also, to have a more effective control, a thicker PZT actuator can be implemented. However, this will make the system heavier. Therefore, a trade-off between the effective control and weight of the system needs to be considered when deciding the thickness of the actuator.

The simulation results show that the vibrations in both systems are being suppressed effectively with all the controllers developed. This result is clear when the simulations of controlled and damped system are compared. In both systems, vector first order form and vector second order form give qualitatively similar results with small numerical differences. System I behaves as though it has lumped masses attached to it. It is more sluggish and takes longer to suppress the vibration. However, for System II, the actuators behave as boundary conditions, and the vibration of the system is suppressed much faster. Also for System II, numerical differences between the vector first order form and vector second order form are much higher compared to System I. This might be the result of accumulated numerical errors due to the structural discontinues.

It should be noted that for certain penalty values of the cost function, Matlab is not even able to solve the Algebraic Riccati Equation. This clearly shows the limits of current computational power and effect of the accumulated numerical errors.

7.2 Future Work

As it can be seen from the literature review, there is not much existing research of the vector second order form. However, as demonstrated with this work, vector second order form has many advantages over vector first order form. It can also be an alternative or complementary to Model Order Reduction techniques. However, it should be noted that there is plenty of work that needs to be done to improve and refine vector second order form methods to establish a common usage in control theory.

One work that needs to be done for vector second order form LQR and Kalman filtering, that are derived using reduced Algebraic Riccati Equation, is establishing a way to have an optimal control always. This may be achieved designing a system for the control theory. This way a system's structural design and control process will be developed in a parallel and iterative manner unlike the traditional approach where structural design and control process are approached separately. Combining these two disciplines will help to have more efficient and reliable designs.

For vector second order form derived using the Hamiltonian method, the generalization of cost function needs to be carried out to have a larger application area. This current formula with only diagonal block matrices has limited applications. Another area that needs to be improved is determining the effect of the eigenvalues and eigenvectors of the system on the control law. As indicated earlier, the modal matrix has great impact on the solution of the system since inverse of the modal matrix is required. When there is a modal matrix with a value close to singular, the inverse may not be possible or reliable.

BIBLIOGRAPHY

[1] Firt, V., *Statistics, Form-finding and Dynamics of Air-Supported Membrane Structures,* Martinus Nijhoff Publishers, The Hague, 1983, pp. 5-6.

[2] http://www.thefarleygroup.com/LATESTPROJECTS/tabid/161/Default.aspx, accessed September, 2014.

[3] Jenkins, H. M. J., (ed.), *Gossamer Spacecraft: Membrane and Inflatable Structures Technology for Space Applications,* AIAA, Reston, VA, 2001, pp. 19.

[4] http://www.nasa.gov/centers/langley/about/project-echo_prt.htm, accessed August, 2014.

[5] Sunny, M. R., Sultan, C., and Kapania, R. K., "Optimal Energy Harvesting From a Membrane Attached to a Tensegrity Structure ", Proc. 54Th AIAA/ASME/ASCE/AHS/ ASC Structures, Structural Dynamics, and Materials Conference, 8-11 April 2013, Boston, MA.

[6] http://psipunk.com/eagle-morphing-into-an-avanced-concept-vehicle-from-nasa/, accessed March, 2015.

[7] Moore Jr, J.D., Patrick, B., Gierow, P. A., and Troy, E., "Design, test, and evaluation of an electrostatically figured membrane mirror", Proc. of SPIE. Vol. 5166, 2004, pp. 188-196.

[8] Junkins, J. L., Kim, Y., *Introduction to Dynamics and Control of Flexible Structures,* AIAA Inc., Washington, D.C. 1993.

[9] Balas, M.J., "Active Control of Flexible Systems", *Journal of Optimization Theory and Applications*, Vol. 25, No. 3, 1978, pp. 1415-1436.

[10] Hughes, P.C., and Skelton, R.E., "Controllability and Observability for Flexiable Spacecraft", Journal of Guidance and Control, Vol. 3, No. 3, 1980, pp. 452-459.

[11] Gibson, J.S., Adamian, A., "Aproximation Theory for Linear –Quadratic-Gaussian Optimal Control of Flexible Structures", *SIAM Journal of Control and Optimization*, Vol. 29, No. 1, 1991, pp. 1-37.

[12] Liu, K., Skelton, R. E., "Integrated Modeling and Controller Design with Application to Flexible Structure Control", *Automatica*, Vol. 29, No. 5, 1993, pp. 1291-1313.

[13] Forward, R. L., "Electronic damping of orthogonal bending modes in a cylindrical mast-experiment", *Journal of Spacecraft and Rockets,* Vol. 18, No. 1, 1981, pp. 11-17.

[14] Sato, T., Ishikawa H., Ikeda, O., Nomura, S., and Uchino, K., "Deformable 2-D mirror using multilayered electrostrictors", *Applied Optics,* Vol. 21, No. 20, 1982, pp.3669-3672.

[15] Sato, T., Ishikawa, H., and Ikeda, O., "Multilayered deformable mirror using PVDF films", *Applied Optics* Vol. 21, No. 20, 1982, pp.3664-3668.

[16] Bailey, T., and Ubbard, J. E., "Distributed piezoelectric-polymer active vibration control of a cantilever beam", *Journal of Guidance, Control, and Dynamics,* Vol. 8, No. 5, 1985, pp. 605-611.29.

[17] Crawley, E. F., and De Luis. J., "Use of piezoelectric actuators as elements of intelligent structures", *AIAA Journal,* Vol. 25, No. 10, 1987, pp. 1373-1385.

[18] Gowronski, W., Lim, K. B., "Balanced actuator and sensor placement for flexible structures", *International Journal of Control*, Vol. 65, No. 1, 1996, pp. 131-145.

[19] Mirza, M. A., Niekerk, J. L. V., "Optimal Actuator Placement for Active Vibration Control With Known Disturbances", *Journal of Vibration and Control,* Vol.5, 1999, pp. 709-724.

[20] Bevan_J. S., *Piezoceramic Actuator Placement for Acoustic Control of Panels*, Ph.D. Dissertation, Aerospace Engineering Dept., Old Dominion Univ., Norfolk, VA, 2001.

[21] Quek, S. T., Wang, S. Y., and K.ANG, K., "Vibration Control of Composite Plates via Optimal Placement of Piezoelectric Patches", *Journal of Intelligent Material Systems and Structures*, Vol. 14, 2003, pp. 229-245.

[22] Halim, D., Moheimani, S. O. R., "An optimization approach to optimal placement of collocated piezoelectric actuators and sensors on a thin plate", *Mechatronics,* Vol. 13, 2003, pp. 27-47.

[23] Yue, H. H., Deng, Z. Q., Tzou, H. S., "Optimal Actuator Locations and Precision Micro Control Actions on Free Paraboloidal Membrane Shells", *Communications in Nonlinear Science and Numerical Simulation*, Vol. 13. 2008. pp. 2298-2307.

[24] Smithmaitrie, P., and Tzou, H. S., "Micro-control actions of actuator patches laminated on hemispherical shells", *Journal of Sound and Vibration,* Vol. 277, No. 4, 2004, pp. 691-710.

[25] Philen, M. K., *Directional Decoupling of Piezoelectric Sheet Actuators for High-Precision Shape and Vibrational Control of Plate Structures*, Ph.D. Dissertation, Department of Mechanical and Nuclear Engineering, Pennsylvania State Univ., State College, PA, 2006.

[26] Bastaits, R., Rodrigues, G., Jetteur, Ph., Hagedorn, P., and Preumont, A., "Multi-layer adaptive thin shells for future space telescopes", *Smart Materials and Structures,*Vol.21, 2012, pp. 1-8.

[27] Hanagud, S., Obal, M. W., and Calise, A. J., "Optimal vibration control by the use of piezoceramic sensors and actuators", *Journal of Guidance, Control, and Dynamics,* Vol. 15, No. 5, 1992, pp.1199-1206.

[28] Scott, R. C., and Weisshaar, T. A., "Panel flutter suppression using adaptive material actuators", *Journal of Aircraft,* Vol.31, No. 1, 1994, pp. 213-222.

[29] Renno J. M. and Inman D. J., "Experimentally Validated Model of a Membrane Strip with Multiple Actuators", *Journal of Spacecraft and Rockets*, Vol. 44, No. 5, pp. 1140-1152, September-October 2007.

[30] Nader, M., Gattringer, H., Krommer, M., and Irschik, H., "Shape control of flexural vibrations of circular plates by shaped piezoelectric actuation", *Journal of Vibration and Acoustics,* Vol. 125, No. 1, 2003, pp. 88-94.

[31] Sun, D., and Tong, L., "Optimum control voltage design for constrained static shape control of piezoelectric structures", *AIAA Journal* Vol. 41, No. 12, 2003, pp. 2444-2450.

[32] Williams, R. B. *Localized Effects of Piezopolymer Devices on the Dynamics of Inflatable Space Based Structures,* MSc. Thesis, Mechanical Engineering Dept., Virginia Polytechnic and State Univ., Blacksburg, VA, 2000.

[33] Jenkins, C., *Recent Advances in Gossamer Spacecraft, Volume 212 of Progress in Astonautics and Aeronautics. AIAA*, Reston, VA. 2006.

[34] Park, G., Kim, M. H., and Inman, D. J.,"Integration of smart materials into dynamics and control of inflatable space structures", *Journal of Intelligent Material Systems and Structures*, Vol. 12, No. 6, 2001, pp. 423-433.

[35] Park, G., Ruggiero, E., and Inman, D.J., "Dynamic testing of inflatable structures using smart materials", *Smart Materials and Structures,* Vol. 11, No. 2, 2002, pp. 147-155.

[36] Hartl, D. J., and Lagoudas, D. C., "Aerospace applications of shape memory alloys", *Proceedings of the Institution of Mechanical Engineers, Part G: Journal of Aerospace Engineering* Vol. 221, No. 4, 2007, pp. 535-552.

[37] Rogers, J. W., and Agnes, G. S., "Modeling Discontinuous Axisymmetric Active Optical Membranes", *Journal of Spacecraft and Rockets*, Vol. 40, No. 4, 2003, pp. 553-564.

[38] Ruggiero, E. J., and Inman, D. J., "Modeling and vibration control of an active membrane mirror", *Smart Materials and structures,* Vol. 18, No. 9, 2009, pp. 1-10.

[39] Ruggiero, E. J., *Modeling and Control of Spider Satellite Components*, Ph.D. Dissertation, Mechanical Engineering Dept., Virginia Polytechnic and State Univ., Blacksburg, VA, 2005.

[40] Renno, J. M., and Inman, D. J., "Modeling and Control of a Membrane Strip Using a Single Piezoelectric Bimorph", *Journal of Vibration and Control*, Vol. 15, No. 3, 2009, pp. 391-414.

[41] Renno, J. M., *Dynamics and Control of Membrane Mirrors for Adaptive Optic Applications*, Ph.D. Dissertation, Mechanical Engineering Dept., Virginia Polytechnic and State Univ., Blacksburg, VA, 2008.

[42] Tarazaga, P. A., *Dynamics and Control of Pressurized Optical Membranes*, Ph.D. Dissertation, Mechanical Engineering Dept., Virginia Polytechnic and State Univ., Blacksburg, VA, 2009.

[43] Kiely, E., Washington, G., and Bernhard, J., "Design and development of smart microstrip patch antennas", *Smart materials and structures,* Vol. 7, No. 6, 1998, pp. 792-800.

[44] Varadarajan, S., Chandrashekhara, K., and Agarwal, S., "Adaptive shape control of laminated composite plates using piezoelectric materials," *AIAA Journal,* Vol. 36, No. 9, 1998, pp.1694-1698.

[45] Ferhat, I., and Sultan. C., "LQG Control and Robustness Study for a Prestressed Membrane with Bimorph Actuators", Proc. of ASME International Design Engineering Technical Conferences and Computers and Information in Engineering Conference, 17-20 August, 2014, Buffalo, NY.

[46] Hom, C. L., Dean, P. D., and Winzer, S. R., "Simulating electrostrictive deformable mirrors: I. Nonlinear static analysis", *Smart Materials and Structures,* Vol. 8, No. 5, 1999, pp. 691-699.

[47] Jenkins, C. H., Kalanovic, V. D., Padmanabhan, K., and Faisal, S. M., "Intelligent shape control for precision membrane antennae and reflectors in space", *Smart Materials and Structures,* Vol. 8, No. 6, 1999, pp. 857-867.

[48] Maji, A. K., and Starnes, M. A., "Shape measurement and control of deployable membrane structures", *Experimental Mechanics,* Vol. 40, No. 2, 2000, pp. 154-159.

[49] Paterson, C., Munro, I., and Dainty, J., "A low cost adaptive optics system using a membrane mirror", *Optics Express*, Vol. 6, No. 9, 2000, pp.175-185.

[50] Martin, J. W., and Main, J. A., "Noncontact electron gun actuation of a piezoelectric polymer thin film bimorph structure", *Journal of intelligent material systems and structures*, Vol. 13, No. 6, 2002, pp. 329-337.

[51] Dürr, J.K., Honke, R., von Alberti M., and Sippel, R., "Development and manufacture of an adaptive lightweight mirror for space application", *Smart materials and structures*, Vol. 12, No. 6, 2003, pp. 1005-1016.

[52] Rodrigues, G., Bastaits, R., Roose, S., Stockman, Y., Gebhardt, S., Schoenecker, A., Villon, P., and Preumont, A., "Modular bimorph mirrors for adaptive optics", *Optical Engineering*, Vol. 48, No. 3, 2009, pp. 1-7.

[53] Sodano, H. A., *Development of Novel Eddy Current Dampers for the Suppression of Structural Vibrations*, Ph.D. Dissertation, Mechanical Engineering Dept., Virginia Polytechnic and State Univ., Blacksburg, VA, 2005.

[54] Zhao, H., *Passive, Iterative, and Repetitive Control for Flexible Distributed Parameter Systems*, Ph.D. Dissertation, Department of Mechanical and Nuclear Engineering, Pennsylvania State Univ., State College, PA, 2005.

[55] Horn, W., Sokolowski, J. "A model for passive damping of a membrane", *Control and Cybernetics*, Vol. 34, No. 1, 2005, pp. 325-337.

[56] Nguyen, Q. C., Hong, K. S., "Transverse Vibration Control of Axially Moving Membranes by Regulation of Axial Velocity', *IEEE Transactions on Control Systems Technology*, Vol. 20, No. 4, 2013, pp. 1124-1131.

[57] Renno, J. M., Kurdila, A. J., and Inman, D. J., "Switching Sliding Mode Control for a Membrane Strip with MFC Actuators", Proc. of the SPIE 6926, Modeling, Signal Processing and Control for Smart Structures Conference, 9 March 2008, San Diego, CA.

[58] Renno, J. M., and Inman, D. J., "Nonlinear Control of a Membrane Mirror Strip Actuated Axially and in Bending", *AIAA Journal*, Vol. 47, No. 3, 2009, pp. 484-493.

[59] Ruppel, T., Dong, S., Rooms, F., Osten, W., and Sawodny, O., "Feedforward Control of Deformable Membrane Mirrors for Adaptive Optics", Proc. 54th AIAA/ASME/ASCE/ AHS/ASC Structures, Structural Dynamics, and Materials Conference, 8-11 April 2013, Boston, MA.

[60] Jha, A.K., and Inman, D.J., "Sliding mode control of a gossamer structure using smart materials", *Journal of Vibration and Control,* Vol. 10, No. 8, 2004, pp. 1199-1220.

[61] Xu, Y., Guan, F. L., "Structure design and mechanical measurement of inflatable antenna", *Acta Astronica*, Vol. 76, 2012, pp. 13-25.

[62] Hughes, P. C., Skelton, R. E., "Controllability and Observability of Linear Matrix-Second-Order Systems", *Journal of Applied Mechanics*, Vol. 47, 1980, pp. 415-420.

[63] Laub, A. J., Arnold, W. F., "Controllability and Observability Criteria for Multivariable Linear Second-Order Models", *IEEE Transactions on Automatic Control*, Vol. 29, No. 2, 1984, pp. 163-165.

[64] Wu, Y. L., and Duan, G. R., "Unified parametric approaches for observer design in matrix second-order linear systems", International of Control, Automation, and Systems, Vol. 3, No.2, 2005, pp. 159-165.

[65] Shieh, L. S., Mehio, M. M., Dib, H. M., "Stability of the Second-Order Matrix Polynomial", *IEEE Transactions on Automatic Control,* Vol. 32, No. 3, 1987, pp. 231-233.

[66] Bernstein, D. S., Bhat, S. P., "Lyapunov Stability, Semistability, and Asymptotic Stability of Matrix Second Order Systems", Proc, American Control Conference, June 1994, Baltimore, MD.

[67] Diwekar, A. M., Yedavalli, R. K., "Stability of Matrix Second Order Systems, New Conditions and Perspectives", *IEEE Transactions on Automatic Control*, Vol. 44, No. 9, 1999, pp. 1773-1777.

[68] Skelton, R. E., Hughes, P. C., "Modal Cost Analysis for Linear Matrix Second Order Systems", *Journal of Dynamics Systems, Measurement and Control*, Vol. 102, 1980, pp. 151-158.

[69] Skelton, R. E., "Adaptive Orthogonal Filters for Compensation of Errors in Matrix Second Order System", *Journal of Guidance and Control*, Vol. 4, No. 2, 1981, pp. 214-221.

[70] Sharma, J. P., George, R. K., "Controllability of Matrix second Order Systems a Trigonometric Matrix Approach", *Electronic Journal of Differential Equations*, No. 80, 2007, pp. 1-14.

[71] Skelton, R. E., *Dynamics Systems Control, Linear system Analysis and Synthesis*, John Wiley & Sons, New York, 1988, Chaps. 5, 6 and 8.

[72] Yipaer, F. Sultan C., “Modern Control Design for a Membrane with Bimorph Actuators”, 54th IAA/ASME/ASCE/AHS/ASC Structures, Structural Dynamics, and Materials Conference, 8-11 April, 2013, Boston, MA.

[73] Ferhat, I. and Sultan C., “System Analysis and Control Design for a Membrane with Bimorph Actuator.” *AIAA Journal*, (to be published)

[74] Ram, Y. M., and Inman, D. J., “Optimal Control for Vibrating Systems”, *Mechanical Systems and Signal Processing*, Vol. 13, No. 6, 1999, pp. 879-892.

[75] Zhang J. F., “Optimal Control for Mechanical Vibration Systems Based on Second-Order Matrix Equations”, *Mechanical Systems and Signal Processing*, Vol. 16, No. 1, 2002, pp. 61-67.

[76] Ferhat, I. and Sultan C., “LQR using Second Order Vector Form for a Membrane with Bimorph Actuators”, AIAA Sci-Tech, 5-9 January 2015, Kissimmee, FL.

[77] Hashemipour, H. R., Laub, A. J., “Kalman Filtering for Second-Order Models”, *Engineering Notes*, Vol. 11, No. 2, 1988, pp. 181-186.

[78] Y. Oshman, Y., Inman, D. J., Laub, A. J., “Square Root Estimation for Second Order Large Space Structures Models”, *Journal of Guidance*, Vol. 12, No. 5, 1989, pp. 698-708.

[79] Juang, J. N., Maghami, P. G.,”Robust Eigensystem Assignment for State Estimators Using Second Order Models”, *Journal of Guidance, Control and Dynamics*, Vol. 15, No. 4, 1992, pp. 920-927.

[80] Juang, J. N., Phan, M., “Robust Controller Designs for Second Order Dynamic Systems, A Virtual Passive Approach”, *Journal of Guidance, Control and Dynamics*, Vol. 15, No. 5, 1992, pp. 1192-1198.

[81] Datta, B. N., Rincon, F., “Feedback Stabilization of a Second-Order System A Nonmodal Approach”, *Linear Algebra and Its Applications*, Vol. 188, 189, 1993, pp. 135-161.

[82] Chu, E. K., Datta B. N., “Numerically Robust Pole Assignment for Second-Order Systems”, *International Journal of Control*, Vol. 64, No. 6, 1995, pp. 1113-1127.

[83] Chu, E. K., “Pole Assignment for Second Order Systems”, *Mechanical Systems and Signal Processing*, Vol. 16, No. 1, 2002, pp. 39-59.

[84] Diwekar, A. M., Yedavalli, R. K., “Smart structure Control in Matrix Second Order Form”, *Smart Materials and Structures*, Vol. 5, 1996, pp. 429-436.

[85] Duan, G. R., Liu, G. P.,"Complete Parametric Approach for Eigenstructure Assignment in a Class of Second Order Linear Systems", *Automatica*, Vol. 38, 2002, pp. 725-729.

[86] Duan, G. R., Parametric Eigenstructure Assignment in Second Order Descriptor Linear Systems", *IEEE Transactions on Automatic Control*, Vol. 49, No. 10, 2004, pp. 1789-1795.

[87] Wang, G. S., Duan, G. R., "Robust Pole Assignment via P-D Feedback in A Class of Second Order Dynamic Systems", 8th International Conference on Control, Automation, Robotics, and Vision, 6-9 December 2004, Kumming, China.

[88] Ventsel, E., and Krauthammer, T., *Thin Plates and Shells, Theory, Analysis and Applications*, Marcel Dekker, Inc., New York, NY, 2001.

[89] Szilard, R., *Theories and Applications of Plate Analysis*, John Wiley & Sons, Inc., Hoboken, NJ, 2004, Chapter 1, 3.

[90] Wang, C. M., Reddy, J. N., and Lee, K. H., *Shear Deformable Beams and Plates, Relationships with Classical Solutions*, Elsevier Science Ltd., Oxford, UK, 2000.

[91] Ugural, A. C., and Fenster, S. K., *Advanced Strength and Applied Elasticity*, Elsevier, New York, 1981, pp. 394.

[92] Leissa, A. W., *Vibration of Plates*, NASA, Washington D.C. 1969, pp. 267, 331-338.

[93] Vepa, R., *Dynamics of Smart Structures*, John Wiley & Sons Ltd. Publication, Chichester, West Sussex, United Kingdom, 2010.

[94] Chopra, I., Sirohi, J., *Smart Structures Theory*, Cambridge University Press, New York, NY, 2014.

[95] Leo, J.D., *Engineering Analysis of Smart Material Systems*, John Wiley & Sons Inc. Hoboken, NJ. 2007

[96] Manbachi, A., and Cobbold, R. S. C., "Development and application of piezoelectric materials for ultrasound generation and detection", *Ultrasound*, Vol. 19, No. 4, 2011, pp. 187-196.

[97] http://www.unictron.com/wordpress/technology/piezo-introduction/, accessed March, 2015.

[98] http://www.piezo.com/index.html, accessed March, 2015.

[99] Reddy, J. N., *An Introduction to the Finite Element Method*, McGraw Hill, Boston, 2006, Chaps. 6, 8 and 12.

[100] Khalil, H.K, *Nonlinear Systems*, Prentice Hall, Upper Saddle River, NJ, 2002.

[101] Meirovitch, L., *Dynamics and control of structures*, John Wiley & Sons, 1990. pp. 70.

[102] Dorato, P., Abdallah, C.T., and Cerone, V., *Linear Quadratic Control: An Introduction*, Krieger Pub Co, 2000, pp.

[103] Doyle, J. C., "Guaranteed Margins for LQG Regulators", *Technical Notes and Correspondence*, 1978, Vol. 23, No. 4, pp. 756-757.

[104] Massioni, P., Raynaud, H. F., Kulcsar, C., and Conan, J. M., "An Approximation of the Riccati Equation in Large-Scale Systems With Application to Adaptive Optics." IEEE Transactions on Control Systems Technology, Vol. 23, No. 2, 2015, 479-487 .

[105] Anderson B. D. O., and Moore J. B., 1990. *Optimal Control, Linear Quadratic Method*s, Prentice Hall, NJ, pp. 218-221.